

Development of a reliable single-cell aCGH suitable for clinical samples



DISSERTATION ZUR ERLANGUNG DES DOKTOGRADES DER
NATURWISSENSCHAFTEN (DR. RER. NAT.) DER FAKULTÄT FÜR BIOLOGIE UND
VORKLINISCHE MEDIZIN DER UNIVERSITÄT REGENSBURG

vorgelegt von
Zbigniew Tadeusz Czyż

aus
Czarnków, Polen

im Jahr
2014

Zusammensetzung des Prüfungsausschusses

- | | |
|---------------------|------------------------------|
| 1. Vorsitzender: | Prof. Dr. Stephan Schneuwly |
| 2. Erstgutachter: | Prof. Dr. Thomas Dresselhaus |
| 3. Zweitgutachter: | Prof. Dr. Christoph A. Klein |
| 4. Drittprüfer: | Prof. Dr. Gunter Meister |
| 5. Ersatzgutachter: | Prof. Dr. Richard Warth |

Das Promotionsgesuch wurde eingereicht am:
14.11.2014

Die Arbeit wurde angeleitet von:
Prof. Dr. Christoph A. Klein

Unterschrift:

Pracę tę dedykuję moim rodzicom,
Hannie i Tadeuszowi Czyż,
w podzięcie za ich miłość, nieustające wsparcie,
i nieoceniony wysiłek włożony
w każdy etap mojego wychowania.

This work I dedicate to my parents,
Hanna and Tadeusz Czyż,
thanking for their love, unfailing support
and invaluable efforts invested
in every stage of my upbringing.

“Pain is temporary.

It may last for a minute, or an hour, or a day, or (even) a year,
but eventually it will subside
and something else will take its place.

If I quit, however, it lasts forever”.

– Lance Armstrong

Index of contents

Index of contents.

List of abbreviations.....	10
1. Introduction.....	12
1.1. Metastasis as the major cause of cancer related deaths.....	12
1.1.1. Incidence and caused of cancer related deaths.	12
1.1.2. Metastasis as a multistep, evolutionary process.	12
1.1.3. Models of metastatic cancer progression.....	13
1.2. Detection and analysis of metastatic cancer spread.	15
1.2.1. Overview of methods for detection of minimal residual disease.	15
1.2.2. Overview and clinical application of immunological assays for detection of occult micrometastatic tumor cells.....	17
1.2.3. The need for more detailed analysis of micrometastatic cancer cells.	19
1.3. Genomic analysis of single cells.....	19
1.3.1. Overview of the methods available for the analysis of single cell genomes.	19
1.3.2. Comprehensive analysis of single cell genomes.	21
1.4. Aim of dissertation.....	24
2. Materials and methods.....	25
2.1. Materials.....	25
2.1.1. Reagents.	25
2.1.2. Enzymes.	27
2.1.3. Kits.	27
2.1.4. Consumables.	28
2.1.5. Laboratory Hardware.....	29
2.1.6. Buffers and solutions.....	30
2.1.7. Patients.	32
2.1.8. Cell lines.....	33
2.2. Methods.....	33
2.2.1. Fluorescent in situ hybridization (FISH).	33
2.2.2. Tissue processing and immunocytochemical screening for DCCs.....	34
2.2.3. Laser microdissection.....	35
2.2.4. Primary whole genome amplification (WGA).	35
2.2.5. Re-amplification of the WGA products.....	38
2.2.6. Quality control of the WGA products.	38
2.2.7. Isolation of bulk genomic DNA.	40
2.2.8. DNA labeling and CGH hybridization on metaphase spreads (mCGH).	40

Index of contents

2.2.9.	DNA labeling and aCGH hybridization on oligonucleotide microarrays.....	41
2.2.9.1.	Random-primed DNA labeling approach (RP labeling).	41
2.2.9.2.	PCR-based labeling techniques for WGA products generated by SCOMP.	43
2.2.9.2.1.	PCR-based labeling using dye-conjugated universal primer (PCR-T1).....	43
2.2.9.2.2.	PCR-based labeling using incorporation of dye-conjugated dNTPs (PCR-T2).45	
2.2.9.3.	Array comparative genomic hybridization on oligonucleotide arrays.....	46
2.2.9.4.	Processing and analysis of the aCGH data.	46
2.2.9.5.	Identification of minimal regions of aberration (MRAs).	47
2.2.9.6.	ROC analysis and hierarchical clustering of the aCGH data.....	47
2.2.10.	DNA labeling and aCGH hybridization on BAC based microarrays.	48
2.2.10.1.	The design of the BAC aCGH microarrays.....	48
2.2.10.2.	Labeling of WGA product.....	48
2.2.10.3.	Hybridization on BAC aCGH microarrays.	49
2.2.10.3.1.	Blocking of the microarray slides and denaturation of BAC DNA probes.	49
2.2.10.3.2.	Hybridization of WGA products on the BAC aCGH microarrays.	50
2.2.10.4.	Washing of the BAC aCGH microarrays.	51
2.2.10.5.	Scanning of the BAC aCGH microarrays.....	51
2.2.10.6.	Analysis of the BAC aCGH microarrays.	51
2.2.11.	Single-cell quantitative PCR (qPCR) assay for detection of genomic gains in ERBB2 locus.	52
2.2.12.	Statistical analysis.	53
3.	Results.	54
3.1.	Development of a new single-cell aCGH assay.....	54
3.1.1.	Optimization and validation of new DNA labeling approaches customized for the processing of SCOMP WGA products.....	54
3.1.2.	Comparison of the PCR-T2 approach with the random primed isothermal amplification DNA labeling system (RP labeling).....	57
3.1.2.1.	Analysis of freshly isolated, unfixed cells.....	57
3.1.2.2.	aCGH analysis of cells after immunostaining.	59
3.1.3.	Reproducibility of the single-cell aCGH analysis.	61
3.1.4.	Selection of the best performing type of reference sample.	62
3.1.5.	Suitability of re-amplified single-cell WGA product for high resolution aCGH	63
3.2.	Performance of the high-resolution single-cell aCGH assay.	64
3.2.1.	Detection of genomic heterogeneity between individual cells.	64
3.2.2.	Quantitative assessment of CNAs in the single cells.	66
3.2.3.	Comparison with previously available methods for single-cell CGH.....	68

Index of contents

3.3. Application of the new single-cell aCGH assay to the analysis of single DCCs.	70
4. Discussion.	74
4.1. Development of a high-resolution aCGH assay for accurate mapping of genomic aberrations in single cells.	74
4.1.1. Selection of the most suitable aCGH platform.	74
4.1.2. Selection of WGA technology.	75
4.1.3. Selection of a strategy for DNA labeling.	76
4.1.4. Selection of reference samples.	77
4.2. Advantages of the novel single-cell aCGH assay.	77
4.3. Applicability of the new analysis to monitor genomic heterogeneity of clinical DCCs – proof-of-principle case report.	78
4.4. Utility of the new method in the era of high-throughput sequencing.	80
5. Summary.	82
6. References.	83
7. Acknowledgments.	95
8. Curriculum vitae.	96

List of abbreviations

List of abbreviations.

#	Abbreviation	Description
1.	μL	Microliter
2.	aCGH	Array comparative genomic hybridization
3.	ADO	Allelic drop-out
4.	AML	Acute myeloid leukemia
5.	APAAP	Alkaline phosphatase - anti-alkaline phosphatase technique
6.	ATCC	American Type Culture Collection
7.	ATP	Adenosine triphosphate
8.	AUC	Area under the curve
9.	BAC	Bacterial artificial chromosome
10.	BCIP	5-bromo-4-chloro-3-indolyl phosphate
11.	BSA	Bovine serum albumin
12.	CEP	Centromere enumeration probe
13.	CHORI	Children's Hospital Oakland Research Institute
14.	CKs	Cytokeratins
15.	CNAs	Copy number alterations
16.	CTCs	Circulating tumor cells
17.	DAPI	4',6-diamidino-2-phenylindole
18.	dATP	Deoxyadenosine
19.	DCCs	Disseminated cancer cells
20.	dCTP	Deoxycytidine
21.	DEP	Dielectrophoresis
22.	dGTP	Deoxyguanosine
23.	DLRS	Derivative log2 ratio spread
24.	DMEM	Dulbecco's Modified Eagle's Medium
25.	DNA	Deoxyribonucleic acid
26.	dNTPs	Deoxyribonucleotides
27.	DOP-PCR	Degenerate oligonucleotide-primed PCR
28.	DSMZ	Deutsche Sammlung von Mikroorganismen und Zellkulturen/ German Collection of Microorganisms and Cell Cultures
29.	dTTP	Deoxythymidine
30.	dUTP	Deoxyuridine
31.	ECACC	European Collection of Cell Cultures
32.	EDTA	Ethylenediaminetetraacetic acid
33.	EpCAM	Epithelial cell adhesion molecule
34.	FACS	Fluoresce activated cell sorting
35.	FAST	Fiber-optic array scanning technology
36.	FCS	Fetal Calf Serum
37.	FDA	U.S. Food and Drug Administration
38.	FFPE	Formalin fixed paraffin embedded
39.	FISH	Fluorescent <i>in situ</i> hybridization

List of abbreviations

40.	gDNA	Genomic DNA
41.	GEO	<u>G</u> ene <u>E</u> xpression <u>O</u> mnibus
42.	HPLC	<u>H</u> igh-performance liquid <u>c</u> hromatography
43.	IARC	<u>I</u> nternational <u>A</u> gency for <u>R</u> esearch on <u>C</u> ancer
44.	ISCT	<u>I</u> solation by size of epithelial <u>t</u> umor cells
45.	kb	Kilobase
46.	m/v	Mass to volume
47.	MACS	<u>M</u> agnetic <u>a</u> ctivated <u>c</u> ell <u>s</u> orting
48.	MALBAC	<u>M</u> ultiple <u>a</u> nnealing and <u>l</u> ooping <u>b</u> ased <u>a</u> mplification <u>c</u> ycles
49.	Mb	Megabase
50.	mCGH	<u>M</u> etaphase <u>c</u> omparative <u>g</u> enomic <u>h</u> ybridization
51.	MDA	<u>M</u> ultiple <u>d</u> isplacement <u>a</u> mplification
52.	MEMS	<u>M</u> icro- <u>e</u> lectro- <u>m</u> echanical <u>s</u> ystem
53.	mL	Milliliter
54.	MRA	<u>M</u> inimal <u>r</u> egion of <u>A</u> berration
55.	NBT	<u>N</u> itroblue tetrazolium
56.	NGS	<u>N</u> ext generation sequencing
57.	OPA	<u>O</u> ne-phor- <u>a</u> ll buffer
58.	PBS	<u>P</u> hosphate <u>B</u> uffered <u>S</u> aline buffer
59.	PCR	Polymerase chain reaction
60.	PCR-T1	PCR-based labeling using dye-conjugated universal primer
61.	PCR-T2	PCR-based labeling using incorporation of dye-conjugated dNTPs
62.	PEP-PCR	<u>P</u> rimers- <u>e</u> xtension <u>p</u> reamplification <u>P</u> CR
63.	PFGE	<u>P</u> ulse <u>f</u> ield <u>g</u> el <u>e</u> lectrophoresis
64.	PGD	<u>P</u> reimplantation <u>g</u> enetic <u>d</u> iagnosis
65.	PMT	<u>P</u> hoto <u>m</u> ultiplier <u>t</u> ube
66.	PSA	<u>P</u> rosate <u>s</u> pecific <u>a</u> ntigene
67.	ROC	<u>R</u> eceiver <u>o</u> perating <u>c</u> haracteristic
68.	RP labeling	Random-primed DNA labeling approach
69.	rpm	<u>R</u> evolutions <u>p</u> er <u>m</u> inute
70.	SCOMP	Single-cell comparative genomic hybridization
71.	SDS	<u>S</u> odium <u>d</u> odecyl <u>s</u> ulfate
72.	SSC	<u>S</u> aline- <u>s</u> odium <u>c</u> itrate
73.	TAE	<u>T</u> ris- <u>A</u> cetate- <u>E</u> DTA buffer
74.	TBE	<u>T</u> ris- <u>b</u> orate- <u>E</u> DTA buffer
75.	Thr	Threshold
76.	ULS	<u>U</u> niversal <u>l</u> inkage <u>s</u> ystem
77.	v/v	Volume to volume
78.	WGA	<u>W</u> hole <u>g</u> enome <u>a</u> mplification

1. Introduction.

1.1. Metastasis as the major cause of cancer related deaths.

1.1.1. Incidence and caused of cancer related deaths.

Population based studies showed that cancer is among the leading causes of death worldwide. A recent report of the International Agency for Research on Cancer (IARC) on global patterns of cancer related incidence and mortality indicated that in 2012 alone 8.2 million people died of cancer and another 14.1 million new cases have been diagnosed [1]. Furthermore, it is projected that by 2030 the global cancer incidence will reach 22.2 million causing 13.2 million deaths and thereby becoming the major cause of morbidity and mortality worldwide [2]. The most common cancers are carcinomas, solid tumors arising in epithelial tissues, among which five tumor entities account for close to 50% of all deaths related to cancer: lung, breast, colorectal, prostate and stomach cancers [1]. Moreover, more than 90% of mortality from solid cancers can be attributed to metastasis, defined as the outgrowth of cancer cells in organs anatomically distant to the tissue of cancer origin [3]. Despite significant progress in cancer treatment, in particular introduction of novel therapeutic agents targeting specifically cancer relevant genes (e.g. Trastuzumab, a drug modulating activity of HER2/neu, which drives tumor progression in ~20% of breast cancer patients) [4,5], the prognosis for patients with late stage (metastatic) carcinomas has not changed over the last four decades with majority of patients dying within five years after the initial diagnosis and disease remaining largely incurable at this stage [6,7]. Compared to metastatic patients the average survival rate is higher in individuals with locally confined tumors (e.g. in breast cancer the expected 5-year survival rates estimated at diagnosis for patients with localized and metastatic disease amounts to 98.4 or 23.9%, respectively) [7]. Nevertheless, even in early-stage cancer patients metastatic lesions can arise after long latency periods. For instance, in breast cancer relapse can occur even twenty years after the initial diagnosis and treatment [8]. Consequently, the outcome of cancer treatment largely depends on the capacity to prohibit the process of metastatic spread or inhibit it at the earliest possible stage.

1.1.2. Metastasis as a multistep, evolutionary process.

Metastatic outgrowth and generation of clinically detectable metastases is a final product of a series of events collectively termed invasion metastasis cascade [9]. During the course of this process cancer cells of the primary tumor need to pass through various steps, all of which

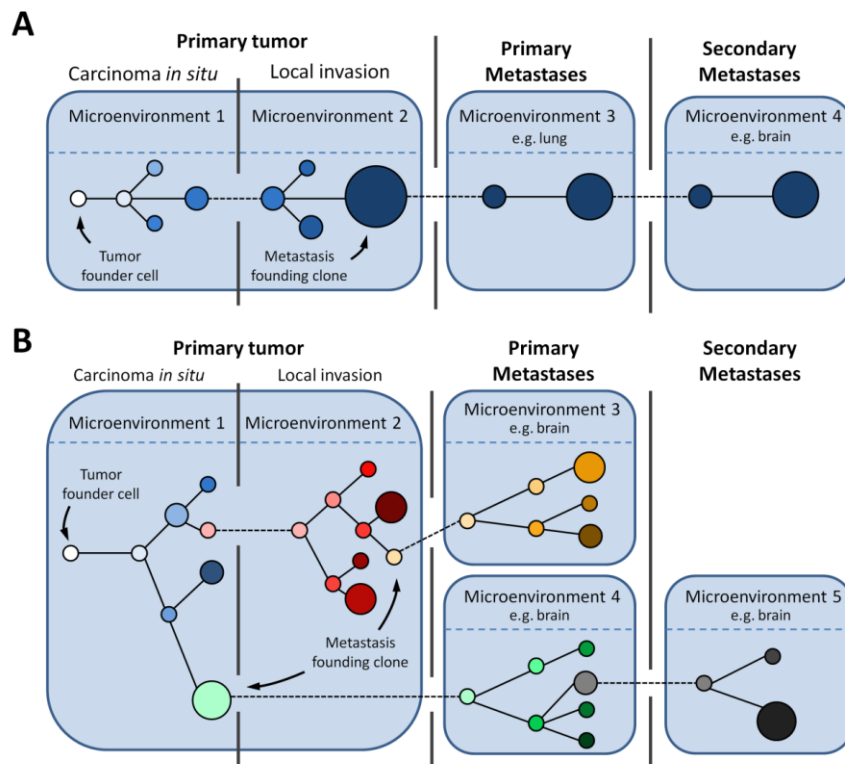
pose a selective pressure for cancer cells: (1) invade locally through extracellular matrix and stromal tissue, (2) enter the hematogenous or lymphatic circulation, (3) survive the transit through the vasculature, (4) arrest at the metastatic site, (5) extravasate into the parenchyma of the distant tissue, (6) survive in the foreign microenvironment of the distant organ, and (7) reinitiate proliferation [9]. Each of these impediments exerts different selective pressure on cancer cells necessitating them to acquire new traits to adapt to the surrounding conditions. Therefore, every step in the metastatic cascade can limit or terminate further spread, proliferation, and survival of cancer cells [9-11]. Consequently, selection of the cellular clone with the highest metastatic potential is likely to be based on the principles of asexual evolution of neoplastic cells [12]. For the succeeding cycles of selection and adaptation to take place, a mechanism is needed providing heterogeneity within the population of metastasizing cancer cells. Heterogeneity of the neoplastic cells may result from genome instability, a characteristic which is considered to be one of the hallmarks of cancer [13]. Acquisition of genetic changes results in generation of heritable phenotypes, which may confer selective advantage to overcome environmental barriers occurring along the metastatic cascade, ultimately leading to selection of full malignancy. Therefore, to effectively treat cancer it is critical to identify key genetic events preceding metastatic outgrowth of tumor cells in ectopic organs.

1.1.3. Models of metastatic cancer progression.

For a long time it was assumed that the genetic evolution of an individual cancer, from its ontogeny to full malignancy, takes place within the microenvironment of the primary tumor. This was supported by an observation that accumulation of genetic and epigenetic alterations was strongly associated with the stepwise acquisition of morphological abnormalities by the tumor tissue [14]. Based on these findings, a linear progression model of metastasis was established (Figure 1A) [14]. According to this paradigm, tumor progression is associated with gradual acquisition of advantageous genetic changes, e.g. activation of oncogenes or inactivation of tumor suppressor genes caused by mutations, allowing clonal expansion of more aggressive cellular variants producing larger and more dysplastic tumors. In this process, the ability of cancer cells to metastasize is strongly associated with the accumulation of genetic and epigenetic changes [14]. Therefore, the capacity to metastasize was largely restricted to cancer cells of large, late-stage tumors only, which already acquired full malignancy. Consequently, the genetic landscape of cancer cells present in the circulation

(both lymphogenous and hematogenous) and the matched primary tumor should be similar. Should this model be true, then the primary tumors could be used as good surrogate markers for selection of therapies, as it would comprise the complete set of genetic event that have led to the development of metastases. Although the linear progression model of cancer has been widely accepted, several clinical observations are not fully compatible with this concept. First, distant metastases can develop at early stages of cancer progression from small tumor lesions. For instance, systemic spread of cancer cells, manifested by the presence of disseminated cancer cells (DCCs) in the bone marrow, could be detected in 13-21% of patients with ductal carcinoma *in situ* (a premalignant lesion of mammary epithelium) [15-17] and in 29% of breast cancer patients with T1 stage tumors (tumor size < 2cm) [18]. Second, 5-10% of cancer patients are diagnosed with so called cancer of unknown primary origin, wherein metastatic disease was detected even though the location of the primary lesion could not be determined [19]. Third, seemingly non-metastatic early-stage cancer may relapse even after a complete resection of the primary tumor [20,21]. Due to these contradictions, a second model of tumor progression was established, termed “parallel progression model” (Figure 1B) [22]. According to this model, cancer cells leave the primary tumor early and simultaneously disseminate to various distant sites, where they progress in parallel with the primary lesion and acquire various traits, while adapting to the local microenvironment. Apart from the clinical observations stated above, this model was further supported by experimental data from studies on murine models of breast cancer. In the study published by Hüsemann and colleagues it was shown that systemic spread of cancer cells can be detected at the premalignant stage of tumor progression [17]. In addition, results of another study, by Podsypanina et al. showed that phenotypically normal, untransformed, mammary epithelial cells may survive in the circulation and, after oncogene activation has occurred, form metastases in distant organs [23]. Given that systemic spread of cancer cells is early, the course of tumor progression at the ectopic sites and in the primary tumor may vary substantially leading to development of distinct cancer genotypes and phenotypes. If this would be the case, then the genetic information confined in the primary tumor alone would have to be deemed insufficient to accurately identify patient subsets that could benefit from targeted anti-cancer therapies necessitating concurrent analysis of cancer cells present in the circulation.

Figure 1.



Models of systemic cancer progression.

In the linear progression model (A) genetic clones of cancer cells (here depicted symbolically as circles; various colors represent unique genetic subclones) accumulate oncogenic changes gradually becoming increasingly malignant. The ability to metastasize is restricted to cells that have acquired full malignant potential. Consequently metastatic spread is a late event in the systemic progression and the level of genetic diversity between primary tumor and metastasis will remain low. In contrast in parallel progression model (B) dissemination starts early – before cancer cells attained a fully malignant potential. Consequently, further steps of cancer progression take place in parallel at multiple anatomical sites (both in primary tumor or distant sites) generating heterogenic cancer clones. Figure adapted from Caldas C. [24] and Greaves M. et al [25].

1.2. Detection and analysis of metastatic cancer spread.

1.2.1. Overview of methods for detection of minimal residual disease.

Multiple assays were developed to identify and enumerate DCCs in lymph nodes or bone marrow and circulating tumor cells (CTCs) in the blood [26-28]. However, due to the extremely low tumor burden in the circulation of cancer patients (approximately 1 tumor cell in 10^5 to 10^7 of nucleated blood or bone marrow cells [29]), which is well beyond the detection limit of standard histopathological analysis, direct detection and isolation of tumor cells is not practical without prior enrichment. This is achieved by means of density centrifugation, selection based on physical properties (such as cell size) or expression of

Introduction

tumor associated markers (Table 1) [30-40]. A variety of methods have been used for the subsequent identification of DCCs or CTCs [41-43]. Detection of tumor cells is based on methods capable of distinguishing cells of different origin, i.e. hematopoietic white blood cells from epithelial tumor cells. Among those, the most widely used protocols are: (i) immunological assays or (ii) molecular methods based on polymerase chain reaction (PCR) (Table 2). Immunological assays utilize monoclonal antibodies to select cells based on the expression of various proteins, e.g. epithelial markers such as epithelial cell adhesion molecule (EpCAM) or cytokeratins (CKs) (used for positive selection) and/or common leukocyte antigen CD45 (used for negative selection) [26,27,44].

Table 1. Methods for enrichment of DCCs and CTCs.

Basis of selection	Selection criteria	Method	Technologies/Media
Physical properties	Buoyant density	Density Centrifugation	Percoll ^[45]
			Ficoll-Isopaque ^[20,21,32,45-48]
			OncoQuick ^[32]
			Leukapheresis ^[49]
	Cell size	Microfiltration	Isolation by Size of Epithelial Tumor Cells (ISET) ^[38]
			Micro-Electro-Mechanical System (MEMS) ^[39]
			ScreenCell ^[50]
Biological properties	Expression of marker proteins	Immunomagnetic cell enrichment	CellSearch ^[33]
			AdnaTest ^[51]
			MagSweeper ^[34]
			Magnetic Activated Cell Sorting (MACS) *
		Immunofluorescence-based enrichment	Fluoresce Activated Cell Sorting (FACS) *
			Fiber-optic array scanning technology (FAST) ^[52]
		Other immunoassays (based on affinity to antibody coated surface)	CTC Chip ^[53]
			EPISPOT ^[54]
			Nanodetector ^[55]

* - multiple reagents and systems customizable to various marker proteins.

Molecular approaches on the other hand, target known genetic alterations of the DNA sequence (e.g. mutations of KRAS or TP53 gene [56,57]) or aberrant expression of tissue specific or tumor associated markers [26,27,29,58,59]. Both detection systems provide clinically relevant information on the prognosis of cancer patients. However, the advantage of the immunological assays is that they allow morphological identification and subsequent isolation of tumor cells for further analyses, thereby allowing more comprehensive studies of

Introduction

DCCs and CTCs, in particular enabling analysis of cellular heterogeneity and clonal composition of these cell populations. Due to this limitation of the molecular detection methods, the remaining part of this chapter will be focused exclusively on the immunocytochemical detection of occult metastatic cells.

Table 2. Methods for detection of DCCs and CTCs.

Detection principle	Methods	Tumor entities	Marker
Immunocytochemical approaches	Immunostaining	Breast cancer	Cytokeratins ^[18,60] , HER2 ^[61] , MUC1 ^[62]
		Colon cancer	Cytokeratins ^[31,63]
		Esophageal cancer	Cytokeratins ^[64] , EpCAM ^[65]
		Gastric cancer	Cytokeratins ^[66]
		Lung (NSCLC)	Cytokeratins ^[67] , EpCAM ^[68]
		Prostate cancer	Cytokeratins ^[69,70]
		Melanoma	HMB45 ^[71] , MCSP ^[72]
Molecular approaches	RT-PCR	Breast cancer	CEA ^[73] , KRT19 ^[74] , SCGB2A2 ^[75] , EpCAM/MUC1/HER2* ^[76] , KRT19/SCGB2A2* ^[77]
		Colon cancer	CEA ^[78,79] , KRT20/CEA* ^[80]
		Lung (NSCLC)	KRT19/UCLL1/FN1/TRIM28* ^[81]
		Pancreatic cancer	KRT20 ^[82]
		Prostate cancer	PSA ^[83]
	Membrane-array	Gastric cancer	KRT19/CEA/hTERT/MUC1* ^[84]
	Mutation analysis	Pancreatic cancer	KRAS ^[57]
		Colon cancer	KRAS ^[56]

* - panels of markers used for detection.

1.2.2. Overview and clinical application of immunological assays for detection of occult micrometastatic tumor cells.

In the late 1980s and early 1990s several immunocytochemistry assays were designed employing monoclonal antibodies to detect occult micrometastatic cells based on the expression of various epithelial markers, including CKs (component of epithelial cytoskeleton), mucin (membrane-bound protein forming protective mucous barriers on epithelial surfaces), prostate specific antigen (PSA) and EpCAM (also known as 17-1A or HEA125) [85,86]. However, the detection rates of these approaches varied considerably

Introduction

depending on the tumor type, tumor stage and the monoclonal antibody used [87,88]. For this reason, attempts have been made to standardize the immunocytochemistry protocols for detection of DCCs [44]. As a result guidelines have been established for detection of DCCs in the bone marrow of breast cancer patients recommending detection of cancer cells by pan-cytokeratin antibodies directed against a wide spectrum of CKs (i.e. antibody A45-B/B3 directed against a common epitope of CKs 8, 18 and 19) [44]. In a similar study, EpCAM was shown to be the most reliable marker for detection of DCCs in the lymph nodes of carcinoma patients [89]. Detection of cytokeratin positive cells in bone marrow or EpCAM positive cells in lymph nodes of non-metastatic cancer patients was strongly associated with an inferior outcome of breast, prostate, lung and esophageal cancer patients indicating that cells detected by both assays are truly cancer cells [18,64,70,90-92]. In a more recent study, similar association was also found between the survival time of breast cancer patients and the presence of occult cytokeratin positive (CK+) cancer cells in the peripheral blood. Strikingly, detection of CK+ cells was prognostically relevant only for metastatic but not for early stage cancer patients [93]. Nevertheless, since the peripheral blood is easy to obtain and its biopsy is less invasive than the aspiration of bone marrow, a series of techniques have been developed to specifically detect CTCs [26,28,59]. The most relevant approach in this context is the CellSearch[®] System, a device allowing semi-automated positive immunomagnetic enrichment (using EpCAM specific antibodies) and subsequent enumeration of CKs⁽⁺⁾/CD45⁽⁻⁾/nucleated (DAPI⁽⁺⁾) cancer cells [33]. In prospective clinical studies positive detection of CTCs by the CellSearch[®] system (defined as ≥ 5 or 3 CTCs in 7.5 mL of blood) showed a significant association with overall and progression-free survival time of patients with metastatic breast, prostate and colon cancer [60,63,69]. These findings led to the clearance of the approach by the U.S. Food and Drug Administration (FDA) for the detection of CTCs in the peripheral blood of patients with afore the mentioned malignancies. More recent reports showed that CTCs detected by the CellSearch[®] System of non-metastatic cancer patients allowed prediction of early recurrence and decreased overall survival in breast cancer patients. This, however, was only possible when using larger sample volumes (i.e. mononucleated cell fraction extracted from the whole circulating blood by means of diagnostic leukapheresis) and/or reduction of the detection thresholds to only one CTC per specimen, thereby reducing the feasibility of these approach [49,94-96]. Therefore, at least for early stage cancer patients, detection and enumeration of occult micrometastatic cells is more reliable if using manual immunologic detection methods mentioned before.

1.2.3. The need for more detailed analysis of micrometastatic cancer cells.

Presence of occult micrometastatic lesions in the circulation of carcinoma patients allows to discriminate between individuals with poor and favorable prognosis. In the future this approach may become a valuable tool for therapeutic decision making and monitoring of the effectiveness of administered therapies. However, to better understand the biology underlying the early stages of systemic cancer spread it is necessary to comprehensively analyze detected metastatic cancer cells and identify the genetic programs governing this stages of disease [97]. Due to extremely low abundance of detectable CTCs and DCCs as well as their genetic heterogeneity, the true extent of genetic alterations in these cell populations can be assessed only at the single-cell level.

1.3. Genomic analysis of single cells.

1.3.1. Overview of the methods available for the analysis of single cell genomes.

Application of single-cell analysis allows to analyze minimal amounts of DNA material and reveals the biological complexity of cell populations, which would be obscured by analyzing bulk DNA. However, owing to the limited amount of genomic DNA in a single cell (approximately 6.5 pg) [98] direct analysis of single-cell DNA is challenging and the number as well as the type of downstream assays becomes significantly diminished allowing simultaneous analysis of a maximum of 96 loci by assays based on PCR or 12 loci by methods based on fluorescent *in situ* hybridization (FISH) [99,100]. Single-cell PCR was first used in the clinic in preimplantation genetic diagnosis (PGD) of monogenic diseases, such as cystic fibrosis, sickle cell anemia or β -thalassemia [101-103], sex determination of embryos at risk of X-linked diseases and, more recently, for the quantitative aneuploidy screening [99]. Single-cell PCR approaches were partially replaced by FISH, as it allowed detection of chromosomal mosaicism within the embryo and screening for translocations [104,105]. However, both methods (PCR and FISH) have several inherent shortcomings, in particular suboptimal reliability and accuracy, as well as limited amount of loci that can be simultaneously tested [106-108]. Hence, over the last twenty five years substantial efforts have been invested to develop and improve methods allowing amplification of the entire human genome [47,109-118]. These approaches, collectively termed whole genome amplification (WGA), were design to provide a comprehensive, accurate and unbiased representation of the starting material in amounts sufficient for extensive downstream testing.

Introduction

Currently existing WGA approaches are based on multiple displacement amplification (MDA) [113-115], variants of polymerase chain reaction (PCR) [47,109-112,116] or a combination of both of these technologies (Table 3) [117,118]. However, none of these technologies is without drawbacks and, due to inherent characteristics of their design, all WGA methods are prone to introduce different types of bias, which may influence the evaluation of downstream analyses.

The WGA-related amplification bias may include the following:

- (i) Quantitative amplification bias causing considerable representation bias of individual loci and random losses of alleles (allelic drop-out; ADO) [113,119-121].
- (ii) Qualitative amplification bias caused by formation of amplification artefacts such as chimeric sequences linking non-contiguous loci in the DNA [115,120,122].
- (iii) Incomplete coverage of the amplified genomes leading to underrepresentation of template DNA [115,120,123].
- (iv) Poor performance with partially degraded template DNA [114,124-127].
- (v) Stochastic priming of template DNA molecules, which may hamper the downstream analysis of WGA products [115,126].

Table 3. Overview of WGA technologies.

WGA Technology	DOP-PCR [109]	PEP-PCR [111]	OmniPlex/ GenomePlex [116,128]	SCOMP/ Ampli1 WGA [47]	RepliG/ GenomiPhi [129,130]	PicoPlex™/ SurePlex™/ EasyAmp™[117]	MALBAC [118]
Mechanism	PCR	PCR	PCR	PCR	MDA	MDA+PCR	MDA+PCR
Primer design	Hybrid ^A	Random	Defined	Defined	Random	Hybrid ^A	Hybrid ^A
Priming pattern	Random	Random	Random	Defined	Random	Random	Random
Applicability to genome-wide analysis of single-cell genomes	mCGH [131-134] aCGH ^(B) [135]	Not applicable	aCGH [136-141] NGS [138,142,143]	mCGH [20,21,45-48,71,72], aCGH [71,144-146] NGS [147]	mCGH [113,148] aCGH [141,149-153] NGS [118,120,138,154]	aCGH [155,156] NGS [120]	NGS [118]
Single-cell genome coverage	Not assessed	Not assessed	up to 38,7% ^[143]	up to 74% ^[147]	up to 72% ^[118]	< 36% ^[120]	up to 93% [118,157-159]
Applicability to analysis of single DCCs or CTCs	Not assessed	Not assessed	Yes [137-139,143]	Yes [20,21,45-48,71,72,144,145]	Yes [138]	Not assessed	Yes [159]

A – primer contain random and defined sequence

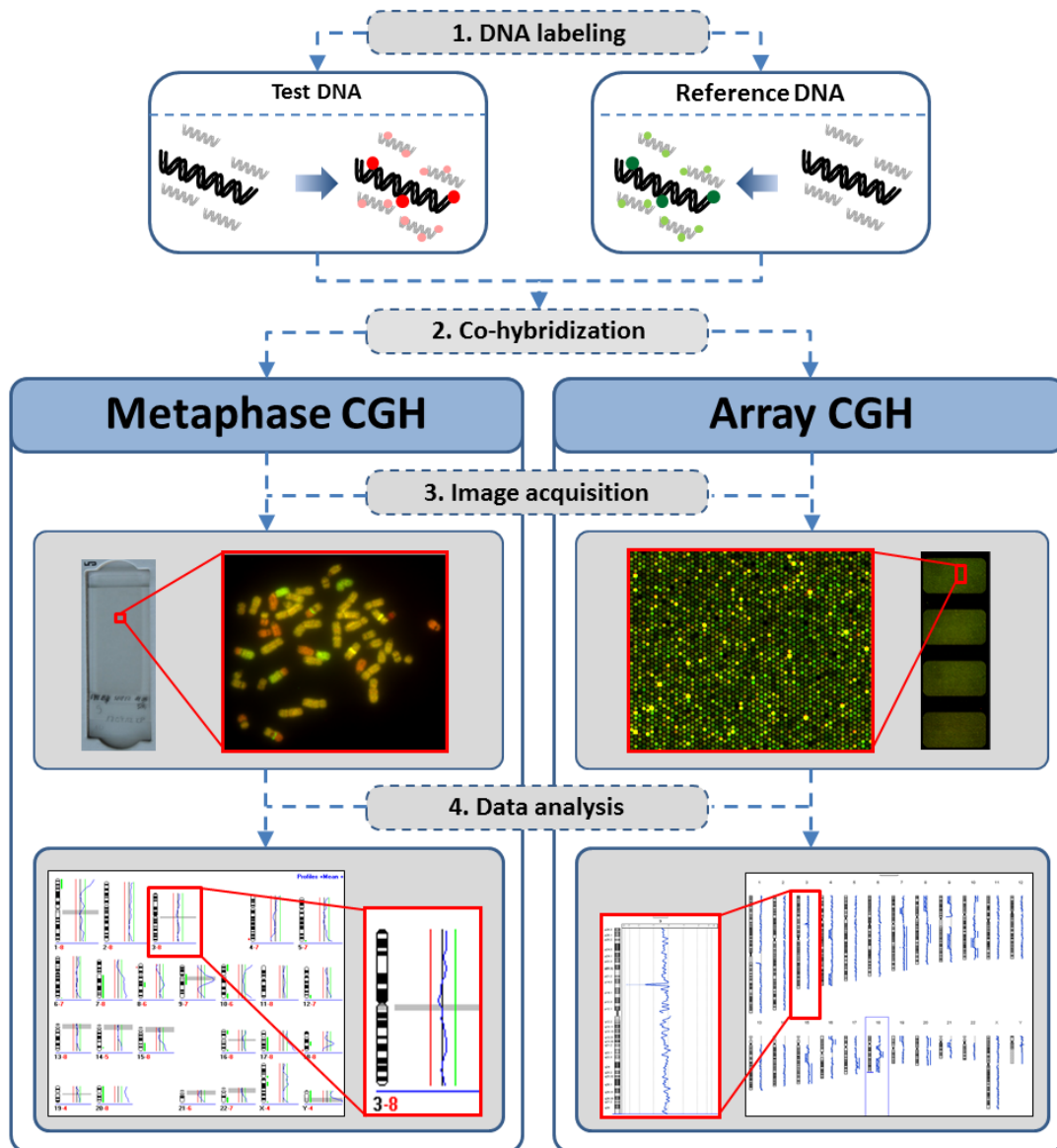
B – poor performance in aCGH

Inherent characteristics of the different WGA approaches make them better suited for specific types of samples, e.g. formalin fixed paraffin embedded (FFPE) tumor tissue specimens [114,125,127], or specific downstream applications [120,141]. For instance, approaches using random primer design, e.g. DOP-PCR, PEP-PCR and MDA are considered to be suboptimal for analysis of partially degraded DNA samples [114,124-127] and PCR-based approaches were shown to be more accurate for the assessment of copy number changes in single-cell WGA products [120,141]. Therefore, WGA methods should be carefully selected depending on the type of analysis to be conducted and the type of samples under investigation. Due to their high reliability of processing samples with compromised DNA quality [125-127] WGA methods based on adaptor mediated PCR, in particular GenomPlex and SCOMP, were used in most studies on CTCs and DCCs [8,20,21,45,46,48,71,137-140,143-146,160]. Genomic profiling of these samples is especially challenging due to fixation of cells performed prior to the amplification of DNA. Therefore, WGA approaches used to process DCCs and CTCs need to be highly robust and show high tolerance to the adverse effects of fixation [144].

1.3.2. Comprehensive analysis of single cell genomes.

With the advent of WGA technologies more comprehensive analysis of single-cell genomes became possible. Combination of WGA approaches with metaphase comparative genomic hybridization (mCGH) allowed genome-wide screening for copy number alterations in single cells [47,131,134]. mCGH utilizes two samples, test (putatively aberrant) and reference (harboring no copy number changes), which after differential labeling are hybridized to metaphase spreads (Figure 2). This approach proved to be very useful for both PGD and analysis of single DCCs allowing to screen the whole complement of chromosomes for the presence of copy number changes [17,20,21,45,47,132,161-164]. However, due to limited resolution (10-20 Mb), high labor intensity and lack of high-throughput capabilities of mCGH it was soon replaced by array-based CGH (aCGH) approaches (Figure 2). Standard DNA microarrays constructed of BAC clone libraries allowed detection of submicroscopic copy number alterations as small as 2.8 Mb in single trophoblast cells and 8.3 Mb in unfixed tumor cells [136,155]. Later, utilization of an improved BAC clone based aCGH platform allowed detection of copy number alterations of 1-2 Mb in unfixed cells and 4.4 Mb in DCCs [145].

Figure 2.



Principle of CGH.

In an CGH experiment test and reference DNA are differentially labeled with two fluorescent dyes (e.g. Cy5 or Cy3, respectively) and co-hybridized on an array of defined DNA probes (array CGH – aCGH) or metaphase spreads (metaphase CGH – mCGH). Following hybridization, fluorescent ratios (Cy5/Cy3) are quantified revealing copy number variations between test and reference samples. Genomic gains and losses are recognized as fluorescent ratios higher or lower than one, respectively. The accuracy of mCGH is limited by the observable banding resolution of metaphase chromosomes to a level of approximately 450 cytobands (5-10 Mb). In contrast, in array aCGH up to several millions of loci (represented by defined DNA probes) can be quantified simultaneously resulting in higher resolution of the method.

Further improvements were achieved by the introduction of modern oligonucleotide aCGH platforms. Denser distribution of probes in the pre-selected regions of interest allowed detection of 1 Mb-sized genomic alteration in unfixed lymphoblastoid cell and 2.6-3.0 Mb in

DCCs [137,156]. However, Möhlendick and coworkers have shown that copy number changes as small as a remarkable 56 kb in size can be detected in unfixed single cells without the need to use targeted array designs [146]. This, however, was only possible when using SCOMP WGA technology [146]. Collectively, studies using single-cell aCGH provided conceptual evidence that cost-effective, high resolution screening for copy number changes in genomes of single CTCs and DCCs is feasible with the use of modern DNA microarray platforms. However, attention needs to be paid to the experimental design and selection of analytical tools. With the advent of next generation sequencing (NGS) technologies, several groups attempted to analyse single-cell genomes with higher resolution. The efficacy of single-cell NGS was first shown by Navin et al., who applied low resolution sequencing to single nuclei of fresh frozen tumor cells allowing to study the genetic structure of cancer cell population in tumor tissue [142]. Subsequently, other groups utilized whole genome or whole exome sequencing approaches on single cells, allowing to study the rate of aneuploidy and *de novo* mutations in human gametes and unfixed cancer cells [118,165,166]. More recently, whole genome and whole exome NGS approaches were also applied to DCCs and CTCs enabling to capture copy number changes or mutation profiles of single cancer cells [138,143,159]. However, given the high cost for sequencing of a single-cell genome and high complexity of the subsequent computational analysis, NGS technologies are not feasible for routine use for screening of large patient collectives. Therefore, if the aim of the analysis is focused on the high-throughput analysis of copy number alterations in single cells, it still seems to be more rational to use more cost effective methods based on DNA arrays.

1.4. Aim of dissertation.

The aim of this thesis was to develop a reliable method for comprehensive, high-resolution copy number analysis of single-cell genomes after whole genome amplification (WGA). At the start of the project, single-cell metaphase CGH (mCGH) or BAC-based array CGH (aCGH) allowed detection of chromosomal imbalances with resolution of 10-20 or 1-2 Mb, respectively, concealing smaller ($< 1\text{Mb}$) aberrations and limiting the accuracy of breakpoint detection. To overcome these limitations, a novel high-resolution aCGH workflow had to be developed allowing more precise mapping of copy number variations in single-cell genomes.

To maximize the reliability and the generality of use, the new method should allow the following: (1) applicability to amplified DNA samples, in particular single-cell WGA products, (2) qualitatively and quantitatively faithful genome-wide assessment of chromosomal imbalances, (3) high sensitivity enabling detection of copy number aberrations with a resolution of $<1\text{Mb}$, (4) high specificity minimizing the rates of false-positive detection of chromosomal imbalances, (5) robustness to process clinical samples with decreased DNA quality such as immunostained DCCs or tumor FFPE tissue specimens, (6) uncomplicated experimental and analytical procedures allowing rapid processing and analysis of samples.

Materials and methods

2. Materials and methods.

2.1. Materials.

2.1.1. Reagents.

#	Description	Manufacturer
1.	1 kb DNA Ladder	Invitrogen
2.	1× TE (pH 8.0), Molecular grade	Promega
3.	2-Log DNA Ladder (0.1-10.0 kb)	New England Biolabs
4.	4',6-Diamidine-2'-Phenylindole Dihydrochloride (DAPI), 10 mg	Roche Diagnostics
5.	AB-Serum (human)	Biotest AG
6.	Acetonitrile	Merck
7.	Adenosine-5'-Triphosphate (ATP)-Lithiumsalt Solution, 100 mM	Roche Diagnostics
8.	Agarose	Sigma Aldrich
9.	Anti-Digoxigenin-FITC, Fab	Roche
10.	Anti-Digoxigenin-Fluorescein, Fab Fragments	Roche Diagnostics
11.	APAAP- Komplex	Dako
12.	Avidin Cy3.5, Purified	Biomol
13.	Avidin-Cy3.5	USBIO
14.	Barrycidal	PAN Biotech
15.	BCIP/NBT (AP Color Reagent)	Bio-Rad
16.	BerEP4 Mouse, Monoclonal, M0804, 250 µg/mL	Dako
17.	Biotin-16-dUTP, 1 mM	Roche
18.	Boric Acid	Sigma Aldrich
19.	Bovine Serum Albumin (BSA), 20mg/ml	Roche Diagnostics
20.	Bovine Serum Albumin (BSA), Factor V	Sigma Aldrich
21.	CEP 17 FISH Probe, 17q11.1-11-1, Alpha Satellite SpectrumGreen	Abbott Molecular
22.	Chloric Acid (HCl), 37% (12M)	J.T. Baker
23.	Cot-1 DNA, 1.0 mg/mL	Roche Diagnostics
24.	Cot-1 DNA, 1.0 mg/mL	Invitrogen
25.	Cy3-dCTP (25 nM)	GE Healthcare
26.	Cy3-dUTP (25 nM)	GE Healthcare
27.	Cy5-dCTP (25 nM)	GE Healthcare
28.	Cy5-dUTP (25 nM)	GE Healthcare
29.	Digoxigenin-11-dUTP, 1 mM	Perkin Elmer
30.	Disodium Phosphate (Na ₂ HPO ₄)	Sigma Aldrich
31.	DMEM/F12 Without L-Glutamate	PAN Biotech
32.	dNTP Set (100 mM Each dATP,dCTP,dGTP,dTTP)	GE Healthcare
33.	Dulbecco's PBS + MgCl ₂ And CaCl ₂	Sigma Aldrich
34.	Eosin	Sigma
35.	Ethanol Abs.	J.T. Baker
36.	Ethidium Bromide, 1%	Fluka
37.	Ethylenediaminetetraacetic Acid (EDTA)	Sigma Aldrich
38.	Expand Long Template PCR System Buffer 1	Roche Diagnostics

Materials and methods

39. FCS/FBS	PAN Biotech
40. Ficoll Paque Plus	GE Healthcare
41. Formamide	Merck
42. Formamide	Sigma Aldrich
43. GelPilot DNA Loading Gel, 5x	Qiagen
44. Hanks' Balanced Salt Solution (HBSS) With Phenol Red	Biochrom AG
45. Hanks' Balanced Salt Solution (HBSS) Without Ca^{2+} , Mg^{2+} , Without Phenol Red, 0.35 g/L NaHCO_3	Biochrom AG
46. Hematoxinilin (Mayer's)	Sigma
47. Heparin	Sigma Aldrich
48. HER-2/neu FISH Probe, 17q11.2-q12 LSI, SpectrumOrange	Abbott Molecular
49. Herring Sperm DNA, 10 mg/mL	Invitrogen
50. Igepal CA-360	Sigma Aldrich
51. KaryoMAX® Colcemid™ Solution	Sigma Aldrich
52. L-Glutamate (L-Glu), 200 μM	PAA
53. Low Molecular Weight DNA Ladder	New England Biolabs
54. Magnesium Acetat Solution Bio Ultra, ~1M in H_2O	Sigma Aldrich
55. Magnesium Chloride	Sigma Aldrich
56. Methanol (CH_3OH)	Merck
57. Monopotassium Phosphate (KH_2PO_4)	Merck
58. MOPC21-Isotypkontroll-Antibody (M5284), 1 mg/mL	Sigma Aldrich
59. Mouse Monoclonal Antibody A45-B/B3, 0.2 mg/mL	Micromet (AS Diagnostics)
60. Mouse Monoclonal Anti-Cytokeratin 18 Antibody, Clone CK2	Roche
61. Natrium Acetat Solution, 3M (pH = 5.2)	Calbiochem
62. Natrium Chloride (NaCl)	AppliChem
63. N-Lauroylsarcosine	Sigma Aldrich
64. Oligo aCGH/ChIP-on-chip Wash Buffer 1	Agilent
65. Oligo aCGH/ChIP-on-chip Wash Buffer 2	Agilent
66. OnePhorAll (OPA) Buffer, 10X	Amersham
67. Pepsin, 1 g	Roche
68. Pepton	GE Healthcare
69. Percoll	GE Healthcare
70. Polyethylene Membrane	P.A.L.M. Microlaser Technologies
71. Potassium acetat solution BioUltra, 5M in H_2O	Sigma Aldrich
72. Potassium chloride (KCl)	Sigma Aldrich
73. Proteinase K recombinant, PCR grade solution	Roche Diagnostics
74. Proteinase K, rec. PCR grade Solution	Roche Diagnostics
75. RPMI Medium without L-Glutamate	PAN Biotech
76. Sephadex G50	Sigma Aldrich
77. Sodium Hydroxide (NaOH)	Sigma Aldrich
78. Sodium Pyruvate	Sigma
79. Stabilization And Drying Solution	Agilent
80. Thermosequenase Buffer	GE Healthcare

Materials and methods

81. Tris(Hydroxymethyl)-Aminomethan (Tris)	AppliChem
82. Trisodium citrate	AppliChem
83. TruI, HC - 50u/μL)	Fermentas
84. Trypan Blue	VWR International
85. TWEEN® 20	Sigma Aldrich
86. TWEEN® 20, For Molecular Biology, Viscous Liquid	Sigma Aldrich
87. Vectashield	Vector Laboratories
88. Water HPLC Grade	Merck
89. Xylol	Carl Roth
90. Penicillin, 10.000 U/mL + Streptomycin, 10 μg/mL (Pen/Strep), 100x	PAN Biotech

2.1.2. Enzymes.

#	Description	Manufacturer
1.	DNA T4 Ligase, 5U/μL	Roche
2.	DNA Taq Polymerase PanScript, 5U/μL	PAN Biotech
3.	DNA Taq Polymerase, 5 U/μL	Roche
4.	Expand Long Template PCR System PolMix	Roche Diagnostics
5.	MseI Restriction Endonuclease Recombinant, 50 U/μL	New England Biolabs
6.	Ribonuclease A (100 mg/ml)	Qiagen
7.	Thermosequenase, 32 U/μl	GE Healthcare
8.	TruI, 50 U/μL	Fermentas
9.	Trypsin (10x)	PAN Biotech

2.1.3. Kits.

#	Description	Manufacturer
1.	Ampli1™ WGA Kit	Silicon Biosystems
2.	DNeasy Blood & Tissue Kit	Qiagen
3.	Oligo aCGH/ChIP-on-chip Hybridization Kit	Agilent
4.	PathVysion HER-2 DNA Probe Kit	Abbott Molecular
5.	SureTag Complete DNA Labeling Kit	Agilent
6.	Light Cycler® SYBRGreenI- Faststart-DNA-Master Mix	Roche

Materials and methods

2.1.4. Consumables.

#	Description	Manufacturer
1.	250 mL capacity slide-staining dish	
2.	96 Well PCR Adhesive Foil	ABGene
3.	96 Well PCR Plate	ABGene
4.	Acu-Jet® Pro Pipette Controller	Brand GmbH + Co KG
5.	Adhesion Slides - 2 Chambers	Carl Roth
6.	Adhesion Slides - 3 Chambers	Carl Roth
7.	Amicon® Ultra-0.5 Centrifugal Filter Devices; 100kDa	Milipore
8.	Amicon® Ultra-0.5 Centrifugal Filter Devices; 30kDa	Milipore
9.	Centrifugation Tubes (Sterile): 15 mL, 50 mL	Greiner Bio-One
10.	Combitips® Plus, Repetitive Positive Displacement Dispenser/ Pipette Tip	Eppendorf
11.	Cover Glass For The Hemocytometer	Schubert & Weiss OMNILAB
12.	Cryogenic Tubes	Nalgene
13.	Dextran Sulfate (Mw > 500000 g/M)	Sigma Aldrich
14.	EASYstrainer™ Cell Sieve 40 µM	Greiner Bio One
15.	EASYstrainer™ Cell Sieve 70 µM	Greiner Bio One
16.	Epoxy Coated Slides	Corning
17.	Eppendorf Repeater® Stream Electronic Pipette	Eppendorf
18.	Eppendorf® Research® Pro Electronic Pipette, 8-Channel, 0.5–10 µL	Eppendorf
19.	Eppendorf® Research® Pro Electronic pipette, 8-Channel, 20–300 µL	Eppendorf
20.	Erlenmeyer Flask	VWR International
21.	Filter 0.22 µM	Millipore
22.	Filter Tips For Micropipette 0.1-10 µL	Eppendorf
23.	Filter Tips For Micropipette 10 µL, 200 µL, 1000 µL	Biozym
24.	Fixogum (Rubber Vement)	Marabu
25.	Forceps	Agilent
26.	Glass Bottle 100 mL, 500mL, 1000 mL, 2000mL, 5000 mL	Schott
27.	Glass Micro-Hematocrit Capillaries	Brand GmbH + Co KG
28.	Hellendahl Cuvette	Carl Roth
29.	Hybridization Chamber, Stainless	Agilent
30.	LifterSlip (70 µL Volume)	Implen
31.	LightCycler® 480 Multiwell Plate 96 With PCR Adhesive Foil	Roche
32.	Magnetic Stir Bar	VWR International
33.	Measuring Cylinder, Glass	Duran Group
34.	Measuring Cylinder, Plastic	VWR International
35.	Microarray Gasket Slide 4-plex format	Agilent
36.	Microtubes 0.2 mL	Thermo Scientific
37.	Microtubes Racks	Brand GmbH + Co KG

Materials and methods

38. Neubauer Hemocytometer	Schubert & Weiss OMNILAB
39. Ozone-Barrier Slide Cover	Agilent
40. Pipettes: P10, P20, P200, P1000	Gilson
41. Polypropylene Reaction tubes: 0.2 mL, 1.5 mL, 2.0 mL	Eppendorf
42. Serological Pipettes (Sterile): 5 mL, 10 mL, 25 mL	Greiner Bio-One
43. Slide Holder	Agilent
44. SurePrint G3 Human CGH Microarray Kit 4×180K (design code: 022060)	Agilent
45. Surgical Disposable Scalpels	Brand GmbH + Co KG

2.1.5. Laboratory Hardware.

#	Description	Manufacturer
1.	Agilent G2565CA Microarray Scanner System	Agilent
2.	Axioskop 40 Zeiss, Mikroskop	Zeiss
3.	Benchtop Microcentrifuge	Grant Bio / Kisker
4.	Centrifuge 5810 R	Eppendorf
5.	DMRXA-RF8 Fluorescence Microscope	Leica
6.	Electrophoresis PerfectBlue Gelsystem	Peqlab Biotechnologie GmbH
7.	HERAsage Laminar Flow Cabinet	Heraeus
8.	Hybridization Oven	Agilent
9.	Hybridization Oven Rotator For Agilent Microarray	Agilent
10.	Incubator	Memmert
11.	Inverted Microscope	OPTECH
12.	Magnetic stir plate with heating element	Chemikalien und Laborbedarf Nierle (CLN)
13.	Medimachine	DAKO
14.	Microcentrifuge, 5417 R	Eppendorf
15.	Microcentrifuge, 5424	Eppendorf
16.	Microdissection Microscope	P.A.L.M. Microlaser Technologies
17.	NanoDrop 2000c	Thermo Scientific
18.	NanoDrop ND-1000	Peqlab Biotechnologie GmbH
19.	Orbital Shaker	Schmidt
20.	PatchMan NP2 Micromanipulator	Eppendorf
21.	Peltier Thermal Cycler Tetrad	Bio-Rad
22.	pH Meter	Sartorius AG
23.	Scale, Electronic	Kern
24.	Thermal Shaker (Thermomixer Confort)	Eppendorf
25.	Thermocycler qPCR, Roche LightCycler®	Roche
26.	Thermocycler, FlexCycler	Analytik Jena

Materials and methods

27. Thermocycler, PCT-200 Thermocycler, MJ Research	Bio-Rad
28. UV-Transilluminator & CCD Camera	Intas
29. Vortex mixer	VELP Scientifica
30. Water bath	Memmert

2.1.6. Buffers and solutions.

Trypsin/EDTA in 1xPBS	5 mL Trypsine (10x), 20 mL PBS (1x)
10x <u>T</u>ris-<u>B</u>orate-<u>E</u>DTA (TBE) Buffer	0.9 M Tris, 0.9 M H ₃ BO ₃ , 20 mM EDTA in H ₂ O (deionized)
10x <u>T</u>ris-<u>A</u>cetate-<u>E</u>DTA (TAE) Buffer	0.4 M Tris, 0.2 M Acetic Acid, 10 mM EDTA in H ₂ O (deionized); pH = 8.0
1x <u>T</u>ris-<u>E</u>DTA (TE) Buffer	10 mM Tris (ultrapure), 1mM EDTA in H ₂ O (HPLC Grade); pH = 8.0
10x <u>P</u>hosphate <u>B</u>uffered <u>S</u>aline (PBS) Buffer	85 mM Na ₂ HPO ₄ , 20 mM KH ₂ PO ₄ , 1.5 M NaCl in H ₂ O (deionized)
20x <u>S</u>aline-<u>S</u>odium <u>C</u>itrate (SCC) Buffer	3M NaCl, 300 mM Trisodium Citrate in H ₂ O (Millipore Grade)
4x SSC	20x SSC (see above) diluted five times with H ₂ O (deionized)
2x SSC	20x SSC (see above) diluted ten times with H ₂ O (Millipore grade)
1x SSC	20x SSC (see above) diluted twenty times with H ₂ O (Millipore grade)
2x SSC with 0.1% NP40	0.1% (v/v) Igepal in 2x SSC
0.4x SSC with 0.3% NP40	0.3% (v/v) Igepal in 0.4x SSC
4x SSC + 0.2% Tween-20	0.2 % (v/v) Tween-20 in 4x SSC; pH = 7.4
2x SSC + 0.1 % SDS	0.1% (v/v) SDS in 2x SSC
30% Dextran Sulfate in 4x SCC	30% (m/v) Dextran Sulfate in 4x SSC

Materials and methods

100% Percoll	100 mL Percoll; 9 mL HBSS without NaHCO ₃ ; pH = 7.4; sterile-filtered
10x PCR Buffer	100 mM Tris-HCl pH 8.5, 500 mM KCl, 10 mM MgCl ₂ in H ₂ O (HPLC Grade)
10x PCR Buffer with dNTPs	5 µL of each 100 mM dATP, dCTP, dGTP, dTTP and 480 µL 10x PCR Buffer
1x <u>T</u>ris/<u>E</u>DTA (TE) Buffer	Tris-HCl (10 mM), EDTA (1mM) in H ₂ O (Millipore Grade); pH = 7.4
7/8 dNTP Mix	dATP, dCTP and dGTP (10 mM each); dTTP (8.75 mM) in H ₂ O (HPLC Grade)
9/10 dNTP Mix	dATP and dGTP (10 mM each); dCTP and dTTP (9 mM each) in H ₂ O (HPLC Grade)
10x <u>O</u>ne-<u>P</u>hor-<u>A</u>ll (OPA) Buffer	Tris-Acetate (100 mM), Magnesium Acetate (100 mM), Potassium Acetate (500 mM) in H ₂ O (HPLC Grade); pH = 7.5
dNTP Mix (10 mM)	dATP, dCTP, dGTP, dTTP, 10 mM each
Blocking Solution Oligonucleotide aCGH	10X Oligo aCGH/ChIP-on-Chip Blocking Agent (complete content of a tube) in 1350 µL H ₂ O (HPLC Grade)
Blocking Solution BAC-array aCGH	2% (m/v) BSA in 1x SSC; pH = 7.4; sterile-filtered
Blocking Solution mCGH	3% (m/v) BSA (Factor V), 5% (v/v) FCS, in 1x PBS/0.2 % (v/v) Tween-20
Hybridization Mix BAC-array aCGH	4% (v/v) N-Lauroylsarcosine, 50% (v/v) Formamide, 8% (m/v) Dextran Sulfate (Mw >500.000 g/M) in 2xSSC; pH =7.4
Fixation Solution mCGH	750 mL Methanol, 250 mL Acetic Acid (3:1 ratio)

Materials and methods

Fixation Solution BAC-array CGH	50% (v/v) Formamide, 15% (m/v) Dextran Sulfate (Mw > 500.000 g/M) in 2x SSC
70% Formamide in 2x SSC	70 mL Formamide, 10 mL 20x SSC, 20 mL H ₂ O (deionized)
DAPI Counterstain Solution	10 µg/ml in 4x SSC + 0.2% Tween-20
Antibody Solution mCGH	20 µL Anti-Digoxigenin-FITC antibody, 2 µL Avidin-Cy3.5, 180 µL 1xPBS with 0.2% (v/v) Tween-20
Cell Culture Medium for OE-19 and PT-1590 esophageal cancer cell lines	10% FCS, 2 mM L-Glutamate, 1x Pen/Strep in RPMI 1640 Medium
Cell Culture Medium for BT474 and SKBR3 breast cancer cell lines	10% FCS, 2 mM L-Glutamate, 1 mM sodium pyruvate, 1x Pen/Strep in RPMI 1640 Medium
Cell Culture Medium for MDA-MB-361 and MDA-MB-453 breast cancer cell lines	10% FCS, 2 mM L-Glutamate, 1x Pen/Strep in DMEM Medium
Ethanol solution 70% (v/v), 85% (v/v), 90% (v/v)	Dilution of absolute ethanol solution in H ₂ O (Millipore or HPLC Grade)

2.1.7. Patients.

The ethics committee of the University of Regensburg (ethics vote number 07-079) approved screening procedures for the detection of DCCs and genomic analysis of the isolated cells. Additionally, as control and reference samples, single mononuclear cells were obtained from peripheral blood of five healthy donors. Within this group, three donors provided written informed consent (in compliance with ethic vote number 12-101-0038 approved by the ethics committee of the University of Regensburg) and two healthy donors provided verbal informed consent only. Since the latter samples were acquired before 2008, neither ethics vote for voluntary blood donation nor a written consent was required for these individuals.

Materials and methods

2.1.8. Cell lines.

Two breast cancer cell lines BT-474 and SKBR3 were obtained from the repository of the German Collection of Microorganisms and Cell Cultures at the Leibniz Institute DSMZ (Braunschweig, Germany). The remaining breast cancer cell lines, MDA-MB-453 and MDA-MB-361, were acquired from the American Type Culture Collection (ATCC). OE-19 esophageal cancer cell line was obtained from the European Collection of Cell Cultures (ECACC). PT1590 cell line was originally generated at the University Medical Center Hamburg-Eppendorf [92]. All cell lines have been maintained in the conditions recommended by the distributor. Identity of all cell lines was confirmed using a PCR-based fingerprinting.

2.2. Methods.

2.2.1. Fluorescent in situ hybridization (FISH).

Two color interphase FISH was performed using PathVysion HER-2 DNA Probe Kit (PathVysion Kit) with spectrum orange conjugated Vysis LSI HER-2/neu probe targeting the locus of ERBB2 gene (17q11.2-12) and spectrum green conjugated Vysis centromere enumeration probe for chromosome 17 (CEP 17) targeting pericentromeric alpha satellite DNA of chromosome 17 (17p11.1-q11.1). Cytospin slides, each containing $1.0\text{--}2.0 \times 10^6$, were thawed at room temperature for 30 min and subsequently washed in 2xSSC for 10 minutes at 37°C. Next, cellular spreads were digested with pepsin for 10 min at 37°C. Thereafter, slides were washed sequentially at room temperature for 5 minutes in 1xPBS temperature, 5 minutes in 1% (v/v) formaldehyde and 5 min in 1xPBS. Next, slides were dehydrated by washing in graded ethanol series: 2 minutes in 70% (v/v) ethanol, 2 minutes in 80% (v/v) ethanol and 2 minutes in 100% (v/v) ethanol. After drying the slide at room temperature, 2.0 µL of FISH probe solution was applied on the slides. Subsequently, after a denaturation step for 5 min at 75°C, hybridization of the FISH probes was conducted at a constant temperature of 39°C for 24 hours. Thereafter, slides were washed sequentially in 0.4x SSC with 0.3% (v/v) NP40 at 73°C for 2 minutes and in 2x SSC with 0.1% (v/v) of NP40 for 1 minute at room temperature. Finally, slides were washed in nuclease-free water and counterstained with DAPI. The results were quantified using the Zeiss Axio Imager 2 system. For each specimen a minimum of 25 cells were analysed and corresponding ERBB2 to CEP17 ratios were calculated.

2.2.2. Tissue processing and immunocytochemical screening for DCCs.

Bilateral bone marrow aspirates were taken from the anterior iliac crest of breast, prostate and esophageal cancer patients after written informed consent was obtained. All bone marrow specimens were screened for the presence of cytokeratin positive (CK+) cancer cells. In addition, in the case of oesophageal cancer patients, lymph nodes collected intraoperatively during the systematic lymphadenectomy were disaggregated and screened for EpCAM positive (EpCAM+) DCCs. The experimental procedures for bone marrow aspiration, lymph node disaggregation, immunocytochemical detection and isolation of DCCs were conducted according to previously published protocols [45,46,92,167]. In brief, bone marrow samples from cancer patients as well as blood specimens from healthy control patients were washed with Hank's solution and subsequently subjected to Ficoll-Paque density gradient centrifugation (density, 1.077 g per mole). Lymph node tissue was washed twice in PBS and subsequently disaggregated mechanically into a single-cell suspension. Mononuclear cell fraction from bone marrow and single-cell suspension obtained from lymph nodes were collected, transferred on adhesion slides (0.25×10^6 cells per 227 mm^2), dried overnight and stored at -20°C until further use. If available, 2×10^6 cells (2 slides) were screened for the presence of DCCs. Immunocytochemical detection of DCCs from bone marrow was performed using either the monoclonal antibody A45-B/B3 recognizing a common epitope of CKs 8, 18 and 19 or the monoclonal antibody clone CK2 directed against CK 18 [18,46], whereas cancer cells from lymph node samples were identified utilizing BerEP4 monoclonal antibody against EpCAM [65]. Cells collected from peripheral blood of healthy donors were stained using the monoclonal antibody (clone V9, Dako) against the intermediate filament vimentin. In parallel to cytokeratin or EpCAM staining, another slide was stained with isotype matched antibody (IgG1 Kappa) specific against non-human antigen (MOPC21 clone). This isotype control staining was utilized as negative control. Positively stained cells were visualized using the alkaline phosphatase and monoclonal anti-alkaline phosphatase (APAAP) technique, with 5-bromo-4-chloro-3-indolyl phosphate and nitroblue tetrazolium (BCIP/NBT) used as substrates for the alkaline phosphatase. Single positive cells were picked from the slide utilizing micromanipulator mounted on an inversed microscope. After visual confirmation that only a single cell was picked, the isolated cell was collected in 1 μL of 1xPBS and subjected to WGA.

Materials and methods

2.2.3. Laser microdissection.

FFPE tissue specimens were microdissected using the PALM Laser-Microbeam system according to the previously described protocol [127]. Briefly, FFPE tumor tissue blocks were cut into sequential 5 μm thick sections using a microtome with a disposable blade. Next, two sequential sections were further processed; one was stained with the conventional hematoxylin and eosin (H&E) staining for morphological inspection of the tissue, whereas the other was mounted on polyethylene membrane and subjected to microdissection. The unstained section was deparaffinized with xylene and subsequently rehydrated in a series of graded ethanol solutions (100%, 85%, and 70%). Following a hematoxylin staining, tissue sections were dehydrated in an increasing ethanol series and subsequently dried overnight in the presence of a desiccant. Using the PALM system selected areas of the section were microdissected and catapulted into the inner side of a 0.2 mL tube cap, which had been previously coated with PCR oil. In a subsequent centrifugation step, 14,000g for 5 minutes, tissue sections were transferred to the bottom of the tube and mixed with 3 μL of the proteinase K digestion mix composed as outlined in Table 4.

Table 4. Composition of the proteinase K digestion mix.

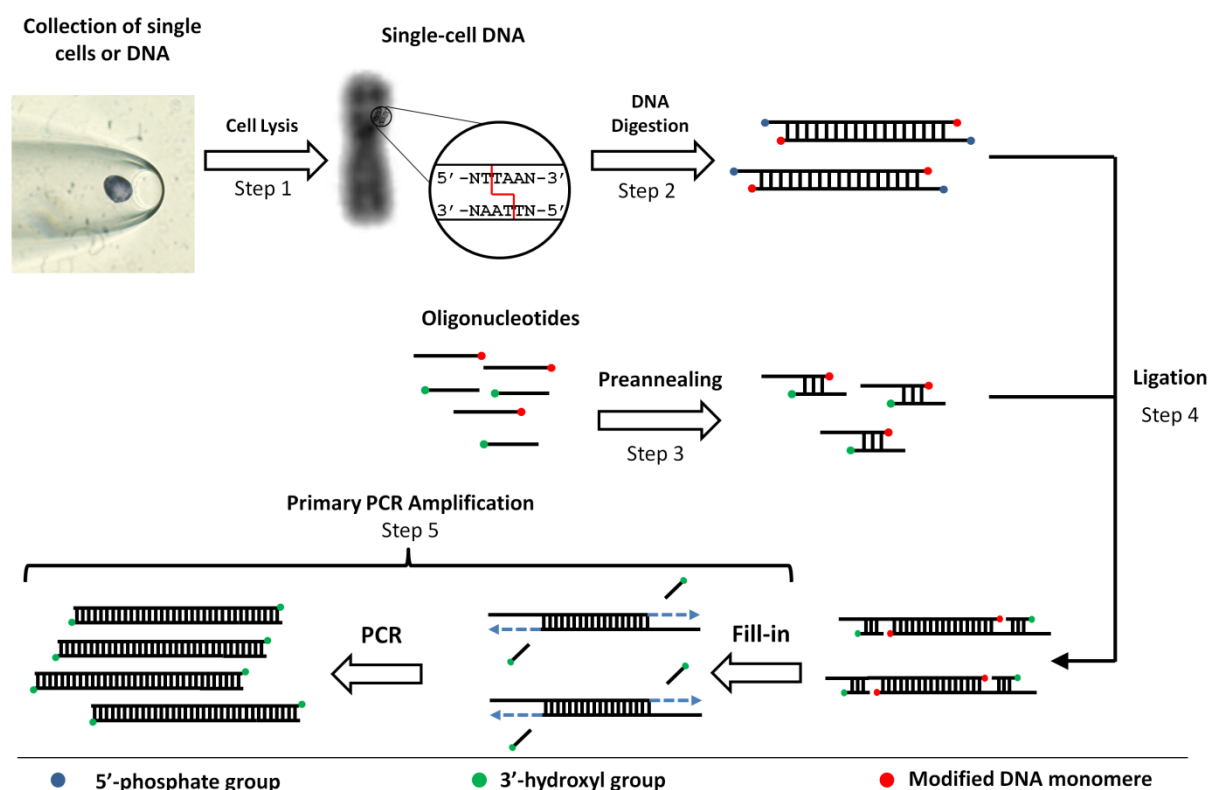
No.	Reagent	Volume
1.	10x One-Phor-All-Plus Buffer *	0.2 μL
2.	Tween-20 (10% v/v)	0.13 μL
3.	Igepal (10% v/v)	0.13 μL
4.	Proteinase K (10mg/ml)	0.26 μL
5.	PCR-grade H_2O	1.28 μL

* 10x One-Phor-All-Plus Buffer (OPA): 10 mM/L Tris-acetate, pH 7.5, 10 mM/L Mg-acetate, 50 mM/L K-acetate

2.2.4. Primary whole genome amplification (WGA).

All single cells, cell pools (approximately 100-1000 single cells) and FFPE tumor tissue were amplified using the SCOMP WGA technology [46,47,127], which is based on ligation mediated PCR, wherein genomic sequence is deterministically fragmented with MseI endonuclease prior to ligation and amplification steps (Figure 3).

Figure 3.



Overview of the processes underlying SCOMP WGA.

SCOMP WGA consists of five consecutive steps: (1) cell lysis, (2) digestion of template, (3) preannealing of PCR adaptors, (4) ligation and (5) PCR-based amplification. Utilization of restriction endonuclease (MseI) at the second step of the procedure assures deterministic and reproducible pattern of DNA fragmentation and priming. Moreover, the use of dedicated design of oligonucleotide comprising PCR adaptors prevents their self-ligation, thereby increasing the efficiency of PCR.

Single cells or cell pools were collected in a 1.0 μ L of PBS and added to 2 μ L of the proteinase K digestion buffer (Table 4), which had been previously dispensed into 0.2 mL reaction tube. The digestion was conducted in a PCR cycler with heated lid at 42°C for 10 hours in the case of single cell and cell pools or 15 hours for the FFPE tissue specimens. Subsequently proteinase K was heat-inactivated at 80°C for 10 min. Next, the sampled DNA was digested with MseI restriction endonuclease by adding 0.2 μ L 10x OPA buffer, 10 U of MseI and water to a total volume of 5 μ L. The restriction digestion was performed for 3 hours at 37°C and thereafter enzyme was heat-inactivated at 65°C for five minutes. Simultaneously, to the MseI digestion, PCR adaptors were prepared for the subsequent ligation mediated PCR. The PCR adaptors consisted of two oligonucleotides, either LIB1 (5'-AGT GGG ATT CCT GCT GTC AGT-3') and ddMse11 (5'-TAA CTG ACA GCdd-3') or, in the case of DCCs of breast cancer DCCs collected at the first analytical time point (details to be found in the result

Materials and methods

section), MseLig 21 (5'-AGT GGG ATT CCG CAT GCT AGT-3') and MseLig 12 (5'-TAA CTA GCA TGCdd-3'), which were mixed in equimolar concentrations (0.5 μ L of 100 μ M stock solution, each) with 0.5 μ L of 10x OPA Buffer and 1.5 μ L of H₂O. The annealing of the oligonucleotides forming the PCR adaptors occurred during an incubation step, in which the temperature was initially raised to 65°C and then decreased with a constant ramp of 1°C/minute to 15°C. Next, 1 μ L of ATP (10 mM) and 1 μ L T4-DNA-Ligase (5 units) were added to the pre-annealed PCR adaptors, which were then ligated over night at 15°C with the genomic DNA previously processed with MseI. The resulting genomic representation was amplified in a subsequent PCR reaction consisting of reagents outlined in Table 5. For this procedure, the MJ thermocycler was programmed using the settings listed in Table 6. Alternatively, for samples processed with MseLig 21-MseLig 12 adaptors, PCR was conducted as previously specified [47].

Table 5. Composition of the primary WGA reaction.

No.	Reagent	Volume
1.	Expand-Long-Template PCR System Buffer 1	3.0 μ L
2.	dNTPs (10 mM, each)	2.0 μ L
3.	Expand-Long-Template PCR System Polymerase Mix (5 U/ μ L)	1.0 μ L
4.	PCR-grade H ₂ O	35 μ L

Table 6. PCR program used to run the primary WGA reaction.

Step	Temperature	Time	Repetitions
1.	68°C	3:00 min	
2.	94°C	0:40 min	15x
3.	57°C	0:30 min	
4.	68°C	1:30 min + 1 sec/cycle	
5.	94°C	0:40 min	9x
6.	57°C + 1°C/cycle	0:30 min	
7.	68°C	1:45 min + 1 sec/cycle	
8.	94°C	0:40 min	23x
9.	65°C	0:30 min	
10.	68°C	1:53 min + 1 sec/cycle	
11.	68°C	3:40 min	
12.	4°C	for ever	

Materials and methods

2.2.5. Re-amplification of the WGA products.

Re-amplification of the primary WGA product was conducted according to the protocol described by Czyz ZT et al. [144]. The composition of the re-amplification reaction and the corresponding PCR-program are outlined in Table 7 and Table 8, respectively. Typically three reactions were run in parallel, which were pooled and used as template for DNA labeling and aCGH. A negative (no template) control was included in every run.

Table 7. Composition of the reaction used to re-amplify primary WGA products.

No.	Reagent	Volume
1.	Expand-Long-Template PCR System Buffer 1	5.0 μ L
2.	LIB1 (10 μ M)	5.0 μ L
3.	dNTP mix (10 mM)	1.75 μ L
4.	BSA	1.25 μ L
5.	Expand-Long-Template PCR System Polymerase Mix (5 U/ μ L)	0.5 μ L
6.	PCR-grade H ₂ O	35.5 μ L
7.	Template (undiluted WGA product)	1.0 μ L

Table 8. Conditions of the PCR reaction used to re-amplify the primary WGA products.

Step	Temperature	Time	Repetitions
1.	94°C	1:00 min	1x
2.	60°C	0:30 min	
3.	65°C	2:00 min	
4.	94°C	0:30 min	11x
5.	60°C	0:30 min	
6.	65°C	2:00 min + 20 sec/cycle	
11.	4°C	for ever	

2.2.6. Quality control of the WGA products.

The quality of WGA products was assessed by means of PCR as previously described [145], with minor modifications. The tested genomic loci and corresponding PCR primers are listed in Table 9. PCR was composed and run according to the specifications outlined in Table 10 and Table 11, respectively. Five-fold dilution of the WGA product was used as template for the PCR. Due to inherent characteristics of the WGA products generated from FFPE

Materials and methods

specimens, in particular significant fragmentation of input DNA caused by the fixation and storage, the quality of these samples could not be assessed prior to the aCGH analysis. Positivity for 7-8 PCR products indicated very good quality of the WGA products, whereas samples with 6-7 positive reactions were classified as good. Samples positive for 5 markers or less were not included in further analyses.

Table 9. Markers and corresponding PCR primers used to assess the quality of the WGA products.

No.	Gene/Marker	Forward Primer	Reverse Primer	Annealing Temperature
1.	D3S1514	5'-CAGCCAGCAGAATTATGAG-3'	5'-GGCAACAGAGCAAGATGC-3'	59°C
2.	D5S2117	5'-CCAGGTGAGAACCTAGTCAG-3'	5'-ACTGAGTCCTCCAACCATGG-3'	58°C
3.	D6S1633	5'-CTCATGGAGCTTATAGCCTG-3'	5'-TGTCCTTCTGGCTAGCATG-3'	59°C
4.	D17S1322	5'-CTAGCCTGGGCAACAAACGA-3'	5'-GCAGGAAGCAGGAATGGAAC-3'	55°C
5.	BCR	5'-CGTGGACAACCTACGGAGTTG-3'	5'-TCAGCCTCAGGACTCTGTG-3'	58°C
6.	KRT19	5'-GAAGATCCGCGACTGGTAC-3'	5'-TTCATGCTCAGCTGTGACTG-3'	58°C
7.	TP53	5'-GAAGCGTCTCATGCTGGATC-3'	5'-CAGCCCAAGCCTTGTCCTTA-3'	58°C
8.	TP53	5'-AGGACCTGATTTCCTTACTGC-3'	5'-GAGGTCCCAAGACTTAGTAC-3'	58°C

Table 10. Composition of the PCR used to assess the quality of WGA products.

No.	Reagent	Volume
1.	10x PCR buffer with dNTP Mix (10 mM, each)	1.0 µL
2.	Forward primer (8 µM)	0.5 µL
3.	Reverse primer (8 µM)	0.5 µL
4.	BSA	0.25 µL
5.	Taq polymerase (5U/µL)	0.1 µL
6.	PCR-grade H ₂ O	7.25 µL
7.	Template	1.0 µL

Table 11. Conditions of the PCR used to test the quality of WGA products.

Step	Temperature	Time	Repetitions
1.	94°C	2:00 min	1x
2.	55/58/59°C *	0:30 min	
3.	72°C	2:00 min	
4.	94°C	0:15 min	15x
5.	55/58/59°C *	0:30 min	
6.	72°C	0:20 min	
7.	94°C	0:15 min	25x
8.	55/58/59°C *	0:30 min	
9.	72°C	0:30 min	
10.	72°C	2:00 min	
11.	4°C	for ever	

*Annealing temperature depended on marker tested (Table 9).

2.2.7. Isolation of bulk genomic DNA.

High-molecular-weight genomic DNA was isolated either from mononuclear cell fraction of the peripheral blood of healthy donors or cancer cell line cells collected from adherent cell cultures. Unamplified genomic DNA was isolated using the Qiagen DNeasy® Blood & Tissue Kit according to the manual provided by the manufacturer (DNeasy Blood & Tissue Handbook 07/2006). In brief, a maximum of 5×10^6 cells were collected and resuspended in 200 μ L of sterile 1x PBS buffer. Next, cell suspension was supplemented with 20 μ L of Proteinase K (concentration not indicated by the manufacturer), 4 μ L of RNase A (100 mg/ml) and 200 μ L of Buffer AL, mixed thoroughly by vortexing and incubated at 56°C for 10 minutes. The resulting cell lysate was mixed with 200 μ L of 96% (v/v) ethanol, loaded on the assembled DNeasy mini spin column and spun down at 6.000g for 1 minute. After discarding the flow-through, the column was loaded with 500 μ L of Buffer AW1 and centrifuged for 1 min at 6.000g. Again, the flow-through was discarded and the column was loaded with 500 μ L of Buffer AW2. Thereafter, columns were centrifuged for 3 min at 20.000 g, flow-through was discarded and the spin column assembly was centrifuged again (1 min at 20.000g) to remove the residual buffers. Subsequently, DNeasy Mini Column was transferred to a clean microcentrifuge tube and the high-molecular-weight DNA was eluted with 2x75 μ L of H₂O. DNA was collected in a two subsequent centrifugation steps for 1 min at 6.000g. The quantity and the purity of isolated DNA were quantified using a NanoDrop ND-1000 spectrophotometer. In addition, the integrity of isolated DNA was assessed on 0.8% agarose gel supplemented with ethidium bromide. Herefore, 300 ng of DNA was applied on a gel and run for 1.5 hour at 3 V/cm.

2.2.8. DNA labeling and CGH hybridization on metaphase spreads (mCGH).

Sample preparation and mCGH was performed according to a previously described protocol [47,168]. In brief, DNA was labeled indirectly using either digoxigenin (test) or biotin (reference). The PCR was composed and run according to specifications outlined in Table 12 and Table 13, respectively. Labeled test and reference DNA were mixed and hybridized on the metaphase spreads in the presence of 80 μ g of Human Cot1-DNA, and 100 μ g of Herring Sperm DNA. The hybridization was carried out at 37°C for 48 hours. Subsequently, the metaphase spreads were washed, their images were acquired and test to reference

Materials and methods

fluorescence ratios were quantified as described before [169]. The mCGH experiments included in this thesis were conducted as part of the dissertation of Dr. Bernhard Polzer [168].

Table 12. Composition of the reaction used to label WGA products prior to mCGH.

No.	Reagent	Volume
1.	Expand-Long-Template PCR System Buffer 1	4.0 μ L
2.	LIB1 (10 μ M)	8.0 μ L
3.	7/8 dNTP mix *	1.5 μ L
4.	Digoxigenin-11-dUTP/Biotin-16-dUTP (1.0 mM)	1.75 μ L
5.	Taq Polymerase (5 U/ μ L)	1.25 μ L
6.	PCR-grade H ₂ O	35.5 μ L
7.	Template (undiluted WGA product)	1.0 μ L

* 7/8 dNTP mix consisted of dATP, dGTP, dCTP (10 mM, each) and dTTP (8.75 mM).

Table 13. Conditions of the PCR used to label WGA products prior to mCGH.

Step	Temperature	Time	Repetitions
1.	94°C	1:00 min	1x
2.	60°C	0:30 min	
3.	72°C	2:00 min	
4.	94°C	0:30 min	11x
5.	60°C	0:30 min	
6.	65°C	2:00 min + 20 sec/cycle	
11.	4°C	for ever	

2.2.9. DNA labeling and aCGH hybridization on oligonucleotide microarrays.

2.2.9.1. Random-primed DNA labeling approach (RP labeling).

Test and reference DNA samples were labeled using SureTag DNA Labeling Kit (Agilent Technologies) according to the instruction provided by the supplier (Agilent Oligonucleotide Array-Based CGH for Genomic DNA Analysis, version 7.1, December 2011), also summarized by Möhlendick et al. and Czyz et al. [144,146]. Briefly, 1.5 - 2.0 μ g of purified DNA (WGA product or unamplified genomic DNA) was mixed with 5 μ L of Random Primer Mix and filled up with H₂O to a total volume of 31 μ L. Unamplified DNA and WGA product samples were denatured at 95°C for 10 or 3 minutes, respectively. Sample tubes were transferred on ice and incubated for 5 min. The labeling reaction with exo-Klenow fragment

Materials and methods

consisted of 31 μL of denatured DNA supplemented with random primers, 10 μL of 5x Reaction Buffer, 5.0 μL of 10x dNTP Mix, 3.0 μL of Cy5-dUTP (test) or Cy3-dUTP (reference) and 1.0 μL of Exo(-) Klenow fragment. Labeling reaction was run at 37°C for two hours, followed by an inactivation step at 65°C for 10 minutes. Labeled DNA was purified using Amicon Ultra 0.5 purification system with a size cut-off of 30 kDa. Herefore, the labeled DNA was filled up with H₂O to a total volume of 480 μL DNA, loaded on the Amicon Ultra spin column assembly and centrifuged for 10 min at 14.000 g. Next, the flow-through was discarded, the column was loaded with 480 μL of H₂O and the samples were centrifuged again at 14.000 g for 10 min. Subsequently, the purification column were removed and mounted in an upside-down position in a new collection tube. The DNA was eluted during a subsequent centrifugation step at 1.000 g for 1 min. Next, samples were measured with the NanoDrop ND-1000 spectrophotometer. The DNA yields and dye incorporation rates (specific activity) were quantified using Equation 1 and Equation 2, respectively.

Equation 1. DNA Yield.

$$DNA\ Yield\ [\mu g] = \frac{DNA\ Concentration\ \left[\frac{ng}{\mu L}\right] \times Sample\ Volume\ [\mu L]}{1000}$$

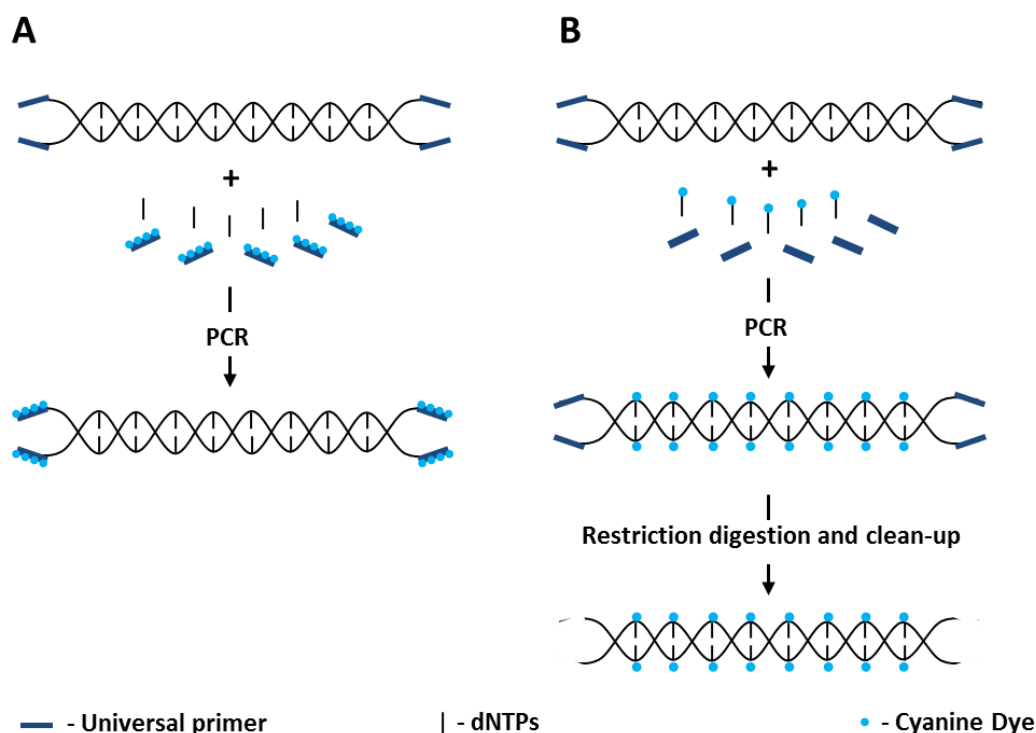
Equation 2. Specific activity (dye incorporation rate).

$$Specific\ Activity\ \left[\frac{pmol}{\mu g}\right] = \frac{Dye\ Concentration\ \left[\frac{pmol}{\mu L}\right]}{DNA\ Concentration\ \left[\frac{\mu g}{\mu L}\right]}$$

2.2.9.2. PCR-based labeling techniques for WGA products generated by SCOMP.

Schematic overview depicting the principles of PCR-based labeling techniques used to process WGA products generated by SCOMP is presented in the Figure 4.

Figure 4.



Schematic overview of PCR-based labeling techniques for SCOMP WGA products.

PCR-T1 (A) utilized dye-conjugated universal primer identical to that used in SCOMP. This facilitated even incorporation of the dye into the amplicons of a WGA product irrespective of their size. In contrast, PCR-T2 (B) facilitated labeling of WGA products though incorporation of dye-conjugated nucleotides. This approach permitted removal of PCR-adaptor sequence prior to hybridization on the array.

2.2.9.2.1. PCR-based labeling using dye-conjugated universal primer (PCR-T1).

Conjugation of the dye directly to the universal primer provides the advantage that all restriction digestion fragments present in the WGA product, irrespective of their size, will be labeled with the same amount of dye. To avoid cross-hybridization of adaptor sequences flanking amplicons in the WGA products, test and reference samples were labeled using different PCR-adaptors. Test samples were labeled with the PCR-adaptor used in the SCOMP primary WGA (paragraph 2.2.4. of this manuscript), while all the reference DNA samples were amplified using the following adaptors: MIB5 (5'-TGAGCTGGTCATTGCGCATGGT-

Materials and methods

3') and ddMse XI (5'-TAACCATGCGC-3'). Universal primers used in the labeling reaction were directly conjugated with either Cy5 in the case of LIB1 primer [5'-TAGTGGGATTCCTGCTGTCAGT-3'] or Cy3 in the cases of MIB5 primer [5'-TGAGCTGGTCATTGCGCATGGT-3'] (underscores indicate placement of the dye). The labeling PCR was assembled according to the specifications outlined in Table 14. The labeling reaction was run in a MJ thermocycler utilizing settings listed in Table 15. Products were purified using the Amicon Ultra 0.5 System (cut-off size 100 kDa), utilizing the same protocol as in the paragraph 2.2.9.1., and quantified with the NanoDrop ND-1000 instrument (see paragraph 2.2.9.1.).

Table 14. Composition of PCR-based labeling reaction using dye-conjugated primer.

No.	Reagent	Volume
1.	Expand-Long-Template PCR System Buffer 1	5.0 μ L
2.	Cy5-LIB1/Cy3-MIB5 (20 μ M)	6.0 μ L
3.	dNTP mix (10 mM)	1.75 μ L
4.	BSA	0.5 μ L
5.	Expand-Long-Template PCR System Polymerase Mix (5 U/ μ L)	0.75 μ L
6.	PCR-grade H ₂ O	35.5 μ L
7.	Template (undiluted WGA product)	0.5 μ L

Table 15. Conditions of the PCR used for labeling of WGA samples prior to oligonucleotide aCGH.

Step	Temperature	Time	Repetitions
1.	94°C	0:15 min	11x
2.	60°C	0:30 min	
3.	65°C	3:30 min	
4.	94°C	0:15 min	3x
5.	60°C	0:30 min	
6.	65°C	3:30 min + 10 sec/cycle	
7.	65°C	7:00 min	
8.	4°C	for ever	

Materials and methods

2.2.9.2.2. PCR-based labeling using incorporation of dye-conjugated dNTPs (PCR-T2).

WGA products were labeled by PCR in the presence of Cy5 or Cy3 conjugated dCTP and dUTP. Incorporation of the fluorescent dyes using the labeled dNTPs provided the advantage that adaptors flanking each amplicon in the WGA product could be removed prior to the aCGH hybridization, thereby avoiding unspecific cross-hybridization of test sample with reference DNA and oligonucleotide probes on the array. For each sample, two PCR-T2 reactions were run in parallel using the thermal profile outlined in Table 15. Each reaction was composed according to the recipe listed in the Table 16.

Table 16.

Composition of the PCR-based labeling reaction using incorporation of dye-conjugated dNTPs.

No.	Reagent	Volume
1.	Expand-Long-Template PCR System Buffer 1	5.0 μ L
2.	LIB1 (20 μ M)	6.0 μ L
3.	9/10 dNTP mix (10 mM) *	1.75 μ L
4.	Cy5-dCTP/Cy3-dCTP (1 mM)	1.75 μ L
5.	Cy5-dUTP/Cy3-dUTP (1 mM)	1.75 μ L
6.	BSA	0.5 μ L
7.	Expand-Long-Template PCR System Polymerase Mix (5 U/ μ L)	1.5 μ L
8.	PCR-grade H ₂ O	31.25 μ L
9.	Template (undiluted WGA product)	0.5 μ L

* 9/10 dNTP mix comprised dATP, dGTP (10 mM each) as well as dCTP and dTTP (9 mM each)

The resulting PCR products were subjected to digestion with Tru1I restriction endonuclease to cleave off the PCR-adaptors. For this purpose each PCR product was supplemented with 5.6 μ L of 10x Buffer R and 30 U of Tru1I. Digestion was performed at 65°C for 3 hours. Resulting products generated for each individual WGA product were pooled and purified using the Amicon Ultra 0.5 System (100 kDa cut-off) using the same procedure as outlined before for the purification system with 30 kDa cut-off (paragraph 2.2.9.1.). DNA yields and dye incorporation rates were quantified using the NanoDrop ND-1000 Instrument (see paragraph 2.2.9.1.).

2.2.9.3. Array comparative genomic hybridization on oligonucleotide arrays.

Array CGH was performed on oligonucleotide-based SurePrint G3 Human CGH 4x180K microarray slides (catalog design; code 022060) according the protocol provided by the manufacturer (Agilent Oligonucleotide Array-Based CGH for Genomic DNA Analysis, version 7.1, December 2011). Slight modifications were introduced for WGA products processed with the PCR-based labeling approaches. Here, the hybridization mix consisted of 5.0 µg of Cot1-DNA (Roche Diagnostics), 12 µL of 10x Blocking Reagent (Agilent Technologies), 60 µL of 2x Hi RPM Hybridization Buffer, 1% (v/v) of each Tween20 and Igepal, and 19 µL of each test and reference DNA. Hybridization mix was denatured at 95°C for 3 min and subsequently incubated for 30 min on a thermoblock set to 37°C allowing the Cot-1 DNA to block the repetitive DNA sequences in test and reference DNA. Next, corresponding test and reference samples were mixed and subjected to hybridization on oligonucleotide array slides. For each hybridization 100 µL of the hybridization mix was applied on the microarray and hybridized at 65°C for 24 h. Following the hybridization the slides were washed twice for 2:30 min in Oligo aCGH/ChIP-on-Chip Wash Buffer 1 (Agilent Technologies) at room temperature and twice for 30 sec in Oligo aCGH/ChIP-on-Chip Wash Buffer 2 (Agilent Technologies) at 37°C. Washed slides were immersed in acetonitrile to remove all remaining traces of the wash buffers. Finally, each slide was placed in the Agilent Slide Holder and scanned using an Agilent Microarray Scanner Type C using the following settings: Slide ID: <Auto Detect>; Channels: red and green (R + G); Scan region: 61 x 21.6 mm; scan resolution: 3 µm double pass; Tiff: 16 bit; R photo multiplier tube (PMT): 100%; G PMT: 100%; XDR: <No XDR>.

2.2.9.4. Processing and analysis of the aCGH data.

Microarray TIFF image files were processed with the Agilent Genomic Feature Extraction Software (version 10.7) using the standard protocols for aCGH arrays (CGH_107_Sep09). The resulting text files were imported and analysed with Agilent Genomic Workbench Software (version 6.5 Lite). Saturated and non-uniform outlier features were excluded prior to data analysis. Aberrant regions were recognized using ADM-2 algorithm with threshold set to 6.5 for unamplified DNA and 7.0 for WGA samples generated from immunostained cells and FFPE tissue specimens. Centralization algorithm was set to a threshold of 6.0 and bin size of 10. To avoid false positive calls, aberration filters were applied to define the minimum log2 ratio (0.25 for unamplified DNA or WGA products from freshly picked cell and 0.3 for WGA

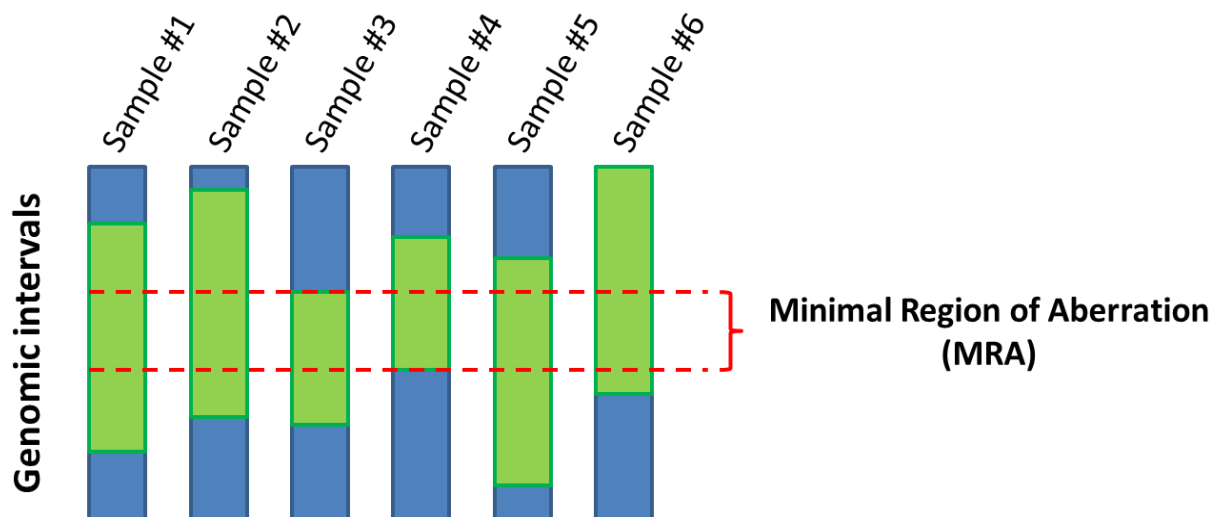
Materials and methods

product from cell subjected to immunostaining) and the minimum number of probes in an aberrant interval (5 for unamplified DNA, 10 for WGA products from fresh picked cells and 30 for WGA products generated from immunostained cells, and FFPE tissue specimens). The microarray data presented in this manuscript has been deposited in Gene Expression Omnibus (GEO) database (accession number: GSE52366).

2.2.9.5. Identification of minimal regions of aberration (MRAs).

MRA refers to the smallest region of genomic copy number alteration shared across an analysed set of aCGH profiles (Figure 5).

Figure 5.



Detection of a minimal region of aberrations.

Scheme depicting exemplary the process MRA detection. Blue bars indicate balanced genomic intervals, whereas green color indicate aberrant regions detected in the tested samples.

2.2.9.6. ROC analysis and hierarchical clustering of the aCGH data.

Accuracy of the new single-cell aCGH assay was assessed using separate ROC curves for gains and losses. To this end, segmentation profiles obtained by the ADM-2 algorithm were binarized according to threshold values (Thr): for gains, values \geq Thr were set to unity or 0 otherwise, for losses: values \leq -Thr were set to unity or 0 otherwise. Reference profiles were binarized according to a fixed threshold of Thr = 0.25, while test profiles were binarized for

different values of Thr. ROC curves were obtained by comparing a reference binarization to test binarizations for different positive threshold values. For clustering, segmentation profiles were discretized according three levels, i.e. values \geq Thr were labeled as gains by 1, values \leq -Thr were labeled as losses by -1, and all other values were labeled by zero. Hierarchical clustering was performed using Euclidean distance and agglomeration by complete linkage. Analyses were done using R [R: A Language and Environment for Statistical Computing, R Core Team, R Foundation for Statistical Computing, Vienna, Austria, 2013, url = <http://www.R-project.org>].

2.2.10. DNA labeling and aCGH hybridization on BAC based microarrays.

2.2.10.1. The design of the BAC aCGH microarrays.

Microarrays manufactured and processed according to the previously published protocol [145] with minor modifications [170]. All BAC clones use to manufacture the arrays were obtained from BACPAC Resources at the Children's Hospital Oakland Research Institute (CHORI). The design included 863 BAC clones representative for chromosome 17 and 368 clones specific for chromosome 6. Both these BAC clone subsets originated from Human Genome High-Resolution BAC Re-Arrayed Clone Collection (the "32k set") providing final tiling-resolution of 46 kb (url = <https://bacpac.chori.org/pHumanMinSet.htm>). Additionally, for the purpose of normalization of the aCGH data, the array design was expanded by addition of 192 BAC clones from the FISH Mapped Clone Collection V1.3., which is a subset of "Human BAC Resource Consortium_1 Set [171]. All the BAC clones were spotted on the epoxide coated slides with 250 μ m spacing between individual spots [170].

2.2.10.2. Labeling of WGA product.

Test and reference sample were labeled by incorporation of dNTPs directly conjugated with cyanine dyes during a PCR based re-amplification of the WGA products. Except for color switch experiments, test samples were labeled with Cy5, whereas Cy3 was incorporated into the reference samples. The PCR was composed and run according to specifications outlined in Table 17 and Table 18, respectively.

Materials and methods

Table 17.

Composition of the labeling reaction prior to hybridization on BAC aCGH microarrays.

No.	Reagent	Volume
1.	10x ThermoSequenase Reaction Buffer	5.0 μ L
2.	LIB1 (100 μ M)	5.0 μ L
3.	9/10 dNTP mix (10 mM) *	2.0 μ L
4.	Cy5-dCTP/Cy3-dCTP (1 mM)	2.0 μ L
5.	Cy5-dUTP/Cy3-dUTP (1 mM)	2.0 μ L
6.	ThermoSequenase (5U/ μ L)	1.0 μ L
7.	PCR-grade H ₂ O	84.0 μ L
8.	Template (undiluted WGA product)	1.6 μ L

* 9/10 dNTP mix comprised dATP, dGTP (each 10 mM) as well as dCTP and dTTP (each 9 mM).

Table 18.

Conditions of the labeling reaction conducted prior to the hybridization on BAC aCGH microarrays.

Step	Temperature	Time	Repetitions
1.	94°C	1:00 min	10x
2.	60°C	0:30 min	
3.	72°C	5:00 min	
4.	4°C	for ever	

Products of the labeling reaction were purified on 1 mL columns filled with Sephadex-G50 [30 g/L in 1xTE Buffer supplemented with 0.1% (v/v) SDS, pH = 8.0]. Next, corresponding test and reference samples were mixed with 80 μ g human Cot1-DNA. Then, following addition of sodium acetate (final concentration 0.3 M) and 2.5 volumes of ethanol, DNA was precipitated over night at -20°C.

2.2.10.3. Hybridization on BAC aCGH microarrays.

The BAC aCGH experiments included in this thesis were conducted as part of the dissertation of Dr. Daniel Will [170].

2.2.10.3.1. Blocking of the microarray slides and denaturation of BAC DNA probes.

Prior to the hybridization of DNA samples BAC microarrays were blocked with a blocking solution #1 composed of 2% (v/v) solution of BSA in 1x SSC buffer; pH = 7.4. Microarray

Materials and methods

slides were immersed in the blocking solution #1 and incubated on an orbital shaker for 30 min at 42°C with a constant stirring rate of 140 rpm. Subsequently, double stranded DNA of the BAC probes was denatured for 10 min at room temperature in 75 mM solution of sodium hydroxide. Afterwards, microarrays were washed three times for 7 minutes (room temperature, 140 rpm) in 2x SSC buffer. Finally, microarray slides were washed for 1 minute (room temperature, 140 rpm) in water and dried by centrifugation at 450g for 2 minutes at room temperature. Next, slides were incubated with blocking solution #2 composed of 250 µg of herring sperm DNA and DNA originating from six negative control WGA products dissolved in 80 µL of the hybridization mix [4 % (v/v) N-lauroylsarcosine, 50 % (v/v) formamide, 8 % (v/v) dextran sulfate in 2x SSC]. As it is assumed that minimal residual amounts of E.coli DNA (contaminating enzymes used in the WGA protocol) are amplified during the WGA, the negative control WGA products were used to block the residual E.coli DNA sequences present in BAC DNA probes spotted on the microarray slides. The blocking solution #2 was applied on the active surface of the microarray slides, which were then sealed with a LifterSlip™ cover slides creating hybridization chamber with 70 µL volume. Subsequently, slides were incubated with the blocking solution #2 for 1 hour at 42°C.

2.2.10.3.2. Hybridization of WGA products on the BAC aCGH microarrays.

After precipitation, labeled DNA samples (obtained in the step 2.2.14.2.) were centrifuged (25000g; 4 °C; 45 min) and the resulting pellets were washed in 800 µL of 70 % (v/v) ethanol. In parallel to the labeled test and reference DNA, six negative control WGA products were precipitated and isolated using the same protocol as for the labeled DNA samples. Following the second round of centrifugation, ethanol was removed and the DNA pellets were dried briefly at 42°C. Next, labeled DNA samples and negative WGA products were resuspended in 40 µL of the Hybridization Mix BAC-array aCGH and mixed on a thermoblock for 1 h at 42 °C with constant stirring at 400 rpm. Subsequently, labeled DNA and negative control WGA products were merged, mixed and heat-denatured for 10 min at 75°C. Thereafter, the samples were incubated for 45 min at 42°C allowing the hybridization of repetitive sequences in the labeled samples with Cot-1 DNA. After the blocking step was completed, the samples were applied on the active surface of the microarray slides, which were then sealed with the LifterSlip™ cover slides (with 70 µL of hybridization volume). The aCGH hybridization was performed for 20 hours in a SlideBooster microarray incubator with temperature set to 42°C and mix/pause intervals set to 3 s/7 s.

2.2.10.4. Washing of the BAC aCGH microarrays.

Following the hybridization the BAC aCGH microarray slides were removed from the Slide Booster microarray incubator and LifterSlip™ 70 µL cover slides were carefully removed. The slides were first washed four times in 1x PBS supplemented with 0.05% (v/v) Tween-20 (5 min, room temperature, 140 rpm) and subsequently three times in 1x SSC (5 min, 60°C, 140 rpm). Following the washing, slides were dehydrated in 70% (v/v) ethanol (1 min, room temperature) and dried by centrifugation at 450g.

2.2.10.5. Scanning of the BAC aCGH microarrays.

The BAC aCGH microarrays were scanned using the GenePix® microarray scanner 4400A and GenePix Pro 7 software. The device collected fluorescent signal intensities of Cy3 and Cy5. The PMT settings were selected automatically to assure optimal overlap over the signal intensities in both channels and assure a maximum of 5% of saturated features. Additionally, to minimize the noise of the hybridization, each location on the slide was scanned three times (lines to average = 3). The resulting images were saved in TIFF format.

2.2.10.6. Analysis of the BAC aCGH microarrays.

The following evaluation steps were conducted only for BAC clones representative for chromosome 17. TIFF files generated after scanning were first processed with GenePix Pro 7 software. Herewith, normalized background corrected fluorescence intensity values were quantified. Subsequently, M- (Equation 3) and A-values (Equation 4) were calculated for each feature

Equation 3. Computation of the M-value.

$$M - value = \ln \frac{FI_{Cy5}}{FI_{Cy3}}$$

FI_{Cy5} – background corrected normalized fluorescence intensity of Cy5.

FI_{Cy3} – background corrected normalized fluorescence intensity of Cy3.

Equation 4. Computation of the A-value.

$$A - value = 0.5 \times \ln (FI_{Cy5} \times FI_{Cy3})$$

All features with overall low intensity (A-value < 2) were excluded from further evaluation. Subsequently, whenever possible, mean M-values were calculated for replicate features. Additionally, M-values were normalized by setting the variance of the M-value spread to 0 and mean value to 1. The profiles were corrected for the WGA-associated bias by subtraction of mean Cy5/Cy3 ratio values generated across ten independent single-cell aCGH experiments performed using cells of healthy donors. Thereafter, mean normalized M-values computed for each feature were plotted against the physical position in the human genome of the corresponding BAC clone. The data was smoothened using the Savitzky-Golay filter.

2.2.11. Single-cell quantitative PCR (qPCR) assay for detection of genomic gains in ERBB2 locus.

Detection of genomic gains at the ERBB2 locus was conducted with the use of a qPCR-based approach (Pasch S. et al., manuscript in preparation). For each single-cell WGA product three amplicons in the target locus (ERBB2) and six reference loci (ATGR, CACNA, GZMB, RUFY2, OPN1SW and SMYD1; one amplicon for each locus) were quantified with LightCycler® 480 System using SYBR Green detection system. 100x diluted aliquots of the original WGA product were used as template for the qPCR. All reactions were conducted in duplicates and the resulting crossing point (Cp) values were computed with the LightCycler 480 software (v 1.5.0). Samples with three or more unsuccessful measurements (crossing point > 30) for the reference loci or at least two unsuccessful measurements of the target locus were excluded from further evaluation. For each target/reference pair (18 pairs in total) relative locus ratio was computed (**Equation 5**).

Equation 5. Computation of calibration normalized efficiency corrected relative locus ratio.

$$\text{Relative Locus Ratio} = \frac{(E_{reference})^{Cp_{sample}}}{(E_{target})^{Cp_{sample}}} \div \frac{(E_{reference})^{Cp_{calibrator}}}{(E_{target})^{Cp_{calibrator}}}$$

E – Efficiency of the PCR

Cp – Crossing point

The further steps of data evaluation were programmed and conducted in R programming language (R Development Core Team: R: A Language and Environment for Statistical Computing. Vienna, Austria, 2008). For the assessment of the data, an additive model based on median polish algorithm was used [172], which was trained with a collective of single-cell WGA products obtained from healthy individuals. Using this approach sample specific qPCR measurement was calculated for each single-cell WGA product. The mean and standard deviation of the qPCR values (relative locus ratios) was used to compare its distribution between the training cell collective and tested cells, thereby allowing to calculate the amplification probability for each tested cells. The amplification probability was computed using *pnorm* function implemented in R. Amplification of the ERBB2 locus were called if the amplification probability was greater than 0.95.

2.2.12. Statistical analysis.

The outcome of the PCR-T1 and PCR-T2 reactions (DNA yield, signal to noise ratios and intensity of fluorescent signals) were compared using the two-tailed unpaired Student's t-test. The p-values (P) were calculated using an online t-test calculator ([url = http://www.graphpad.com/quickcalcs/ttest1/](http://www.graphpad.com/quickcalcs/ttest1/)). In each comparison, the difference between the values was considered as statistically significant if p-value was lower than 0.05.

3. Results.

The result section is subdivided into three parts: (i) description of steps undertaken to establish a new single-cell aCGH protocol (3.1.), (ii) performance assessment of the new workflow (3.2.) and (iii) exemplary demonstration of the utility of the new method for the analysis of single DCCs of cancer patients (3.3.).

3.1. Development of a new single-cell aCGH assay.

3.1.1. Optimization and validation of new DNA labeling approaches customized for the processing of SCOMP WGA products.

Uniform labeling of test and reference samples is crucial for the success of aCGH analysis. Taking into consideration the underlying principle of SCOMP, it was speculated that the most optimal labeling will be achieved when using a PCR-based approach. This way, all the amplicons comprised in a single-cell SCOMP genomic representation should be effectively and comprehensively labeled. To this end, two different PCR-based DNA labeling methods were developed, both using the same universal primer as used in the SCOMP WGA protocol. The first PCR-based labeling technique (PCR-T1) utilized directly conjugated oligomers as PCR primers, allowing incorporation of fluorescent dyes into the adaptor sequences flanking each amplicon in the WGA representation (Figure 4A). This allows uniform labeling of each amplicon, regardless of its size. The second PCR-based approach (PCR-T2) incorporated dye conjugated nucleotides into the WGA products (Figure 4B). This technique, although prone to preferentially label longer amplicons, permits removal of the PCR-adaptor sequences, whose presence could interfere with the subsequent aCGH hybridization. The accuracy and reliability of PCR-T1 and PCR-T2 were tested on PT1590 esophageal cancer cell line cells [92], which are known to harbour a complex pattern of copy number alterations (CNAs) including amplification of the ERBB2 locus on chromosome 17q21 [21,173]. Four single cells, three cells from PT-1590 cell line and one from a healthy female donor were isolated and subjected to SCOMP. Additionally, four cell pools (approximately 100-1000 cells), three from PT-1590 cell line and one from healthy donor, were processed with the identical protocols as the single cells and used as controls. The resulting WGA products were subjected to aCGH hybridization on Agilent SurePrint G3 Human 4x180k arrays. Fluorimetric analysis of the DNA labeling products revealed that PCR-T1 enabled more efficient incorporation of the fluorescent dyes, whereas PCR-T2 provided consistently higher DNA yields (Table 19).

Results

Table 19.

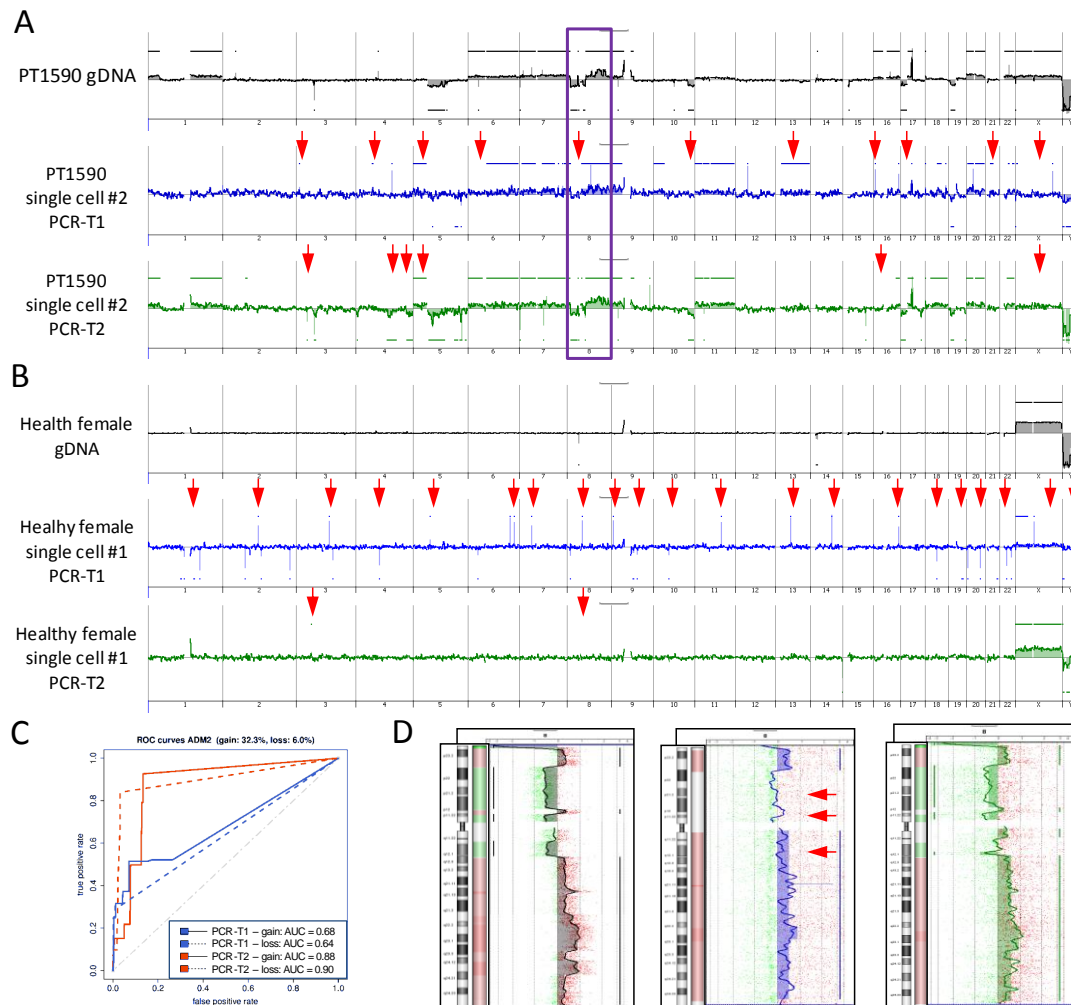
	Cell Pool			Single Cell		
	PCR-T1	PCR-T2	Student's t-test	PCR-T1	PCR-T2	Student's t-test
Test DNA (cell pool/single cell) [μg]	4.1 (0.1)	13.4 (1.0)	p=0.003	5.2 (0.6)	15.8 (1.1)	p<0.0001
Reference DNA (cell pool) [μg]	4.6 (0.2)	14.1 (1.6)	p<0.0001	N/A	N/A	N/A
Dye Incorporation Test (Cy5) [$\frac{pMol(Dye)}{\mu g(DNA)}$]	58.2 (12.9)	9.0 (2.2)	p=0.0011	44.6 (3.5)	12.4 (2.1)	p<0.0001
Dye Incorporation Reference (Cy3) [$\frac{pMol(Dye)}{\mu g(DNA)}$]	60 (5.6)	6.9 (1.5)	p<0.0001	N/A	N/A	N/A
Signal Intensity - Red (Cy5) [FU]	194.3 (28.6)	999.6 (150.1)	p=0.0021	189.8 (118.3)	1586.1 (434.3)	p=0.0025
Signal Intensity - Green (Cy3) [FU]	42.0 (6.3)	316.2 (96.2)	p<0.0001	N/A	N/A	N/A
Signal-to Noise Ratio - Red (Cy5)	2.3 (1.0)	49.6 (24.1)	p=0.0591	2.9 (2.3)	53.8 (10.4)	p=0.0002
Signal-to-Noise Ratio - Green (Cy3)	1.9 (0.6)	55.8 (21.8)	p=0.0003	N/A	N/A	N/A

Hybridization characteristics of samples processed with PCR-based DNA labeling techniques (PCR-T1 and PCR-T2).

For all the variables average values and standard deviation (values in parentheses) are indicated in the table. The values obtained for PCR-T1 and PCR-T2, respectively, were compared using the two-tailed Student's t-test. Corresponding p-values are indicated. N/A – not assessed, as only cell pools were used as reference samples. FU – fluorescence units.

More importantly, samples processed with PCR-T2 provided higher signal intensities and lower signal-to-noise ratios following the aCGH hybridization indicating better performance of the method in the aCGH experiments. To determine true positive CNAs, resulting aCGH profiles of single-cell WGA products were compared to the corresponding profile generated by using unamplified genomic DNA of PT-1590 cells. In all specimens tested, single-cell aCGH profiles generated following the PCR-T1 labeling were less concordant to unamplified DNA than corresponding profiles generated using PCR-T2 (Figure 6 A-B). Higher accuracy of the latter approach was confirmed in the subsequent analysis of ROC curves (Figure 6C). Direct comparison bulk DNA revealed that multiple genomic alteration present in the bulk DNA were detectable in single-cell WGA products only upon utilization of PCR-T2 (Figure 6D). It was speculated that the poorer sensitivity of aCGH following the PCR-T1 is associated with the unspecific hybridization of the adaptor sequences to the probes on the array. This would particularly affect short amplicons, i.e. shorter than <100 bp, where PCR adaptors comprise a significant part of the amplification product. To minimize the bias introduced by the unspecific hybridization of the PCR-adaptor sequence, 100x or 1000x excess of unlabeled complementary oligonucleotides were added into the hybridization mix. This intervention, however, gradually decreased the sensitivity and the reliability of the method by abrogating the detection of otherwise detectable alterations and resulted in introduction of artefacts (Figure 7). Consequently, due to poorer sensitivity of the aCGH the use of PCR-T1 was discontinued and PCR-T2 became the method of choice for the DNA labeling of WGA products.

Figure 6.



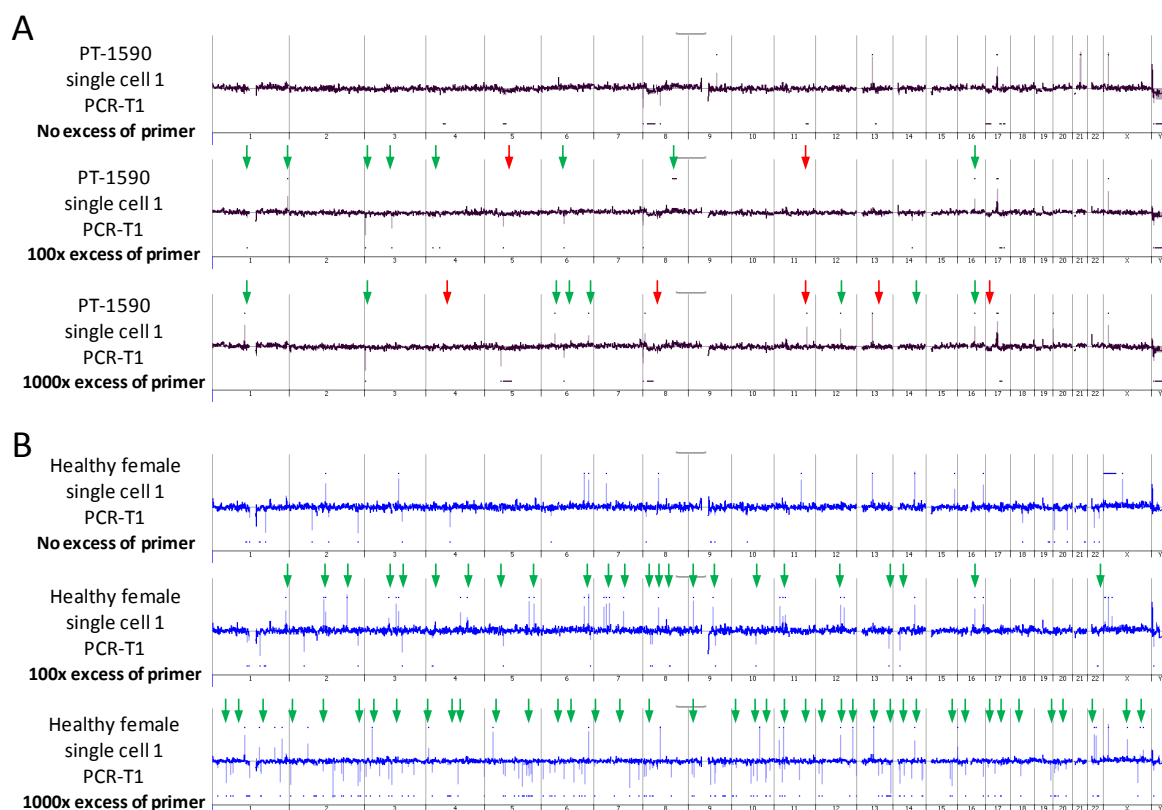
Selection of best performing PCR-based labeling technique.

A,B) Exemplary horizontal aCGH profiles of PT-1590 oesophageal cancer cells (A) or healthy female donor (B). Unamplified gDNA (upper panel) was used as benchmark and compared with the corresponding results obtained with a single-cell WGA product processed with either PCR-T1 (middle panel) or PCR-T2 (lower panel). All samples were hybridized against DNA samples (cell pool WGA products) originating from a healthy male. Deviations between the aCGH profiles of unamplified gDNA and single-cell WGA products are indicated by red arrows. X-axis genomic position. Y-axis \log_2 ratio of the normalized fluorescence values obtained for test and reference samples. DNA gains and losses are indicated by positive and negative \log_2 ratio values, respectively.

C) ROC-curves comparing the accuracy of single-cell aCGH upon application of PCR-T1 (blue lines) and PCR-T2 (red lines) on a single-cell WGA product depicted in panel A. Accuracy of detection of DNA gains and losses are depicted separately with solid and dashed lines, respectively. ROC analysis was performed based on the genome-wide patterns of CNAs with unamplified gDNA of PT-1590 cells used as reference. A larger area under the curve (AUC) indicates higher accuracy of the method.

D) Vertical aCGH profiles of chromosome 8 of PT-1590 cells (placed in violet bracket in panel A) generated with unamplified DNA (left panel) and single-cell WGA products processed with either PCR-T1 (middle panel) or PCR-T2 (right panel). Arrows indicate genomic loci falsely recognized as balanced in the sample subjected to PCR-T1 protocol. Genomic gains and losses are marked with red and green color, respectively, on the ideograms depicted on the left side of each panel. Discrepancies in the aCGH profiles are indicated with red arrows.

Figure 7.



Blocking the hybridization of PCR-adaptor sequences present in the products of PCR-T1 DNA labeling.

A, B) Horizontal aCGH profiles depicting single-cell WGA product of a PT-1590 cell (A) or a healthy female donor processed with PCR-T1. Hybridization of the PCR-adaptor sequences on the aCGH probes was blocked by the addition of 100x or 1000x excess of the unlabeled complementary DNA oligomere. Green arrows indicate false positive CNAs introduced by the addition of unlabeled primer sequences, whereas red arrows show genomic loci at which true positive CNAs were falsely classified as balanced intervals.

3.1.2. Comparison of the PCR-T2 approach with the random primed isothermal amplification DNA labeling system (RP labeling).

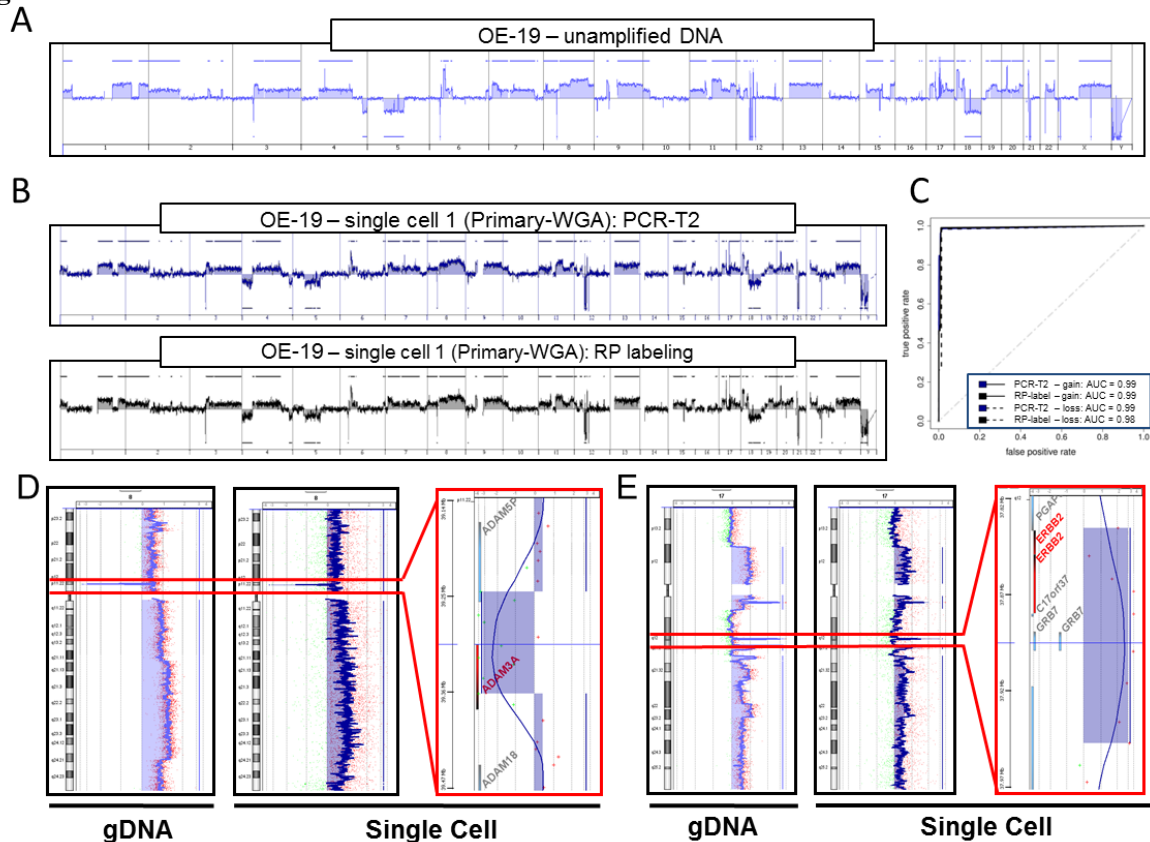
3.1.2.1. Analysis of freshly isolated, unfixed cells.

DNA labeling based on random primed isothermal amplification is the widest used system in two-color aCGH experiments. This system utilizes Klenow fragment of the *Escherichia coli* DNA polymerase I, which following the priming of random octamers facilitates incorporation of modified nucleotides into the target DNA [174]. In the past, this system already has been successfully applied to label single-cell WGA products [136-139,150,152,153,156,175,176]. In a recent publication Möhlendick and co-workers demonstrated that combined use of SCOMP with RP-labeling allows detection of CNAs in single cells with resolution of 100 kb

Results

or less [146]. This protocol was directly compared with the PCR-T2 to stringently test the performance of the newly developed DNA labeling technique. To this end, freshly picked single cells of OE-19 esophageal cancer cell lines were subjected to SCOMP and subsequently processed in parallel by both PCR-T2 and RP-labeling. The OE-19 cell line is known to harbour complex patterns of genomic aberrations including focal homozygous DNA loss of ADAM3A locus (0.1 Mb in size) on chromosome 8 and amplification of ERBB2 locus (0.1 Mb in size) on chromosome 17 (<http://www.broadinstitute.org/ccle/home>) [177].

Figure 8.



Comparison of PCR-T2 with RP-labeling on cell line cells.

A, B) Horizontal aCGH profiles of OE-19 cells generated using unamplified gDNA (A) or single-cell WGA products processed with either PCR-T2 (B, upper panel) or RP-labeling (B, lower panel).

C) ROC-curves assessing the accuracy of the single-cell aCGH upon using PCR-T2 (blue lines) and RP-labeling techniques (black lines). Genome-wide pattern of CNAs of single-cell WGA products was compared against the aCGH results generated with unamplified gDNA of OE-19 cells. Area under the curve (AUC) corresponds to the accuracy of the assay.

D, E) Vertical aCGH profiles of chromosome 8 (D) and chromosome 17 (E) of OE-19 cells. Left and middle panel depicts aCGH profiles generated using unamplified gDNA and single-cell WGA products labeled using PCR-T2, respectively. Right panel displays a graphical magnification of the loci in which CNAs were recognized.

Regardless, of the labeling approach used, aCGH profiles of single OE-19 cells were highly concordant with the results obtained with unamplified bulk genomic DNA (Figure 8 A-C). Significantly, in both cases both labeling techniques allowed reliable and reproducible detection of CNAs as small as 100 kb (Figure 8 D-E). This indicated that PCR-T2 and RP-

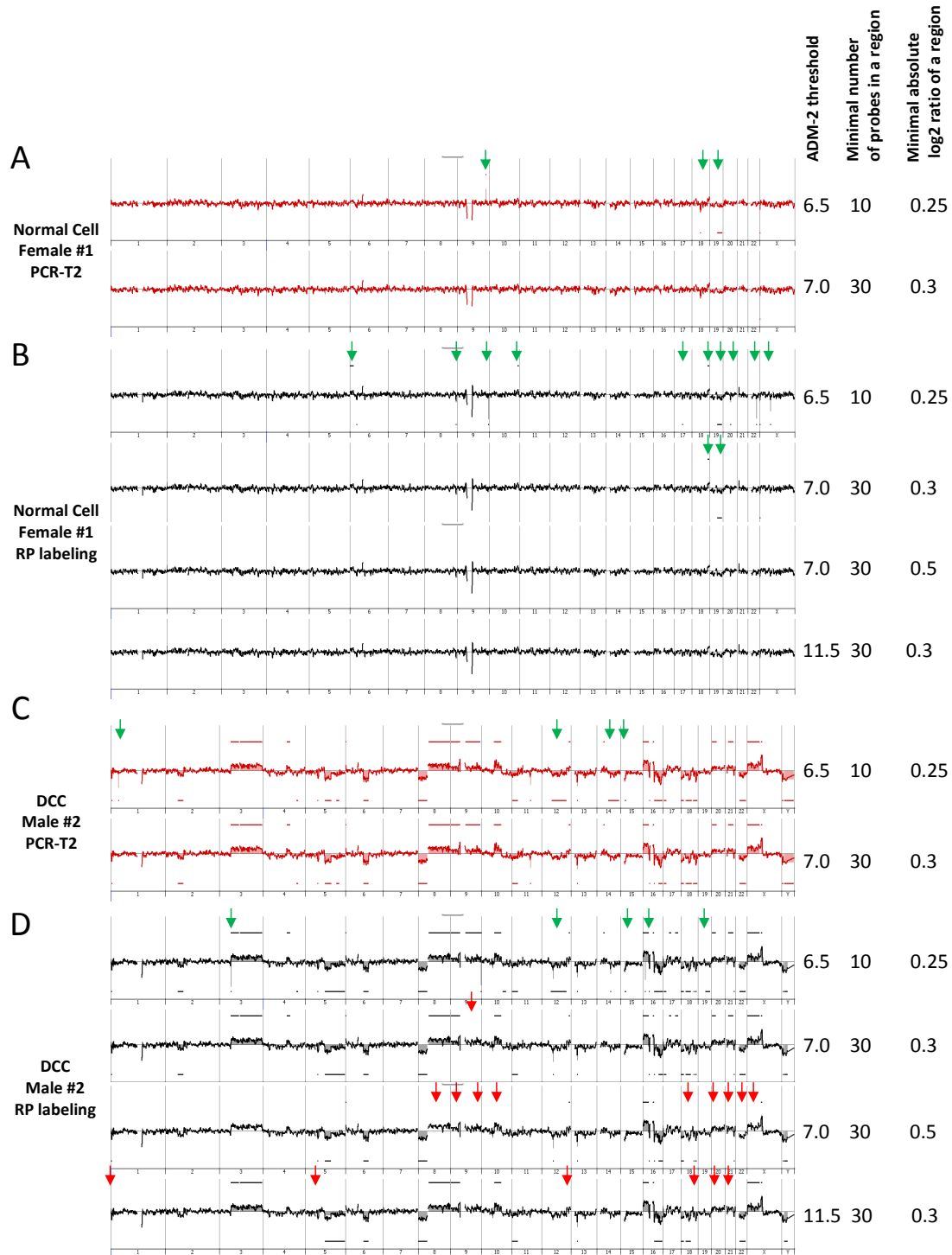
labeling are equally reliable for the detection of CNAs in single-cell WGA products generated from freshly isolated, unfixed material.

3.1.2.2. aCGH analysis of cells after immunostaining.

Detection of DCCs is typically conducted with the use of immunostaining assays targeting epithelial markers e.g. CKs 8/18/19 [178]. These protocols comprise the use of fixative agents, e.g. paraformaldehyde, that negatively affect the quality of single-cell DNA. Consequently, the analytic workflows used for the analysis of DCCs must be highly resistant to bias introduced during the course of sample processing. To determine the most robust workflow for immunostained cells both RP-labeling and PCR-T2 were applied on DCCs from two prostate cancer patients. Additionally, single cells from the peripheral blood of five healthy donors (three females and two males) were isolated and used as controls. Since leukocytes of healthy individuals do not express CKs, these cells were stained for vimentin utilizing the same immunocytochemistry staining protocol as used for detection of DCCs. Following the immunostaining, single marker positive cells were picked and subjected to WGA and subsequently analysed by aCGH. Analysis of the aCGH profiles of control cells revealed in all tested samples presence of focal shifts of log₂ ratio values manifested as both DNA gains and losses ranging from 0.1 to 20.7 Mb in size (Figure 9 A-B). Since their distribution was random and their detection was independent of the DNA labeling protocol used, these aberration calls were classified as artefacts. To prevent their detection, the standard settings for the alteration detection algorithm (ADM-2) and the minimum absolute log₂ ratio of aberrant regions were modified to 7.0 and 0.3, respectively (Figure 9 A-B). Since the average length of detected artificial CNAs was longer in samples processed with the RP labeling (Student's t-test $P < 0.05$), modification of the aberration filter proved to be more effective for specimen subjected to the PCR-T2 labeling (Figure 9 A-B). Elimination of artefacts generated by the RP-labeling required the use of high threshold values for the absolute average log₂ ratios of aberrant regions (>0.5) or the ADM-2 aberration algorithm (>11.5). However, this strongly reduced sensitivity of the assay (Figure 9 C-D). Due to the discrepancies in the sensitivity of the single-cell aCGH assay depending on the DNA labeling technique used, the use of RP-labeling was abandoned and PCR-T2 was utilized for all further aCGH experiments involving single-cell WGA products.

Results

Figure 9.



Comparison of PCR-T2 with RP-labeling on prostate cancer DCCs and lymphocytes of healthy donors.

A-B) Horizontal aCGH of a single-cell WGA obtained from a control cell (vimentin positive) of a healthy female donor processed with PCR-T2 (A) or RP-labeling (B). Analytical settings were varied to allow elimination of false positive CNAs.

C-D) Horizontal aCGH of a single-cell WGA generated from a DCC of a prostate cancer patient and subjected to PCR-T2 (C) or RP-labeling (D).

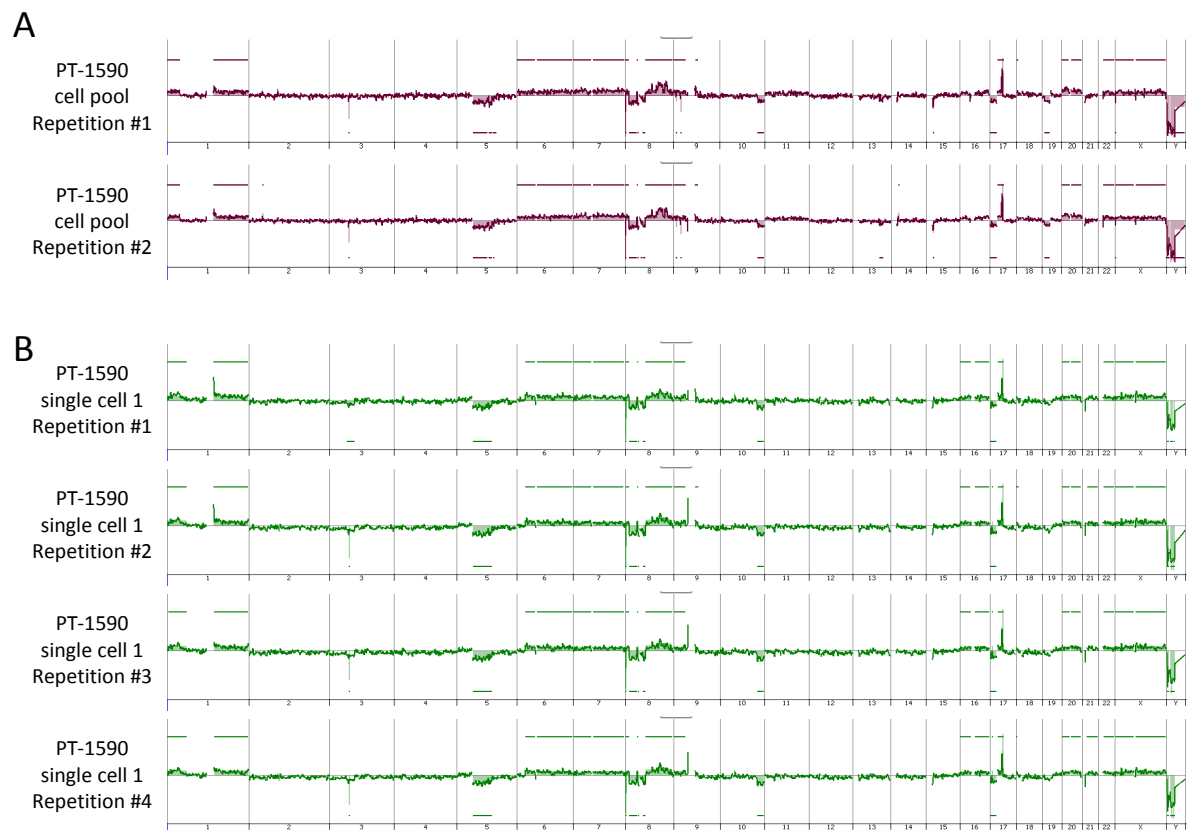
Green arrows indicated artificial alterations detected in single-cell WGA products, whereas red arrows show CNAs which escaped detection upon adjustment of the analytical settings to remove the artificial aberration calls.

Results

3.1.3. Reproducibility of the single-cell aCGH analysis.

Reliable assays designated for the analysis of clinical patient material should provide highly reproducible data. To assess the reproducibility of the single-cell aCGH assay, WGA products of PT-1590 cell, were repeatedly hybridized on aCGH arrays as technical replicates. Repeated hybridization of single-cell WGA products processed with PCR-T2 gave highly reproducible results, with the correlation coefficient (c_{xy}) of log2 ratios across different experiments ranging from 0.897 to 0.948 (Figure 10).

Figure 10.



Reproducibility of the single cell aCGH assay using PCR-T2 labeling approach.

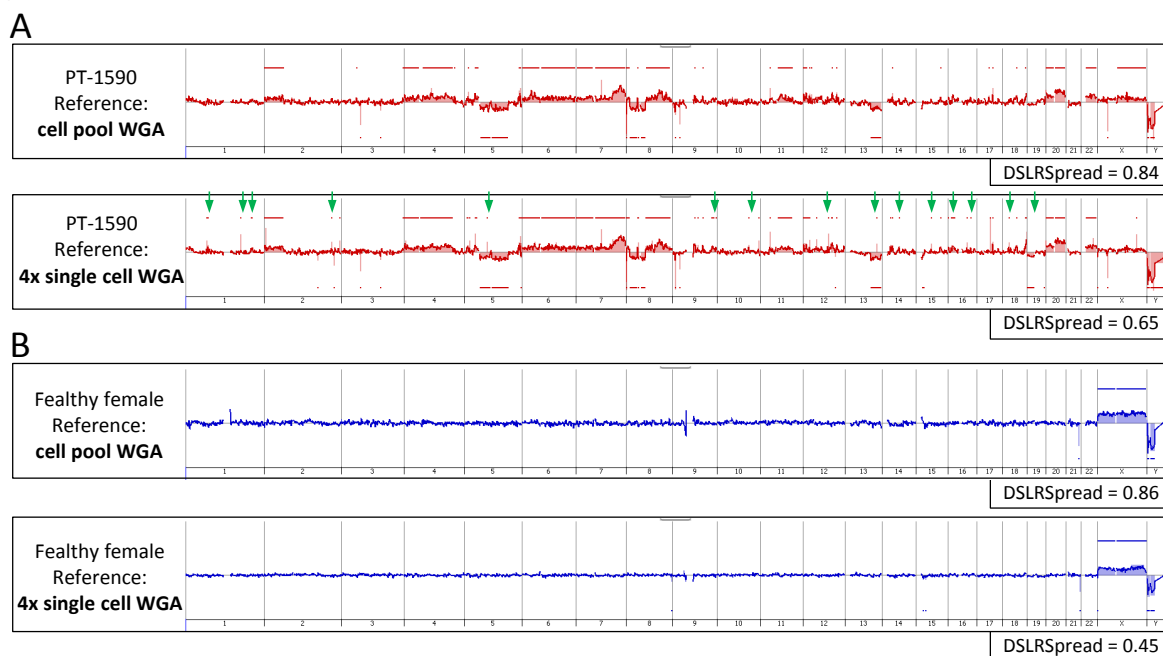
A,B) Horizontal aCGH profiles of WGA products generated using either cell pool (A) or single-cell (B) WGA products of PT-1590 oesophageal cancer cell line cells. Each profile represents a technical replicate of an aCGH experiment.

Results

3.1.4. Selection of the best performing type of reference sample.

The applied reference sample is a crucial component of every aCGH experiment. Since CGH compares the relative amounts of DNA in the two samples, i.e. test and reference, aberrance in DNA quantity or quality between test and reference sample may introduce systematic bias, thereby making the detection of CNAs unreliable. For this reason two types of samples were tested for their applicability as reference in single-cell aCGH experiments: (i) WGA products generated from cell pools (approximately 100-1000 cells) and (ii) samples obtained by pooling four independently amplified single-cell WGA products. In both cases, cells were collected from the mononuclear fraction of peripheral blood of healthy male or female donors. Both types of references were used in subsequent aCGH experiments and hybridized against single-cell WGA products of PT-1590 cell lines or a healthy female donor. Direct comparison of the resulting aCGH profiles revealed that derivative log₂ ratio spread (DLRS) values, a measurement of hybridization noise, were consistently higher in testing series using cell pool WGA product as reference DNA compared to experiments utilizing reference samples consisting of amplified single-cell DNA (average DLRS 0.85 and 0.55, respectively, Figure 11).

Figure 11.



Selection of the best performing reference DNA sample.

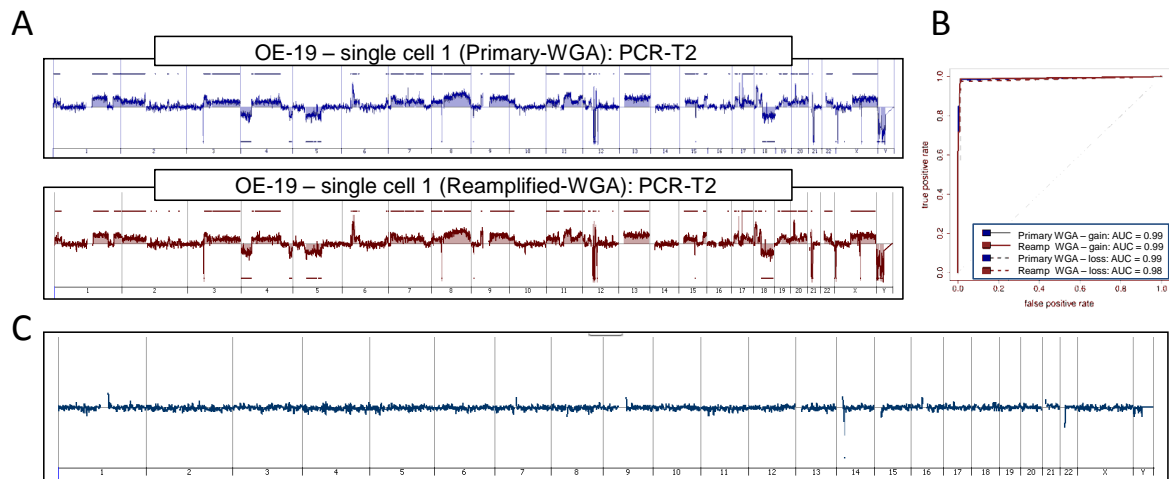
A, B) Horizontal aCGH profiles of single-cell WGA products generated with either a PT-1590 cell (A) or a cell isolated from a healthy female donor (B). Test samples were hybridized against either WGA products generated from cell pool (upper panels) or a pool of four single-cell WGA products (lower panels). Green arrows indicate CNAs detected exclusively upon utilization of single-cell WGA products as reference DNA.

Reduced level of technical noise of the hybridization upon application of reference samples consisting of single-cell WGA product enabled detection of additional CNAs which otherwise would remain undetected when cell pool based reference was utilized (Figure 11). As a consequence all subsequent experiments included a pool of four single-cell WGA products originating from one healthy individual as a reference sample.

3.1.5. Suitability of re-amplified single-cell WGA product for high resolution aCGH .

WGA techniques provide sufficient amounts of DNA material for multiple downstream analysis. Nevertheless, the yield of each WGA is limited, which may preclude some high-throughput analyses, e.g. whole genome sequencing, where large amount of input material is needed. One of the ways to increase the DNA yield originating from a single-cell is to subject the primary WGA to a second round of amplification (re-amplification). PCR-based WGA approaches utilizing non-degenerated primer during the exponential phase of amplification, e.g. SCOMP, GenomePlex, PicoPlex and MALBAC, enable comprehensive re-amplification of the entire single-cell genomic representation. However, the additional round of amplification may introduce bias into the original sample representation noticeable as e.g. false positive CNAs in the aCGH analysis. To exclude the introduction of artificial CNAs by the second round of WGA amplification, primary WGA products need to be directly compared with the re-amplified counterparts. For this purpose, single-cell WGA products originating from OE-19 cells or from healthy donors were analysed by aCGH. The aCGH profiles generated with re-amplified single-cell WGA products showed a high level of concordance with the corresponding results obtained with unamplified DNA (Figure 12A). Subsequent ROC analysis confirmed highly accurate detection of CNAs in OE-19 cells with the use of re-amplified WGA products (Figure 12B). Moreover, re-amplified single-cell WGA products obtained from healthy donors showed balanced aCGH profiles (Figure 12C). This indicates that second round of amplification does not introduce significant amplification bias into the original DNA representation and its use does not affect the outcome of the aCGH analysis. For this reason, all subsequent aCGH experiments were constricted to re-amplified WGA products only.

Figure 12.



Suitability of re-amplified WGA products for single-cell aCGH.

A) Horizontal aCGH profiles of primary (upper panel) or re-amplified WGA products (lower panel) of a single OE-19 cell.

B) ROC curves comparing the accuracy of the single-cell aCGH assay after analysis of primary (blue lines) and reamplified WGA products (brown lines). Corresponding aCGH profiles are depicted in panel A. Genome-wide pattern of CNAs of single-cell WGA products was compared against the aCGH products generated with unamplified gDNA of OE-19 cells. Area under the curve (AUC) corresponds to the accuracy of the assay.

C) Horizontal aCGH profile of a healthy male donor hybridized against male reference DNA.

3.2. Performance of the high-resolution single-cell aCGH assay.

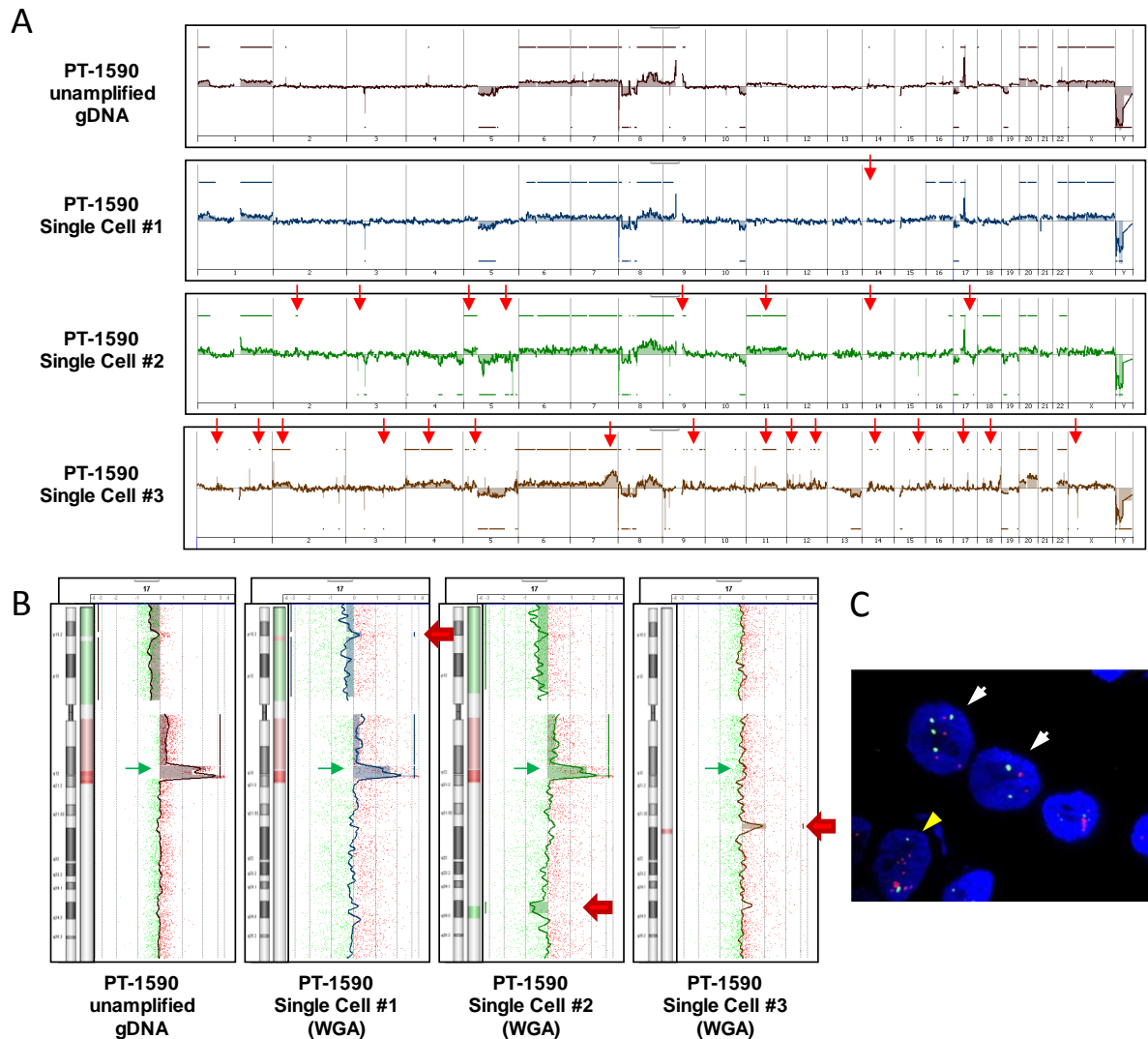
3.2.1. Detection of genomic heterogeneity between individual cells.

High level of genomic diversity is considered as the hallmark of benign tumor lesions, which enables the selection of cells or cellular clones bearing the most aggressive phenotype leading to malignant progression of the disease [97]. Unravelling the evolution of early tumor lesions is dependent on the sensitivity of the method used to assess the extent of genomic diversity within the sampled specimens. These, have to be able to reliably detect genomic discrepancies between tumor cell clones or, ideally, distinguish between individual tumor cells. To this end it was important to validate the ability of the new single-cell aCGH assay to detect genomic heterogeneity at the single-cell level. Previous studies have shown that at the single-cell level PT-1590 oesophageal cancer cells show detectable genomic heterogeneity [92,173]. Therefore, previously generated single-cell aCGH datasets (see sections 3.1.1., 3.1.3. and 3.1.4) were reanalysed, in an attempt to identify genomic discrepancies between the individual PT-1590. Subsequent analysis showed that the majority of detected genomic aberrations were common to all of the samples, e.g. DNA gains of chromosome 6 and 7, DNA

Results

loss of chromosome 5q11.2-5q14.2 as well as complex pattern of gains and losses on chromosome 8 (Figure 13A). However, some aberrations, e.g. DNA gain on chromosome 17p13.1 in single-cell 1, DNA loss of chromosome 17q24.3-25.1 in single-cell #2 and DNA gain on chromosome 17q22 in single-cell #3, were present only in individual cells but not in the bulk genomic DNA (Figure 13B).

Figure 13.



Detection of single cell heterogeneity.

A) Horizontal aCGH profiles generated using either unamplified gDNA or single-cell WGA products of PT-1590 cells. Red arrows show genomic loci at which the single-cell WGA profiles diverged from the results obtained for unamplified genomic DNA.

B) Magnified vertical aCGH profiles of chromosome 17 of samples presented in the panel A. Red arrows indicate discrepancies in the aCGH profiles of single PT-1590 cells and green arrows indicated localization of the ERBB2 locus.

C) Representative FISH images of PT1590 cells. Red signals indicate ERBB2 locus and green CEP17. White arrows label cells with balanced copy number of ERBB2 vs. CEP17. Yellow arrowhead shows cells with high-level amplification of the ERBB2 locus.

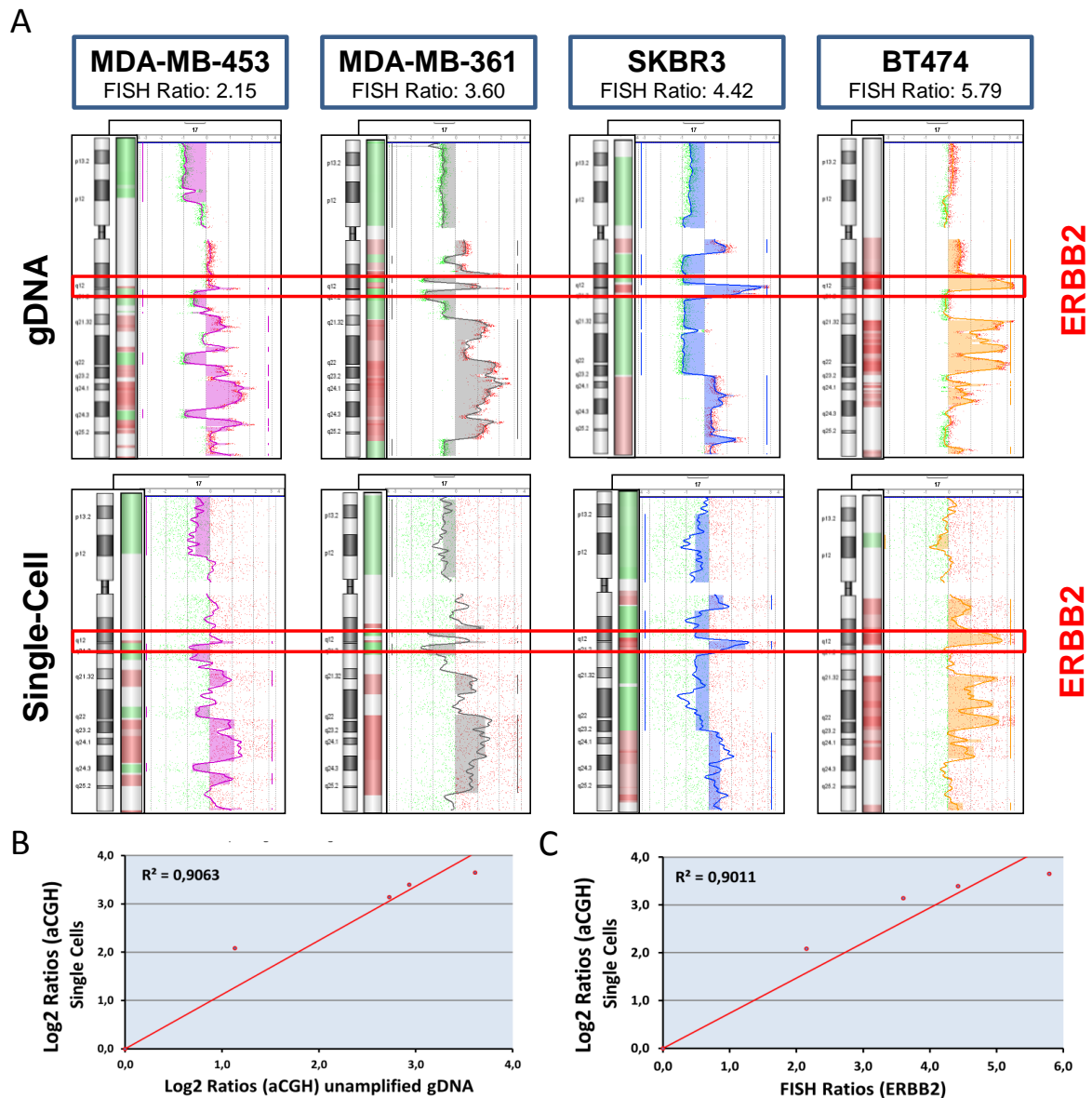
Despite previous reports indicating the relevance of the ERBB2 amplification in the PT-1590 cells [21], one out of three tested PT-1590 cells did not harbour this alteration (Figure 13B). To exclude artificial character of this observation, PT-1590 cells were analysed by FISH targeting centromere of chromosome 17 as well as ERBB2 locus, showing that 10% of PT-1590 cells display balanced copy number of the ERBB2 locus (Figure 13C). Thus, CNAs detected in the individual cells but not the bulk DNA could represent true positive alterations that affect only these particular cells or small cellular subfractions and thereby remained undetectable for the standard aCGH analysis.

3.2.2. Quantitative assessment of CNAs in the single cells.

It is expected that a reliable assay for the assessment of CNAs in single-cell will be able to accurately quantify the level of copy number changes of a given loci. For this reason, the new single-cell aCGH assay was tested for its precision to quantify various levels of copy number changes. To this end, bulk DNA and single-cell WGA products from a panel of four breast cancer cell lines (MDA-MB-453, MDA-MB-361, SK-BR-3 and BT-474) were tested for accuracy of the copy number assessment at the ERBB2 locus. With FISH ratios of ERBB2 to CEP17 ranging from 2.15 to 5.79, each cell line included in the analysis represented a different copy number of the ERBB2 locus (Figure 14A). The average log2 ratios of probes specific for ERBB2 locus obtained in single-cell experiments were extracted and correlated with the corresponding values acquired from the unamplified DNA and the ratios of ERBB2 to CEP17 obtained in the FISH experiments (Figure 14 B-C). In both comparisons, single-cell aCGH vs. standard aCGH and single-cell aCGH vs. FISH, the measures of the ERBB2 copy number were highly convergent showing Pearson's correlation coefficient of 0.99 and 0.94, respectively (Figure 14 B-C). This shows that in the copy number range of 2 to 10 copies, single-cell aCGH workflow allows accurate quantitative assessment of CNAs.

Results

Figure 14.



Quantitative assessment CNAs by the new single-cell aCGH assay.

A) Vertical aCGH profiles of chromosome 17 of four breast cancer cell lines (MDA-MB-453, MDA-MB-361, SKBR3 and BT474) with increasing copy number of ERBB2 locus (FISH ratio 2.15, 3.60, 4.42 and 5.70, respectively) generated using unamplified DNA (upper row) or single-cell WGA products (lower row). Red brackets indicate the position of the ERBB2 locus. Corresponding FISH ratios (ERBB2 vs. CEP17) of all cell lines are indicated in blue brackets.

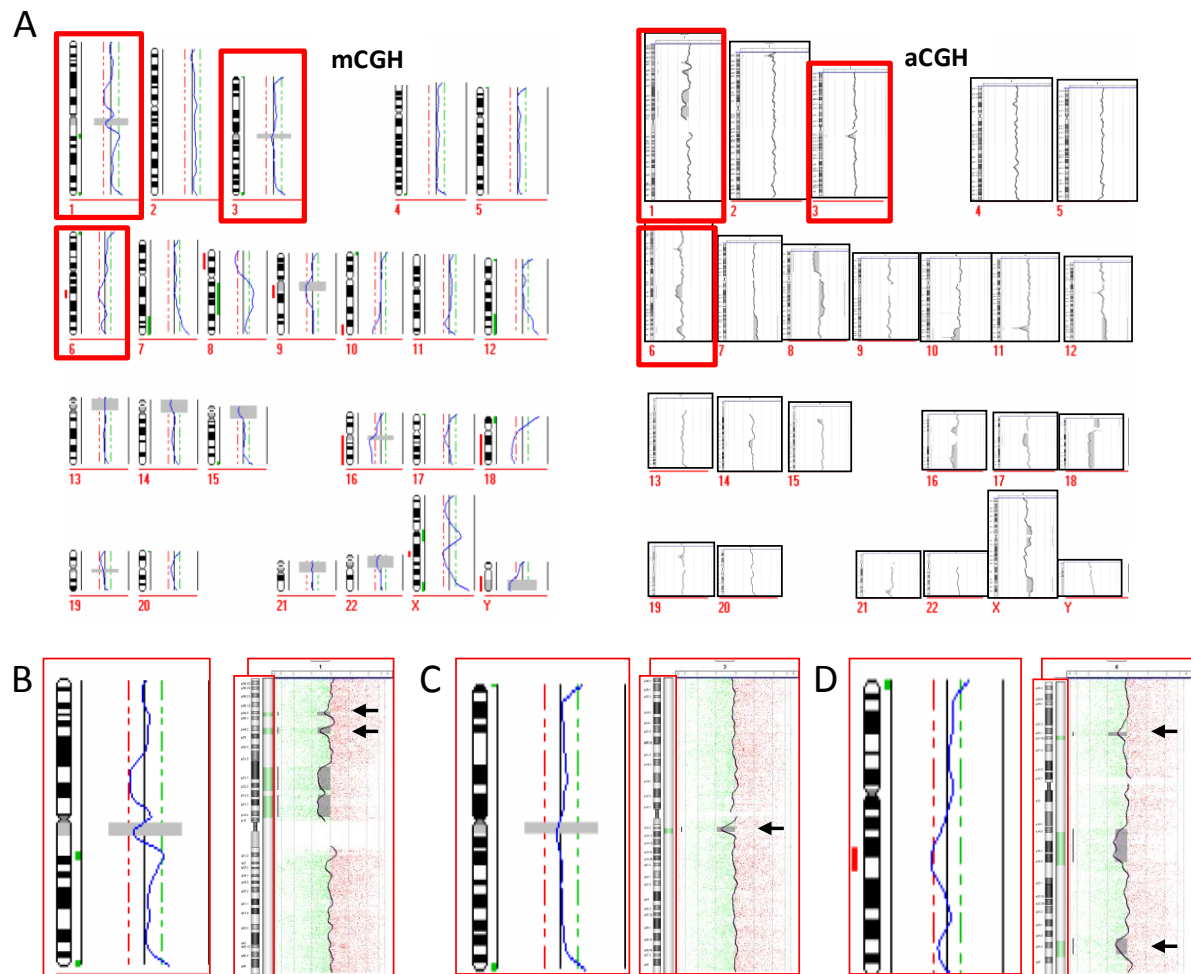
B) Correlation of average log2 values of aCGH probes specific for ERBB2 locus obtained in single-cell aCGH experiments (Y-axis) vs. corresponding values obtained with unamplified DNA (X-axis). DNA samples from four breast cancer cell lines (MDA-MB-453, MDA-MB-361, SKBR3, BT474) have been included in the analysis. Pearson's correlation coefficient = 0.99.

C) Correlation of average log2 values of aCGH probes specific for ERBB2 locus obtained in single-cell aCGH experiments (Y-axis) vs. FISH ratios (ERBB2/CEP17) calculated for four breast cancer cell lines: MDA-MB-453, MDA-MB-361, SKBR3, BT474. Pearson's correlation coefficient = 0.94.

3.2.3. Comparison with previously available methods for single-cell CGH.

Previously, single-cell WGA products generated with SCOMP have been already analysed using metaphase CGH (mCGH) and BAC-based aCGH arrays [47,145]. The later approach allowed detection of CNAs in breast cancer DCCs as small as 4.4 Mb in size. More recently, the detection limit of this method was further increased by the application of tiling resolution BAC-based aCGH platform ([170], unpublished data). To demonstrate the performance of the new aCGH workflow for the analysis of DCCs, the new method was compared with the previously used analytical approach based on mCGH. To this end, two prostate cancer DCCs previously analysed by mCGH were now re-analysed using the new high-resolution oligonucleotide arrays. Direct comparison between the results obtained using mCGH and the new aCGH-based workflow showed high level of concordance. However, in one of the prostate cancer DCCs several focal alterations escaped the detection by mCGH indicating higher sensitivity of the aCGH-based approach, e.g. DNA losses of chromosome 1p35.3-35.2, 3q12.2-13.11 and 6p21.33-21.31 (Figure 15). With sizes of 3.5 Mb, 3.4 Mb and 2.4 Mb, respectively, these aberrations were beyond the level of detection provided by the mCGH-based approach. To additionally challenge the new assay, its performance was directly compared with a recently developed single-cell aCGH approach using array design consisting of chromosome 17 specific tiling resolution BAC clone library [170]. Due to the specific design of the BAC clone-based arrays, the comparison of the aCGH platforms was restricted to chromosome 17 only. Four oesophageal cancer DCCs were selected for the comparison of the aCGH platforms. These specimens were previously analysed using BAC clone-based aCGH, mCGH and a qPCR assay. Using qPCR it was possible to detect amplification of the ERBB2 locus in two analysed cells (3266 Lk4T2 and 3270 Lk6T2). Consistently with the results of qPCR, single-cell mCGH and oligonucleotide aCGH but not BAC clone-based aCGH detected copy number gains in a genomic region encompassing the ERBB2 locus on chromosome 17q12 (Figure 16). Furthermore, in all samples tested BAC clone-based aCGH failed to detect CNAs, which were otherwise identified by mCGH and the new oligonucleotide aCGH assay (Figure 16). Significantly, the latter two approaches provided very concordant profiles of copy number changes, although the boundaries of CNAs could be detected more precisely using the oligonucleotide aCGH, thereby showing higher sensitivity of this approach (Figure 16). Collectively, these results indicate that the single-cell aCGH assay using oligonucleotide arrays provides more accurate assessment of CNAs than mCGH and the aCGH approach using BAC clone-based arrays.

Figure 15.

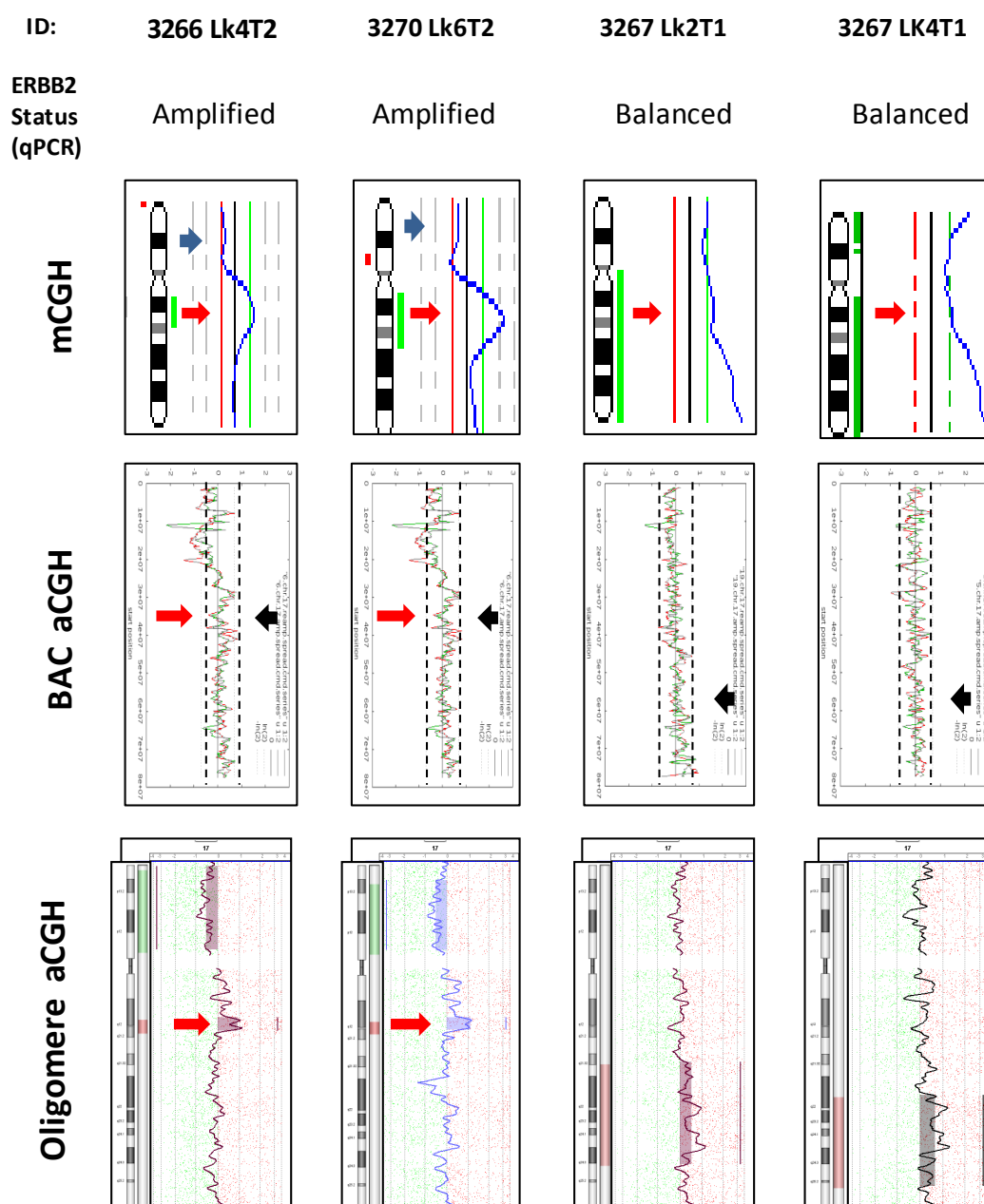


Comparison of the new single-cell aCGH workflow with the mCGH based approach.

A) Exemplary vertical single-cell mCGH (left panel) and aCGH (right panel) profiles of a DCC of a prostate cancer patient. In the mCGH plots, DNA gains and losses are indicated by red or green bars, respectively. CNAs detected by aCGH are indicated by gray shading depicted in the profiles.

B, C, D) Horizontal mCGH (left panel) and aCGH profiles of chromosome 1, 3 and 6 of the prostate cancer DCC depicted in panel A. Black arrows indicate CNAs which were detected by aCGH and escaped detection by mCGH.

Figure 16.



Comparison of single-cell aCGH approaches based on patient derived DCCs.

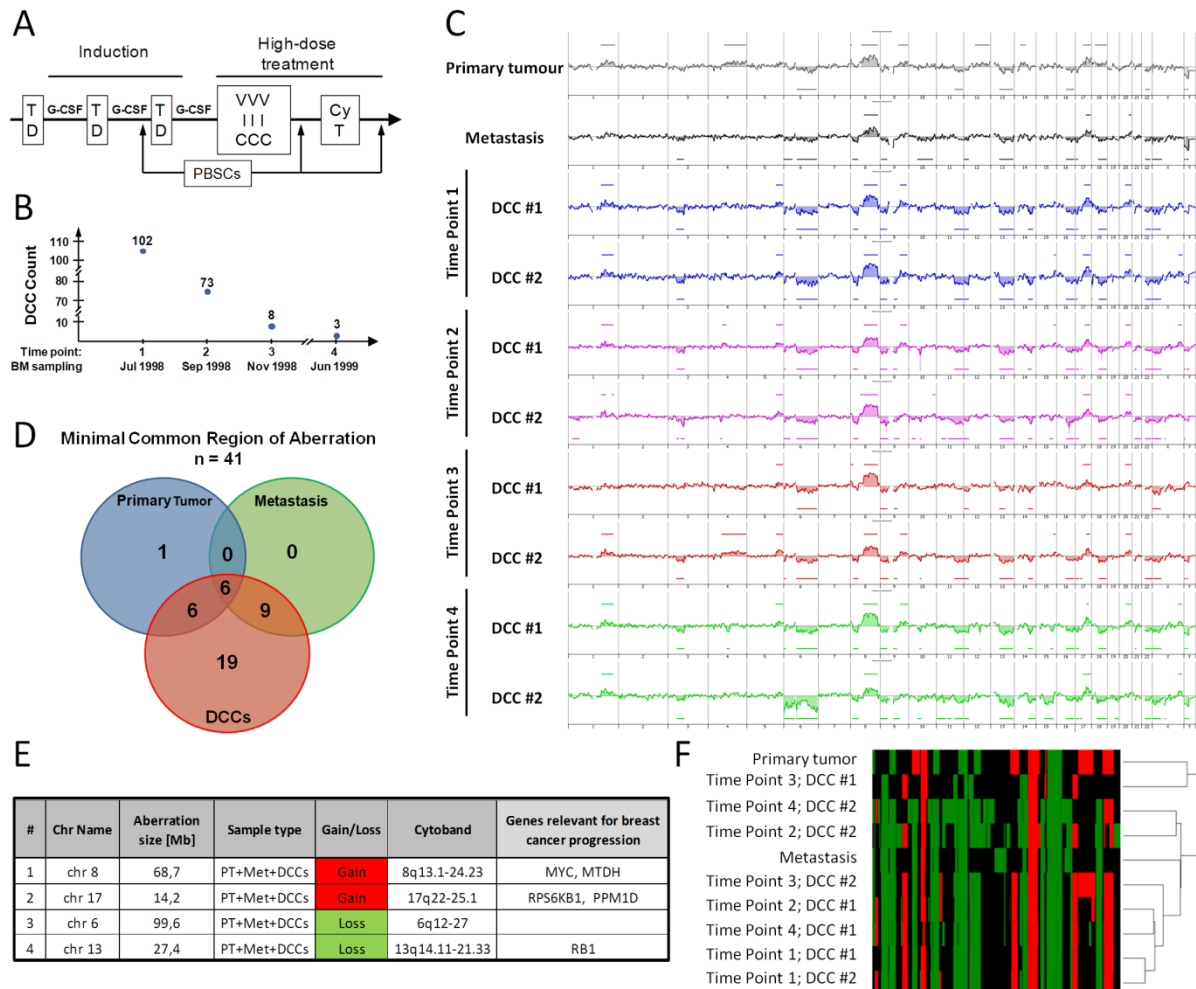
Vertical mCGH (upper row) or aCGH profiles generated using either a BAC clone-based (middle row) or oligonucleotide (lower row) platform. Only chromosome 17 specific profiles of four oesophageal cancer cells are depicted. Red arrows indicate the location of the amplified ERBB2 loci in the depicted cells. Black arrows show locations at which BAC clone-based aCGH assay failed to detect CNAs.

3.3. Application of the new single-cell aCGH assay to the analysis of single DCCs.

Tumor heterogeneity and the resulting clonal evolution pose a challenge for molecular diagnostics and treatment of cancer. DCCs or CTCs have the potential to be used for monitoring the progression of malignant disease. Molecular analysis of these cells at different

Results

time points of disease could allow to control the tumor burden more efficiently, monitor the process of clonal selection and study the mechanism of drug resistance. In a proof-of-principle study the new single-cell aCGH assay was used to demonstrate the utility of DCCs to monitor the clonal evolution of cancer cells during the malignant progression. For this, a breast cancer patient was selected who was consecutively tested for the presence of DCCs throughout the course of treatment. The patient was diagnosed initially with advanced, stage IV breast cancer (PT4b, N1bii, pM1, G3, ER+, PR+, HER2-), with metastatic lesions detected in the lymph nodes and bones. During the subsequent eleven months the patient was subjected to high dose chemotherapy treatment (Figure 17A). During this time the presence of DCCs was quantified four times: once at the time point of the primary tumor resection (July 1998) and three consecutive times during the course of treatment (September 1998, November 1998 and July 1999) (Figure 17B). The DCC count (DCC/ 1×10^6 white blood cells) was steadily decreasing, with 102, 73, 8 and 3 detected DCCs, respectively (Fig 17B). This indicated that the tumor burden decreased as a consequence of the administered treatment. Two single DCCs from each of the time points were subjected to WGA and subsequently analysed by aCGH. Additionally, the analysis included two formalin FFPE tumor tissue specimens; one from the primary tumor and the other from the lymph node metastasis. Investigation of the resulting aCGH profiles revealed multiple CNAs in all samples tested (Figure 17C). Further analysis revealed forty one minimal regions of common aberration (MRAs) (Figure 17D). Nineteen aberrant regions (both DNA gains and losses) were found in DCCs only, no CNAs were found to be specific for the metastatic lesion and only one CNA was detected exclusively in the primary tumor (Table 20, Figure 17D). This indicates that DCCs may represent a more advanced stage of the disease. Among the remaining MRAs, nine were found present in the metastatic compartment (metastatic lesion and DCCs) but not in the primary tumor (Table 20, Figure 17D). Interestingly, this group included genomic losses only (Table 20) indicating that these regions may harbour metastatic suppressor genes. Further analysis of the aCGH datasets revealed six MRAs shared by samples representing all analysed sites (primary tumor, metastatic lesion and at least one DCCs) (Table 20, Figure 17D). Within this group four aberrant regions were present in all tested specimens – gains on 17q and 8q and losses on chromosomes 6 and 13 (Figure 17E). These regions harbour multiple oncogenes and tumor suppressor genes, e.g. MYC, MTDH and RB1, that were previously associated with the progression of breast cancer. High penetrance of CNAs in these regions suggests that these aberrations were among the earliest genomic events that had occurred during the course



A) The overview of the chemotherapy treatment. The patient was first subjected to three cycles of 7

B) The course of bone marrow sampling. DCC count indicate the amount of detected DCCs in 1.0×10^6 mononuclear cells.

C) Horizontal aCGH profile of samples included in the study: primary tumor, lymph node metastasis and eight DCCs.

D) Venn diagram depicting the amount of MRAs (both gains and losses) detected in all three types of clinical samples.

E) Table depicting core MRAs that were detected with 100% penetrance across all the analysed samples.

F) Hierarchical clustering (distance: Euclidian; linkage: average) of samples included in the aCGH analysis.

72

Results

progression among tested specimens. Lack of otherwise recurrent CNAs was also detected in the DCC #2 collected at the time point 4 (Figure 17C). Collectively, this proof-of-principle study shows that the new assay is well suited to monitor the clonal selection of DCCs throughout the course of cancer treatment.

Table 20.

Minimal regions of recurrent copy number changes.

#	Chr Name	Aberration size [Mb]	Gain/Loss	Sample type	Penetrance All Samples	Penetrance DCCs only	Cytoband
1	chr6	99,6	Loss	PT+Met+DCCs	100	100	6q12-27
2	chr8	68,7	Gain	PT+Met+DCCs	100	100	8q13.1-24.23
3	chr13	27,4	Loss	PT+Met+DCCs	100	100	13q14.11-21.33
4	chr16	35,1	Loss	PT+Met+DCCs	90	87,5	16q12.2-24.2
5	chr17	14,2	Gain	PT+Met+DCCs	100	100	17q22-25.1
6	chr22	26,8	Loss	PT+Met+DCCs	90	87,5	22q11.21-13.31
7	chr1	35,1	Loss	DCCs	10	12,5	1p36.12-32.1
8	chr4	6,2	Loss	DCCs	10	12,5	4q13.1-13.2
9	chr4	14,7	Loss	DCCs	10	12,5	4q22.1-25
10	chr5	34,5	Gain	DCCs	70	87,5	5q21.3-35.3
11	chr9	14,1	Loss	DCCs	70	87,5	9p21.11-21.32
12	chr10	1,9	Loss	DCCs	20	25	10p15.3-15.2
13	chr11	25,3	Loss	DCCs	20	25	11p14.3-11.12
14	chr11	11,6	Loss	DCCs	20	25	11q12.1-13.3
15	chr12	24,8	Loss	DCCs	80	100	12p13.33-11.23
16	chr12	2,4	Loss	DCCs	10	12,5	12q21.31
17	chr15	14,0	Loss	DCCs	30	37,5	15q24.1-25.3
18	chr15	8,4	Gain	DCCs	30	37,5	15q26.1-26.3
19	chr17	6,9	Loss	DCCs	20	25	17q11.2-12
20	chr18	4,1	Loss	DCCs	10	12,5	18p11.31-11.23
21	chr19	19,7	Loss	DCCs	10	12,5	19q13.2-13.43
22	chr20	28,3	Gain	DCCs	70	87,5	20q11.22-13.33
23	chr21	6,8	Loss	DCCs	30	37,5	21q11.2-21.1
24	chrX	7,4	Loss	DCCs	20	25	Xq11.1-13.1
25	chrX	17,4	Gain	DCCs	40	50	Xq26.2-28
26	chr18	58,3	Gain	PT	10	0	18q11.1-23
27	chr1	22,7	Gain	PT+DCCs	80	87,5	1q24.1-31.1
28	chr1	10,0	Gain	PT+DCCs	80	87,5	1q41-42.12
29	chr4	12,3	Gain	PT+DCCs	30	25	4q21.21-22.1
30	chr8	8,6	Gain	PT+DCCs	20	12,5	8p23.3-23.1
31	chr9	33,5	Gain	PT+DCCs	60	62,5	9p22.33-34.1
32	chr11	43,4	Loss	PT+DCCs	80	87,5	11q14.3-25
33	chr3	35,9	Loss	Met+DCCs	80	87,5	3p21.31-p12.2
34	chr6	11,8	Loss	Met+DCCs	80	87,5	6p25.3-24.1
35	chr8	25,4	Loss	Met+DCCs	80	87,5	8p22-11.22
36	chr9	29,4	Loss	Met+DCCs	90	100	9p24.1-13.3
37	chr10	7,2	Loss	Met+DCCs	50	50	10q21.1-21.2
38	chr14	10,5	Loss	Met+DCCs	90	100	14q24.1-31.1
39	chr17	12,4	Loss	Met+DCCs	80	87,5	17p13.2-11.2
40	chr18	39,5	Loss	Met+DCCs	80	87,5	18q12.3-23
41	chrX	43,4	Loss	Met+DCCs	90	100	Xp22.33-11.3

4. Discussion.

4.1. Development of a high-resolution aCGH assay for accurate mapping of genomic aberrations in single cells.

The aim of this study was to develop a novel method for robust and accurate assessment of copy number aberrations in the genomes of single micrometastatic cancer cells. To facilitate this goal, a novel aCGH protocol was established allowing reliable detection of copy number aberrations as small as 100 kb in single-cell genomes. Critical for achieving this level of accuracy were the following factors: (i) the use of high-resolution aCGH arrays, (ii) application of highly robust SCOMP WGA technology, and (iii) improvements of the experimental procedures for labeling and hybridization of WGA products.

4.1.1. Selection of the most suitable aCGH platform.

Reports published before the beginning of the research project outlined in this thesis indicated that the outcome of single-cell aCGH is highly dependent on the design and quality of the DNA arrays used for the analysis. A study published by Fuhrmann and coworkers showed that depletion of contaminating bacterial DNA from BAC probes by pulse field gel electrophoresis (PFGE) significantly improves the performance of BAC arrays for single-cell aCGH, allowing detection of CNAs at 1-2 Mb resolution [145]. At that time, this platform outperformed all traditional BAC-based and oligonucleotide arrays in terms of sensitivity. However, the laborious fabrication of PFGE-purified BACs [145] and generally low spatial resolution of BAC-based arrays [179] hindered the widespread use of this technology. An opportunity to improve the sensitivity of single-cell aCGH came with the development of technologies for *in situ* synthesis of DNA oligonucleotides on solid surfaces, enabling fabrication of high-resolution arrays [180-182]. In recent years oligonucleotide arrays have been applied in multiple studies analysing single-cell WGA products [137,139,150,153,156,183-188]. However, despite higher probe density of oligonucleotide arrays the sensitivity of resulting single-cell aCGH assays remained inferior to best performing BAC-based platform [145] suggesting that the detection limit of single-cell aCGH had been reached. Only very recently, reports including the study presented here indicated that a reliable detection of CNAs of 1 Mb or smaller is possible using the modern high-resolution oligonucleotide arrays [144,146,156]. Strikingly, these studies utilized oligoarrays manufactured by using the inkjet deposition technology, which suggests that this type of

aCGH platform offers the highest level of accuracy. Indeed, recent reports showed that oligonucleotide arrays generated using inkjet deposition approach allow the most sensitive detection of copy number variations [189,190]. Another explanation for the improved performance of single-cell aCGH in the last studies may be associated with the advances in probe design algorithms and *in silico* probes selection criteria [191-193]. Previous reports suggested that that sensitive detection of copy number variations in single-cell WGA products is only possible when using arrays with ultra-high density (median probe spacing of 65-80 bp) [137,156]. In contrast, data presented in this thesis and the work of others [146] show that arrays with median probe spacing of 13 kb provide already sufficient resolution for precise copy number profiling in single-cell genomes, indicating that performance of individual probes have increased in comparison with previously used platforms. Collectively, these data indicate that selection of both the array platform and design of probes may be critical for performance of single-cell aCGH.

4.1.2. Selection of WGA technology.

A second important factor influencing the accuracy of copy number profiling is the selection of the WGA approach to amplify single cell genomes. Recent reports based on data collected by single-cell aCGH or whole genome sequencing showed that PCR-based WGA approaches, e.g. GenomePlex and PicoPlex, allow more accurate detection of CNAs than MDA-based WGA technologies [120,141,194]. Although the nature of this phenomenon is not fully understood, it seems possible that sequence artefacts and quantitative amplification bias introduced in MDA products may pose putative causes for distort copy number profiles of single-cell MDA products [118,120]. Moreover, due to inherent characteristics of primer design and reduced efficiency to amplify short DNA molecules, MDA seem to be less suitable for analysis of partially degraded, or otherwise fragmented, templates such as DNA extracted from FFPE tissue specimens, thereby limiting the applicability of this method to clinical samples [114,124,151]. In contrast, PCR-based approaches were shown to be able to efficiently amplify DNA from various types of archival clinical material [127,195,196]. Moreover, comparison of various PCR-based WGA methodologies, including GenomePlex, PicoPlex and SCOMP, revealed that the latter technology provides the most accurate single-cell aCGH data suggesting that SCOMP is the most suitable WGA approach for assessment of copy number changes in single-cell WGA products [146]. In accordance, data presented in this thesis show that SCOMP allows highly reliable and accurate profiling of CNAs in single-

cell genomes, suggesting that this WGA approach is highly suitable for high-resolution single-cell aCGH analysis. On the other hand, recent studies indicate WGA approaches employing MDA, in particular MALBAC, attain broader breadth of genomic coverage making them potentially more suitable for applications that are directed at accurate genotyping rather than copy number analysis [118,120,141].

4.1.3. Selection of a strategy for DNA labeling.

Another technical factor that influenced the performance of single-cell aCGH is DNA labeling. Several techniques have been developed for DNA labeling, including nick translation [197,198], random priming (RP labeling) [199,200], non-enzymatic universal linkage system (ULS) [201,202] and direct labeling by PCR [145,203]. However, nick translation, RP-labeling and ULS require high input of DNA (typically $\geq 1 \mu\text{g}$), which can be problematic if applied to unique and precious samples such as single-cell WGA products from micrometastatic cancer cells. To avoid excessive consumption of the WGA products two novel PCR-based DNA labeling approaches were developed designed specifically for WGA products generated by SCOMP (PCR-T1 and PCR-T2, see Figure 4 in Materials and methods section). The new methods require only minute quantities of DNA for labeling, leaving sufficient amount of material for multiple downstream applications, such as qPCR or next generation sequencing (NGS). However, direct comparison of both approaches revealed that PCR-T1 is susceptible to introduce amplification bias into the amplified DNA and therefore is not suitable for single-cell aCGH. This was most likely caused by illegitimate cross-hybridization of adaptor sequences to the DNA probes on the array or suboptimal priming of the dye-conjugated oligonucleotide, indicated by low DNA yields. In contrast, analysis of single-cell WGA product labeled with PCR-T2 showed that this approach allows reliable and reproducible labeling of SCOMP WGA products without introducing any noticeable bias to the original genomic representation. Direct comparison of PCR-T2 with a RP labeling technique recently successfully applied to WGA product generated by SCOMP [146] showed that the new PCR-based technique allows more reliable assessment of CNAs in patient-derived immunostained cells. Although the exact mechanism causing this phenomenon was not elucidated, it seems likely that poorer performance of RP labelling in clinical samples may be caused by shortening of the average length of WGA amplicons brought about by DNA breaks resulting from fixation and sample processing. Due to the use of random primers the products of RP labelling generated from short DNA fragments may carry insufficient amounts

of dye to be efficiently detected. In contrast, the design of PCR-T2 ensures comprehensive labeling of entire WGA amplicons allowing incorporation of higher amounts of dye into the short DNA fragments. As a consequence, PCR-T2 labeling approach facilitates more effective labelling of clinical samples, thereby making this method better suited for processing of patient-derived clinical specimens such as DCCs or CTCs.

4.1.4. Selection of reference samples.

A prerequisite for successful aCGH analysis is comparable representation of genomic sequences in both test and reference sample. However, all WGA procedures are prone to amplification bias [113,118,120,141,147,204] or generate DNA representations which in terms of complexity differ from the unamplified DNA [205,206]. Therefore, co-hybridization of test samples amplified by WGA with unamplified reference specimen may lead to increased hybridization noise or introduction of artefacts to aCGH data. Previous reports showed that bias introduced by hybridization of a single-cell WGA product against non-amplified reference DNA may be compensated by using dedicated computational algorithms [153,207] or by matching the sample characteristics of test and reference DNA i.e. by amplifying both samples with the same WGA procedure [202]. Due to its simplicity the latter approach was used preferentially in the recently published single-cell aCGH analyses [137,139,145,146,156,185]. In many of these studies samples used as reference DNA consisted of WGA product generated from pooled cells [137,139,145]. However, data presented in this thesis showed that, in comparison to WGA product from cell pools, DNA obtained by pooling multiple single-cell WGAs is more suitable for single-cell aCGH analysis as this approach allows reduction of hybridization noise and thereby more confident recognition of copy number aberrations in single-cell WGA products. Similar observations were also made in a study by Bi and coworkers [156]. This indicates that proper selection of reference DNA has a strong impact on the performance of aCGH analysis.

4.2. Advantages of the novel single-cell aCGH assay.

The assay presented in this work proved to be highly reliable and accurate. Comparison of FISH and aCGH data revealed that the new assay allows accurate detection of CNAs over a wide dynamic range of copy number states. Remarkably, the high-quality data provided by the new method allowed detection of aberrations as small as 0.1 Mb in single-cell genomes.

However, it possible that even smaller genetic lesion (<0.1 Mb) could be also detected had they been present in tested cells. This level of sensitivity is superior to most of the available methods for array based profiling of CNAs in single cells and only comparable with the most sensitive single-cell aCGH assay currently available [146]. However, due to the use of RP-labeling the latter methodology is less reliable if applied to single cells that were subjected to immunostaining prior to WGA. Further improvement of resolution may be achieved by application of single-cell methodologies based on NGS. A recently presented method based on pair-end high throughput sequencing allowed detection of CNAs as small as 13-35 kb [120] in single-cell genomes. However, only a small fraction of these events (12-26%) could be confirmed by presence of discordant read pairs and PCR. Notwithstanding, more confident recognition of CNAs by single-cell NGS would necessitate the use of recently emerging technologies for low-error high-throughput sequencing [208]. Beyond the high resolving power, the new assay proved to be remarkably robust providing consistently good quality data for all tested samples, including FFPE specimens and archival WGA products stored for more than 10 years. In comparison, recently presented single-cell aCGH workflow using MDA-based WGA allowed analysis of only 59% of successfully amplified single-cell DNA samples [153,175]. Moreover, unlike to other single-cell aCGH workflows published in the past, evaluation of the data generated by the new method did not necessitate the use of customized scripts for data curation. Despite increased level of hybridization noise typical for single-cell WGA products, copy number aberrations could be identified using standard detection algorithms such as AMD-2 [209] or CBS [210]. Consequently, streamlined experimental design and automatable data evaluation makes the new protocol particularly user-friendly and amenable to routine use in molecular biology laboratories. Beyond that, the new assay presented here can be executed in a short amount of time. While the other protocols [175] require up to a week for completion of the analysis, the assay presented in this work can be executed within 2.5 day. Still, this timeframe is too long to apply the new method for prenatal genetic diagnosis (PGD), wherein the results need to be delivered within 48h to prevent cryopreservation of the embryo.

4.3. Applicability of the new analysis to monitor genomic heterogeneity of clinical DCCs – proof-of-principle case report.

Genetic heterogeneity of malignant diseases is recognized as a major obstacle for eradication of metastases and effective treatment of cancer [211-213]. It may have important clinical

implications for the diagnosis, treatment outcome and identification of putative drug targets [12,213-217]. Therefore, better understanding of the extent of the intratumor heterogeneity is of direct clinical importance. Increasing evidence indicate that efficacy of treatment may depend on the ability to detect rare genetically and functionally distinct tumor subclones that harbour driving mutations or confer resistance to treatment [138,211,213,216,218,219]. However, identification of such clones is technically challenging and would necessitate longitudinal sampling over the course of treatment [213]. Previously, presence of intratumor heterogeneity in both primary tumor [220] as well as in CTCs [221] was associated with emergence of therapy resistance and poor patient outcome. Thus far, however, little is known about the extent of genetic heterogeneity and clonal dynamics of DCCs. Reports published in the past indicated that DCCs are genomically highly divergent in the early systemic cancer and become clonal once metastases have clinical manifested [20,45,46,97]. However, the mode of clonal selection is largely unknown. Using the new single-cell aCGH method it was possible to get an insight into the microevolution of DCCs over a course treatment of metastatic cancer. Genomic analysis revealed the presence of multiple genomically distinct DCC clones and showed a complex phylogenetic history of clonal selection with fluctuations in the subclonal composition. Interestingly, the detection of two clones (here represented by DCC #1 from time point 3 and DCC #2 from time point 4) became possible only after initiation of chemotherapy indicating that selective pressure exerted by therapeutic agents promoted the selection of previously undetectable genetic variants. Such clonal dynamics indicate that chemotherapeutic treatment enhances heterogeneity among DCCs. Strikingly, selected clones harboured high proportion of CNAs co-occurring ubiquitously at all stages of disease (primary tumor, minimal residual disease and metastases). Therefore, chromosomal gains on chromosome 17q and 8q as well as losses on chromosome 6, 12 and 13 can be placed on the shared trunk of phylogenetic tree of tumor progression in the tested patient. As such these aberrations are likely to represent early somatic alterations that are essential for the survival of cancer cells and drive tumor maintenance in the tested patient [215,222]. Predominant occurrence of highly recurrent CNAs in the selected DCC clones suggests their close relatedness to early tumor progenitor cells. It is likely that a small number of these cells survived the clonal sweep and expanded once cancer cells sensitive to chemotherapy have been eradicated. A similar pattern of clonal selection was observed during progression from myelodysplastic syndromes to secondary acute myeloid leukemia (AML) [223,224]. There, a subclone of the tumor founding clone survived therapy, gained additional mutations and expanded causing relapse. The collected data indicate that breast cancer DCCs undergo

similar process. Unfortunately, from the available data it cannot be elucidated whether therapy resistance of arising DCCs clones was a consequence of their intrinsic characteristic or whether it was attained by acquisition of protective mutations. Further studies would be necessary to test this hypotheses. Alternatively, it may be also possible that survival of the DCCs was fostered by phenotes such as clinical dormancy, a state generally associated with persistence of micrometastatic cancer cells [225], which confers resistance to chemotherapeutic drugs [226]. Recent studies showed that cellular phenotypes have also a critical role in development of therapy resistance in breast cancer . However, the interplay between genetic and phenotypic diversity in the evolution of chemoresistance is still not well understood and requires further investigation [227,228]. Collectively, data from the proof-of-principle case indicate that the novel single-cell aCGH method is suitable for long term monitoring of minimal residual disease and capable of providing important insight about the clonal composition of DCCs.

4.4. Utility of the new method in the era of high-throughput sequencing.

Single-cell WGA products have been analysed with a number of high resolution approaches including aCGH, SNP arrays and more recently with NGS. Massive parallel sequencing technologies have several advantages over array-based methodologies. In particular, NGS-based analyses promises genome wide assessment of genetic lesions at base pair resolution. Unfortunately, bioinformatic approaches for reliable detection of structural sequence variants and base pair substitutions in single-cell WGA products are still at their infancy [121]. Recent studies using whole genome or targeted sequencing approaches indicated that reliable calling of base pair substitutions (i.e. SNPs or point mutations) in single-cell NGS data requires the use of cells harbouring polyploid genomes [154], sequencing of multiple kindred cells of the same donor [118,166,229] or application of comparative sequencing strategies necessitating additional deep-sequencing of control samples [138]. This limits the utility of single-cell NGS as stand-alone tool for sequence analysis of rare and heterogeneous cell populations such as DCCs and CTCs. In addition, due to the high costs high-resolution NGS-based analysis is practically not feasible to study intratumor genomic heterogeneity in large sample cohorts. For this type of analysis low-resolution NGS approaches seem to be more suitable. Recently these methodologies have been adapted to study single-cell genomes [142,143,194]. Although low-resolution NGS technologies lack the accuracy of deep-sequencing approaches, they still allow to assess the genomic heterogeneity at the single-cell level. Still, the level of complexity

Discussion

limits the applicability of this method to large molecular biology laboratories only. In contrast, single-cell aCGH assay presented here is relatively simple and cost-efficient. Remarkably, the results presented in this thesis show that single-cell aCGH may even be competitive to low-resolution NGS in terms of sensitivity. The new single-cell aCGH method offers a precise but still affordable solution for screening large number of samples within a short period of time. Unlike single-cell NGS, the newly developed aCGH-based approach does not require sophisticated infrastructure and complex bioinformatic data evaluation allowing its quick implementation in most molecular biology laboratories. Moreover, depending on the aim of a given study it can be easily adjusted to the intended use by application of customized arrays targeting specific regions of interest. Furthermore, the robust design of the new method makes it applicable to a variety of clinical specimens such as FFPE tissue samples and immunostained cells. In the future, combination of the new aCGH methodology with improved low-error NGS approaches [208] could provide a practicable framework for concurrent mapping of copy number and sequence alterations in single cells.

5. Summary.

Metastatic disease is the most common cause of cancer related death. Despite that fact, little is known about the processes underlying systemic progression of cancer. Recently, a number of studies indicated that cancer cells disseminate early and evolve independent to the primary tumor acquiring different oncogenic traits. This results in striking genetic disparity between local disease and systemic cancer. Consequently, analysis of resected primary tumor alone is insufficient to determine the full complexity of oncogenic changes driving tumorigenic progression, emphasizing the need to analyze ectopically residing cancer cells, i.e. single DCCs or CTCs. However, currently available methods provided only low-resolution copy number information of single-cell genomes. For this reason this thesis aimed to develop a high-resolution aCGH for mapping of copy number variations in single-cell genomes. The methods utilized the established SCOMP WGA technology and high-resolution oligonucleotide DNA arrays. In order to increase the accuracy of single-cell aCGH analysis, experimental procedures for DNA labeling and hybridization were optimized to decrease the amplification bias and hybridization noise introduced by the WGA. The sensitivity and specificity of resulting protocol was validated using single cells of well-characterized cancer cell lines and healthy donors showing high concordance with unamplified DNA controls and published copy number profiles. Significantly, the new method allowed reproducible detection of copy number changes as small as 0.1 Mb in size. Therefore, in comparison with previously available methodologies, such as single-cell BAC-based aCGH and mCGH, the new protocol allowed to improve the sensitivity by one to two orders of magnitude, respectively. Analysis of single DCCs showed that fixation and immunostaining procedures used to detect these cells does not have significant impact on the outcome of the new assay, showing high robustness the method. The clinical applicability of the new methodology was demonstrated in a proof-of-concept study conducted on DCCs from an individual breast cancer patient at different time points of high-dose chemotherapy treatment. The analysis uncovered co-occurrence of genomically distinct cellular clones among DCCs and revealed clonal fluctuations driven by therapeutic selection. Strikingly, the pattern of genomic changes detected in DCCs surviving chemotherapy indicated that they originate from genomically less advanced cancer cells population. Collectively, this data indicate that the new single-cell aCGH assay is a highly sensitive tool capable of inferring the clonal dynamics of micrometastatic cells. In the future the new methodology can provide important insights into the mechanisms underlying metastatic progression and therapy resistance.

6. References.

1. Ferlay J SI, Ervik M, Dikshit R, Eser S, Mathers C, Rebelo M, Parkin DM, Forman D, Bray, F. GLOBOCAN 2012 v1.0, Cancer Incidence and Mortality Worldwide. IARC CancerBase No 11 [Internet], Lyon, France: International Agency for Research on Cancer; 2013 Available from: <http://globocan.iarc.fr>, accessed on 03/May/2014
2. Bray F, Jemal A, Grey N, Ferlay J, Forman D (2012) Global cancer transitions according to the Human Development Index (2008-2030): a population-based study. *Lancet Oncol* 13: 790-801.
3. Gupta GP, Massague J (2006) Cancer metastasis: building a framework. *Cell* 127: 679-695.
4. Aggarwal S (2010) Targeted cancer therapies. *Nat Rev Drug Discov* 9: 427-428.
5. Vanneman M, Dranoff G (2012) Combining immunotherapy and targeted therapies in cancer treatment. *Nat Rev Cancer* 12: 237-251.
6. Gabor Miklos GL (2005) The human cancer genome project--one more misstep in the war on cancer. *Nat Biotechnol* 23: 535-537.
7. Howlader N NA, Krapcho M, Garshell J, Miller D, Altekruse SF, Kosary CL, Yu M, Ruhl J, Tatalovich Z, Mariotto A, Lewis DR, Chen HS, Feuer EJ, Cronin KA (eds) SEER Cancer Statistics Review, 1975-2011, National Cancer Institute. Bethesda, MD, http://seer.cancer.gov/csr/1975_2011/, based on November 2013 SEER data submission, posted to the SEER web site, April 2014.
8. Karrison TG, Ferguson DJ, Meier P (1999) Dormancy of mammary carcinoma after mastectomy. *J Natl Cancer Inst* 91: 80-85.
9. Valastyan S, Weinberg RA (2011) Tumor metastasis: molecular insights and evolving paradigms. *Cell* 147: 275-292.
10. Fidler IJ (2003) The pathogenesis of cancer metastasis: the 'seed and soil' hypothesis revisited. *Nat Rev Cancer* 3: 453-458.
11. Luzzi KJ, MacDonald IC, Schmidt EE, Kerkvliet N, Morris VL, et al. (1998) Multistep nature of metastatic inefficiency: dormancy of solitary cells after successful extravasation and limited survival of early micrometastases. *Am J Pathol* 153: 865-873.
12. Merlo LM, Pepper JW, Reid BJ, Maley CC (2006) Cancer as an evolutionary and ecological process. *Nat Rev Cancer* 6: 924-935.
13. Hanahan D, Weinberg RA (2011) Hallmarks of cancer: the next generation. *Cell* 144: 646-674.
14. Fearon ER, Vogelstein B (1990) A genetic model for colorectal tumorigenesis. *Cell* 61: 759-767.
15. Banys M, Hahn M, Gruber I, Krawczyk N, Wallwiener M, et al. (2014) Detection and clinical relevance of hematogenous tumor cell dissemination in patients with ductal carcinoma in situ. *Breast Cancer Res Treat* 144: 531-538.
16. Sanger N, Effenberger KE, Riethdorf S, Van Haasteren V, Gauwerky J, et al. (2011) Disseminated tumor cells in the bone marrow of patients with ductal carcinoma in situ. *Int J Cancer* 129: 2522-2526.
17. Husemann Y, Geigl JB, Schubert F, Musiani P, Meyer M, et al. (2008) Systemic spread is an early step in breast cancer. *Cancer Cell* 13: 58-68.
18. Braun S, Pantel K, Muller P, Janni W, Hepp F, et al. (2000) Cytokeratin-positive cells in the bone marrow and survival of patients with stage I, II, or III breast cancer. *N Engl J Med* 342: 525-533.
19. van de Wouw AJ, Janssen-Heijnen ML, Coebergh JW, Hillen HF (2002) Epidemiology of unknown primary tumours; incidence and population-based survival of 1285 patients in Southeast Netherlands, 1984-1992. *Eur J Cancer* 38: 409-413.
20. Schmidt-Kittler O, Ragg T, Daskalakis A, Granzow M, Ahr A, et al. (2003) From latent disseminated cells to overt metastasis: genetic analysis of systemic breast cancer progression. *Proc Natl Acad Sci U S A* 100: 7737-7742.
21. Stoecklein NH, Hosch SB, Bezler M, Stern F, Hartmann CH, et al. (2008) Direct genetic analysis of single disseminated cancer cells for prediction of outcome and therapy selection in esophageal cancer. *Cancer Cell* 13: 441-453.

References

22. Klein CA (2009) Parallel progression of primary tumours and metastases. *Nat Rev Cancer* 9: 302-312.
23. Podsypanina K, Du YC, Jechlinger M, Beverly LJ, Hambardzumyan D, et al. (2008) Seeding and propagation of untransformed mouse mammary cells in the lung. *Science* 321: 1841-1844.
24. Caldas C (2012) Cancer sequencing unravels clonal evolution. *Nat Biotechnol* 30: 408-410.
25. Greaves M, Maley CC (2012) Clonal evolution in cancer. *Nature* 481: 306-313.
26. Pantel K, Brakenhoff RH, Brandt B (2008) Detection, clinical relevance and specific biological properties of disseminating tumour cells. *Nat Rev Cancer* 8: 329-340.
27. Alix-Panabieres C, Pantel K (2013) Circulating tumor cells: liquid biopsy of cancer. *Clin Chem* 59: 110-118.
28. Barradas AM, Terstappen LW (2013) Towards the Biological Understanding of CTC: Capture Technologies, Definitions and Potential to Create Metastasis. *Cancers (Basel)* 5: 1619-1642.
29. Riethdorf S, Wikman H, Pantel K (2008) Review: Biological relevance of disseminated tumor cells in cancer patients. *Int J Cancer* 123: 1991-2006.
30. Schlimok G, Funke I, Holzmann B, Gottlinger G, Schmidt G, et al. (1987) Micrometastatic cancer cells in bone marrow: in vitro detection with anti-cytokeratin and in vivo labeling with anti-17-1A monoclonal antibodies. *Proc Natl Acad Sci U S A* 84: 8672-8676.
31. Lindemann F, Schlimok G, Dirschedl P, Witte J, Riethmuller G (1992) Prognostic significance of micrometastatic tumour cells in bone marrow of colorectal cancer patients. *Lancet* 340: 685-689.
32. Rosenberg R, Gertler R, Friederichs J, Fuehrer K, Dahm M, et al. (2002) Comparison of two density gradient centrifugation systems for the enrichment of disseminated tumor cells in blood. *Cytometry* 49: 150-158.
33. Allard WJ, Matera J, Miller MC, Repollet M, Connelly MC, et al. (2004) Tumor cells circulate in the peripheral blood of all major carcinomas but not in healthy subjects or patients with nonmalignant diseases. *Clin Cancer Res* 10: 6897-6904.
34. Talasz AH, Powell AA, Huber DE, Berbee JG, Roh KH, et al. (2009) Isolating highly enriched populations of circulating epithelial cells and other rare cells from blood using a magnetic sweeper device. *Proc Natl Acad Sci U S A* 106: 3970-3975.
35. Magbanua MJ, Park JW (2013) Isolation of circulating tumor cells by immunomagnetic enrichment and fluorescence-activated cell sorting (IE/FACS) for molecular profiling. *Methods* 64: 114-118.
36. Gorges TM, Tinhofer I, Drosch M, Rose L, Zollner TM, et al. (2012) Circulating tumour cells escape from EpCAM-based detection due to epithelial-to-mesenchymal transition. *BMC Cancer* 12: 178.
37. Seal SH (1964) A Sieve for the Isolation of Cancer Cells and Other Large Cells from the Blood. *Cancer* 17: 637-642.
38. Vona G, Sabile A, Louha M, Sitruk V, Romana S, et al. (2000) Isolation by size of epithelial tumor cells : a new method for the immunomorphological and molecular characterization of circulating tumor cells. *Am J Pathol* 156: 57-63.
39. Zheng S, Lin H, Liu JQ, Balic M, Datar R, et al. (2007) Membrane microfilter device for selective capture, electrolysis and genomic analysis of human circulating tumor cells. *J Chromatogr A* 1162: 154-161.
40. Lin HK, Zheng S, Williams AJ, Balic M, Groshen S, et al. (2010) Portable filter-based microdevice for detection and characterization of circulating tumor cells. *Clin Cancer Res* 16: 5011-5018.
41. Pantel K, Brakenhoff RH (2004) Dissecting the metastatic cascade. *Nat Rev Cancer* 4: 448-456.
42. Pantel K, Izbicki JR, Angstwurm M, Braun S, Passlick B, et al. (1993) Immunocytological detection of bone marrow micrometastasis in operable non-small cell lung cancer. *Cancer Res* 53: 1027-1031.
43. Ross JS, Slodkowska EA (2009) Circulating and disseminated tumor cells in the management of breast cancer. *Am J Clin Pathol* 132: 237-245.

References

44. Fehm T, Braun S, Muller V, Janni W, Gebauer G, et al. (2006) A concept for the standardized detection of disseminated tumor cells in bone marrow from patients with primary breast cancer and its clinical implementation. *Cancer* 107: 885-892.
45. Weckermann D, Polzer B, Ragg T, Blana A, Schlimok G, et al. (2009) Perioperative activation of disseminated tumor cells in bone marrow of patients with prostate cancer. *J Clin Oncol* 27: 1549-1556.
46. Klein CA, Blankenstein TJ, Schmidt-Kittler O, Petronio M, Polzer B, et al. (2002) Genetic heterogeneity of single disseminated tumour cells in minimal residual cancer. *Lancet* 360: 683-689.
47. Klein CA, Schmidt-Kittler O, Schardt JA, Pantel K, Speicher MR, et al. (1999) Comparative genomic hybridization, loss of heterozygosity, and DNA sequence analysis of single cells. *Proc Natl Acad Sci U S A* 96: 4494-4499.
48. Schardt JA, Meyer M, Hartmann CH, Schubert F, Schmidt-Kittler O, et al. (2005) Genomic analysis of single cytokeratin-positive cells from bone marrow reveals early mutational events in breast cancer. *Cancer Cell* 8: 227-239.
49. Fischer JC, Niederacher D, Topp SA, Honisch E, Schumacher S, et al. (2013) Diagnostic leukapheresis enables reliable detection of circulating tumor cells of nonmetastatic cancer patients. *Proc Natl Acad Sci U S A* 110: 16580-16585.
50. Desitter I, Guerrouahen BS, Benali-Furet N, Wechsler J, Janne PA, et al. (2011) A new device for rapid isolation by size and characterization of rare circulating tumor cells. *Anticancer Res* 31: 427-441.
51. Zieglschmid V, Hollmann C, Gutierrez B, Albert W, Strothoff D, et al. (2005) Combination of immunomagnetic enrichment with multiplex RT-PCR analysis for the detection of disseminated tumor cells. *Anticancer Res* 25: 1803-1810.
52. Hsieh HB, Marrinucci D, Bethel K, Curry DN, Humphrey M, et al. (2006) High speed detection of circulating tumor cells. *Biosens Bioelectron* 21: 1893-1899.
53. Nagrath S, Sequist LV, Maheswaran S, Bell DW, Irimia D, et al. (2007) Isolation of rare circulating tumour cells in cancer patients by microchip technology. *Nature* 450: 1235-1239.
54. Alix-Panabieres C (2012) EPISPOT assay: detection of viable DTCs/CTCs in solid tumor patients. *Recent Results Cancer Res* 195: 69-76.
55. Saucedo-Zeni N, Mewes S, Niestroj R, Gasiorowski L, Murawa D, et al. (2012) A novel method for the in vivo isolation of circulating tumor cells from peripheral blood of cancer patients using a functionalized and structured medical wire. *Int J Oncol* 41: 1241-1250.
56. Hardingham JE, Kotasek D, Sage RE, Eaton MC, Pascoe VH, et al. (1995) Detection of circulating tumor cells in colorectal cancer by immunobead-PCR is a sensitive prognostic marker for relapse of disease. *Mol Med* 1: 789-794.
57. Niedergethmann M, Rexin M, Hildenbrand R, Knob S, Sturm JW, et al. (2002) Prognostic implications of routine, immunohistochemical, and molecular staging in resectable pancreatic adenocarcinoma. *Am J Surg Pathol* 26: 1578-1587.
58. Pantel K, Cote RJ, Fodstad O (1999) Detection and clinical importance of micrometastatic disease. *J Natl Cancer Inst* 91: 1113-1124.
59. Pantel K, Alix-Panabieres C, Riethdorf S (2009) Cancer micrometastases. *Nat Rev Clin Oncol* 6: 339-351.
60. Cristofanilli M, Budd GT, Ellis MJ, Stopeck A, Matera J, et al. (2004) Circulating tumor cells, disease progression, and survival in metastatic breast cancer. *N Engl J Med* 351: 781-791.
61. Wulfing P, Borchard J, Buerger H, Heidl S, Zanker KS, et al. (2006) HER2-positive circulating tumor cells indicate poor clinical outcome in stage I to III breast cancer patients. *Clin Cancer Res* 12: 1715-1720.
62. Mansi JL, Easton D, Berger U, Gazet JC, Ford HT, et al. (1991) Bone marrow micrometastases in primary breast cancer: prognostic significance after 6 years' follow-up. *Eur J Cancer* 27: 1552-1555.

References

63. Cohen SJ, Punt CJ, Iannotti N, Saidman BH, Sabbath KD, et al. (2008) Relationship of circulating tumor cells to tumor response, progression-free survival, and overall survival in patients with metastatic colorectal cancer. *J Clin Oncol* 26: 3213-3221.
64. Thorban S, Roder JD, Nekarda H, Funk A, Siewert JR, et al. (1996) Immunocytochemical detection of disseminated tumor cells in the bone marrow of patients with esophageal carcinoma. *J Natl Cancer Inst* 88: 1222-1227.
65. Izbicki JR, Hosch SB, Pichlmeier U, Rehders A, Busch C, et al. (1997) Prognostic value of immunohistochemically identifiable tumor cells in lymph nodes of patients with completely resected esophageal cancer. *N Engl J Med* 337: 1188-1194.
66. Jauch KW, Heiss MM, Gruetzner U, Funke I, Pantel K, et al. (1996) Prognostic significance of bone marrow micrometastases in patients with gastric cancer. *J Clin Oncol* 14: 1810-1817.
67. Pantel K, Izbicki J, Passlick B, Angstwurm M, Haussinger K, et al. (1996) Frequency and prognostic significance of isolated tumour cells in bone marrow of patients with non-small-cell lung cancer without overt metastases. *Lancet* 347: 649-653.
68. Kubuschok B, Passlick B, Izbicki JR, Thetter O, Pantel K (1999) Disseminated tumor cells in lymph nodes as a determinant for survival in surgically resected non-small-cell lung cancer. *J Clin Oncol* 17: 19-24.
69. de Bono JS, Scher HI, Montgomery RB, Parker C, Miller MC, et al. (2008) Circulating tumor cells predict survival benefit from treatment in metastatic castration-resistant prostate cancer. *Clin Cancer Res* 14: 6302-6309.
70. Weckermann D, Muller P, Wawroschek F, Harzmann R, Riethmuller G, et al. (2001) Disseminated cytokeratin positive tumor cells in the bone marrow of patients with prostate cancer: detection and prognostic value. *J Urol* 166: 699-703.
71. Ulmer A, Dietz K, Hodak I, Polzer B, Scheitler S, et al. (2014) Quantitative measurement of melanoma spread in sentinel lymph nodes and survival. *PLoS Med* 11: e1001604.
72. Ulmer A, Schmidt-Kittler O, Fischer J, Ellwanger U, Rassner G, et al. (2004) Immunomagnetic enrichment, genomic characterization, and prognostic impact of circulating melanoma cells. *Clin Cancer Res* 10: 531-537.
73. Jotsuka T, Okumura Y, Nakano S, Nitta H, Sato T, et al. (2004) Persistent evidence of circulating tumor cells detected by means of RT-PCR for CEA mRNA predicts early relapse: a prospective study in node-negative breast cancer. *Surgery* 135: 419-426.
74. Stathopoulou A, Vlachonikolis I, Mavroudis D, Perraki M, Kouroussis C, et al. (2002) Molecular detection of cytokeratin-19-positive cells in the peripheral blood of patients with operable breast cancer: evaluation of their prognostic significance. *J Clin Oncol* 20: 3404-3412.
75. Ntoulia M, Stathopoulou A, Ignatiadis M, Malamos N, Mavroudis D, et al. (2006) Detection of Mammaglobin A-mRNA-positive circulating tumor cells in peripheral blood of patients with operable breast cancer with nested RT-PCR. *Clin Biochem* 39: 879-887.
76. Tewes M, Aktas B, Welt A, Mueller S, Hauch S, et al. (2009) Molecular profiling and predictive value of circulating tumor cells in patients with metastatic breast cancer: an option for monitoring response to breast cancer related therapies. *Breast Cancer Res Treat* 115: 581-590.
77. Ignatiadis M, Kallergi G, Ntoulia M, Perraki M, Apostolaki S, et al. (2008) Prognostic value of the molecular detection of circulating tumor cells using a multimarker reverse transcription-PCR assay for cytokeratin 19, mammaglobin A, and HER2 in early breast cancer. *Clin Cancer Res* 14: 2593-2600.
78. Liefers GJ, Cleton-Jansen AM, van de Velde CJ, Hermans J, van Krieken JH, et al. (1998) Micrometastases and survival in stage II colorectal cancer. *N Engl J Med* 339: 223-228.
79. Sadahiro S, Suzuki T, Maeda Y, Yurimoto S, Yasuda S, et al. (2007) Detection of carcinoembryonic antigen messenger RNA-expressing cells in peripheral blood 7 days after curative surgery is a novel prognostic factor in colorectal cancer. *Ann Surg Oncol* 14: 1092-1098.

References

80. Iinuma H, Okinaga K, Egami H, Mimori K, Hayashi N, et al. (2006) Usefulness and clinical significance of quantitative real-time RT-PCR to detect isolated tumor cells in the peripheral blood and tumor drainage blood of patients with colorectal cancer. *Int J Oncol* 28: 297-306.
81. Sher YP, Shih JY, Yang PC, Roffler SR, Chu YW, et al. (2005) Prognosis of non-small cell lung cancer patients by detecting circulating cancer cells in the peripheral blood with multiple marker genes. *Clin Cancer Res* 11: 173-179.
82. Soeth E, Grigoleit U, Moellmann B, Roder C, Schniewind B, et al. (2005) Detection of tumor cell dissemination in pancreatic ductal carcinoma patients by CK 20 RT-PCR indicates poor survival. *J Cancer Res Clin Oncol* 131: 669-676.
83. Ghossein RA, Rosai J, Scher HI, Seiden M, Zhang ZF, et al. (1997) Prognostic significance of detection of prostate-specific antigen transcripts in the peripheral blood of patients with metastatic androgen-independent prostatic carcinoma. *Urology* 50: 100-105.
84. Wu CH, Lin SR, Yu FJ, Wu DC, Pan YS, et al. (2006) Development of a high-throughput membrane-array method for molecular diagnosis of circulating tumor cells in patients with gastric cancers. *Int J Cancer* 119: 373-379.
85. Riethmuller G, Johnson JP (1992) Monoclonal antibodies in the detection and therapy of micrometastatic epithelial cancers. *Curr Opin Immunol* 4: 647-655.
86. Braun S, Pantel K (1998) Prognostic significance of micrometastatic bone marrow involvement. *Breast Cancer Res Treat* 52: 201-216.
87. Braun S, Muller M, Hepp F, Schlimok G, Riethmuller G, et al. (1998) Re: Micrometastatic breast cancer cells in bone marrow at primary surgery: prognostic value in comparison with nodal status. *J Natl Cancer Inst* 90: 1099-1101.
88. Braun S, Pantel K (1999) Micrometastatic bone marrow involvement: detection and prognostic significance. *Med Oncol* 16: 154-165.
89. Passlick B, Pantel K (2000) Detection and relevance of immunohistochemically identifiable tumor cells in lymph nodes. *Recent Results Cancer Res* 157: 29-37.
90. Passlick B, Kubuschok B, Izbicki JR, Thetter O, Pantel K (1999) Isolated tumor cells in bone marrow predict reduced survival in node-negative non-small cell lung cancer. *Ann Thorac Surg* 68: 2053-2058.
91. Passlick B, Izbicki JR, Kubuschok B, Nathrath W, Thetter O, et al. (1994) Immunohistochemical assessment of individual tumor cells in lymph nodes of patients with non-small-cell lung cancer. *J Clin Oncol* 12: 1827-1832.
92. Hosch S, Kraus J, Scheunemann P, Izbicki JR, Schneider C, et al. (2000) Malignant potential and cytogenetic characteristics of occult disseminated tumor cells in esophageal cancer. *Cancer Res* 60: 6836-6840.
93. Pierga JY, Bonneton C, Vincent-Salomon A, de Cremoux P, Nos C, et al. (2004) Clinical significance of immunocytochemical detection of tumor cells using digital microscopy in peripheral blood and bone marrow of breast cancer patients. *Clin Cancer Res* 10: 1392-1400.
94. Lucci A, Hall CS, Lodhi AK, Bhattacharyya A, Anderson AE, et al. (2012) Circulating tumour cells in non-metastatic breast cancer: a prospective study. *Lancet Oncol* 13: 688-695.
95. Bidard FC, Mathiot C, Delaloge S, Brain E, Giachetti S, et al. (2010) Single circulating tumor cell detection and overall survival in nonmetastatic breast cancer. *Ann Oncol* 21: 729-733.
96. Rack B, Schindlbeck C, Juckstock J, Andergassen U, Hepp P, et al. (2014) Circulating tumor cells predict survival in early average-to-high risk breast cancer patients. *J Natl Cancer Inst* 106.
97. Klein CA (2013) Selection and adaptation during metastatic cancer progression. *Nature* 501: 365-372.
98. Dolezel J, Bartos J, Voglmayr H, Greilhuber J (2003) Nuclear DNA content and genome size of trout and human. *Cytometry A* 51: 127-128; author reply 129.
99. Treff NR, Tao X, Ferry KM, Su J, Taylor D, et al. (2012) Development and validation of an accurate quantitative real-time polymerase chain reaction-based assay for human blastocyst comprehensive chromosomal aneuploidy screening. *Fertil Steril* 97: 819-824.

References

100. Munne S, Fragouli E, Colls P, Katz-Jaffe M, Schoolcraft W, et al. (2010) Improved detection of aneuploid blastocysts using a new 12-chromosome FISH test. *Reprod Biomed Online* 20: 92-97.
101. Strom CM, Verlinsky Y, Milayeva S, Evsikov S, Cieslak J, et al. (1990) Preconception genetic diagnosis of cystic fibrosis. *Lancet* 336: 306-307.
102. el-Hashemite N, Wells D, Delhanty JD (1996) Preimplantation genetic diagnosis of beta-thalassaemia. *Lancet* 348: 620-621.
103. Xu K, Shi ZM, Veeck LL, Hughes MR, Rosenwaks Z (1999) First unaffected pregnancy using preimplantation genetic diagnosis for sickle cell anemia. *JAMA* 281: 1701-1706.
104. Delhanty JD, Griffin DK, Handyside AH, Harper J, Atkinson GH, et al. (1993) Detection of aneuploidy and chromosomal mosaicism in human embryos during preimplantation sex determination by fluorescent in situ hybridisation, (FISH). *Hum Mol Genet* 2: 1183-1185.
105. Munne S, Sandalinas M, Escudero T, Fung J, Gianaroli L, et al. (2000) Outcome of preimplantation genetic diagnosis of translocations. *Fertil Steril* 73: 1209-1218.
106. Findlay I, Corby N, Rutherford A, Quirke P (1998) Comparison of FISH PRINS, and conventional and fluorescent PCR for single-cell sexing: suitability for preimplantation genetic diagnosis. *J Assist Reprod Genet* 15: 258-265.
107. Ray PF, Handyside AH (1996) Increasing the denaturation temperature during the first cycles of amplification reduces allele dropout from single cells for preimplantation genetic diagnosis. *Mol Hum Reprod* 2: 213-218.
108. Kontogianni EH, Griffin DK, Handyside AH (1996) Identifying the sex of human preimplantation embryos in X-linked disease: amplification efficiency of a Y-specific alphoid repeat from single blastomeres with two lysis protocols. *J Assist Reprod Genet* 13: 125-132.
109. Telenius H, Carter NP, Bebb CE, Nordenskjold M, Ponder BA, et al. (1992) Degenerate oligonucleotide-primed PCR: general amplification of target DNA by a single degenerate primer. *Genomics* 13: 718-725.
110. Kittler R, Stoneking M, Kayser M (2002) A whole genome amplification method to generate long fragments from low quantities of genomic DNA. *Anal Biochem* 300: 237-244.
111. Zhang L, Cui X, Schmitt K, Hubert R, Navidi W, et al. (1992) Whole genome amplification from a single cell: implications for genetic analysis. *Proc Natl Acad Sci U S A* 89: 5847-5851.
112. Dietmaier W, Hartmann A, Wallinger S, Heinmoller E, Kerner T, et al. (1999) Multiple mutation analyses in single tumor cells with improved whole genome amplification. *Am J Pathol* 154: 83-95.
113. Dean FB, Hosono S, Fang L, Wu X, Faruqi AF, et al. (2002) Comprehensive human genome amplification using multiple displacement amplification. *Proc Natl Acad Sci U S A* 99: 5261-5266.
114. Lee CI, Leong SH, Png AE, Choo KW, Syn C, et al. (2006) An isothermal method for whole genome amplification of fresh and degraded DNA for comparative genomic hybridization, genotyping and mutation detection. *DNA Res* 13: 77-88.
115. Zhang K, Martiny AC, Reppas NB, Barry KW, Malek J, et al. (2006) Sequencing genomes from single cells by polymerase cloning. *Nat Biotechnol* 24: 680-686.
116. Langmore JP (2002) Rubicon Genomics, Inc. *Pharmacogenomics* 3: 557-560.
117. Kamberov E, Sun T, Bruening E, Pinter J, Sleptsova I, et al. (2004) Amplification and analysis of whole genome and whole transcriptome libraries generated by a DNA polymerization process. United States Patent Application Publication No. US 2004/0209298 A1.
118. Zong C, Lu S, Chapman AR, Xie XS (2012) Genome-wide detection of single-nucleotide and copy-number variations of a single human cell. *Science* 338: 1622-1626.
119. Spits C, Le Caignec C, De Rycke M, Van Haute L, Van Steirteghem A, et al. (2006) Whole-genome multiple displacement amplification from single cells. *Nat Protoc* 1: 1965-1970.
120. Voet T, Kumar P, Van Loo P, Cooke SL, Marshall J, et al. (2013) Single-cell paired-end genome sequencing reveals structural variation per cell cycle. *Nucleic Acids Res* 41: 6119-6138.

References

121. Macaulay IC, Voet T (2014) Single cell genomics: advances and future perspectives. *PLoS Genet* 10: e1004126.
122. Lasken RS, Stockwell TB (2007) Mechanism of chimera formation during the Multiple Displacement Amplification reaction. *BMC Biotechnol* 7: 19.
123. Yilmaz S, Singh AK (2012) Single cell genome sequencing. *Curr Opin Biotechnol* 23: 437-443.
124. Lee CI, Leong SH, Png AE, Choo KW, Syn C, et al. (2006) An isothermal primer extension method for whole genome amplification of fresh and degraded DNA: applications in comparative genomic hybridization, genotyping and mutation screening. *Nat Protoc* 1: 2185-2194.
125. Arneson N, Moreno J, Iakovlev V, Ghazani A, Warren K, et al. (2012) Comparison of whole genome amplification methods for analysis of DNA extracted from microdissected early breast lesions in formalin-fixed paraffin-embedded tissue. *ISRN Oncol* 2012: 710692.
126. Nowak NJ, Miecznikowski J, Moore SR, Gaile D, Bobadilla D, et al. (2007) Challenges in array comparative genomic hybridization for the analysis of cancer samples. *Genet Med* 9: 585-595.
127. Stoecklein NH, Erbersdobler A, Schmidt-Kittler O, Diebold J, Schardt JA, et al. (2002) SCOMP is superior to degenerated oligonucleotide primed-polymerase chain reaction for global amplification of minute amounts of DNA from microdissected archival tissue samples. *Am J Pathol* 161: 43-51.
128. Gribble S, Ng BL, Prigmore E, Burford DC, Carter NP (2004) Chromosome paints from single copies of chromosomes. *Chromosome Res* 12: 143-151.
129. Dean FB, Nelson JR, Giesler TL, Lasken RS (2001) Rapid amplification of plasmid and phage DNA using Phi 29 DNA polymerase and multiply-primed rolling circle amplification. *Genome Res* 11: 1095-1099.
130. Lizardi PM (2000) Multiple displacement amplification. United States Patent No. US 6124120 A.
131. Wells D, Sherlock JK, Handyside AH, Delhanty JD (1999) Detailed chromosomal and molecular genetic analysis of single cells by whole genome amplification and comparative genomic hybridisation. *Nucleic Acids Res* 27: 1214-1218.
132. Wells D, Delhanty JD (2000) Comprehensive chromosomal analysis of human preimplantation embryos using whole genome amplification and single cell comparative genomic hybridization. *Mol Hum Reprod* 6: 1055-1062.
133. Wells D, Escudero T, Levy B, Hirschhorn K, Delhanty JD, et al. (2002) First clinical application of comparative genomic hybridization and polar body testing for preimplantation genetic diagnosis of aneuploidy. *Fertil Steril* 78: 543-549.
134. Voullaire L, Wilton L, Slater H, Williamson R (1999) Detection of aneuploidy in single cells using comparative genomic hybridization. *Prenat Diagn* 19: 846-851.
135. Hu DG, Webb G, Hussey N (2004) Aneuploidy detection in single cells using DNA array-based comparative genomic hybridization. *Mol Hum Reprod* 10: 283-289.
136. Fiegler H, Geigl JB, Langer S, Rigler D, Porter K, et al. (2007) High resolution array-CGH analysis of single cells. *Nucleic Acids Res* 35: e15.
137. Geigl JB, Obenauf AC, Waldispuehl-Geigl J, Hoffmann EM, Auer M, et al. (2009) Identification of small gains and losses in single cells after whole genome amplification on tiling oligo arrays. *Nucleic Acids Res* 37: e105.
138. Heitzer E, Auer M, Gasch C, Pichler M, Ulz P, et al. (2013) Complex tumor genomes inferred from single circulating tumor cells by array-CGH and next-generation sequencing. *Cancer Res* 73: 2965-2975.
139. Mathiesen RR, Fjellidal R, Liestol K, Due EU, Geigl JB, et al. (2012) High-resolution analyses of copy number changes in disseminated tumor cells of patients with breast cancer. *Int J Cancer* 131: E405-415.
140. Magbanua MJ, Sosa EV, Scott JH, Simko J, Collins C, et al. (2012) Isolation and genomic analysis of circulating tumor cells from castration resistant metastatic prostate cancer. *BMC Cancer* 12: 78.

References

141. Treff NR, Su J, Tao X, Northrop LE, Scott RT, Jr. (2011) Single-cell whole-genome amplification technique impacts the accuracy of SNP microarray-based genotyping and copy number analyses. *Mol Hum Reprod* 17: 335-343.
142. Navin N, Kendall J, Troge J, Andrews P, Rodgers L, et al. (2011) Tumour evolution inferred by single-cell sequencing. *Nature* 472: 90-94.
143. Moller EK, Kumar P, Voet T, Peterson A, Van Loo P, et al. (2013) Next-generation sequencing of disseminated tumor cells. *Front Oncol* 3: 320.
144. Czyz ZT, Hoffmann M, Schlimok G, Polzer B, Klein CA (2014) Reliable Single Cell Array CGH for Clinical Samples. *PLoS One* 9: e85907.
145. Fuhrmann C, Schmidt-Kittler O, Stoecklein NH, Petat-Dutter K, Vay C, et al. (2008) High-resolution array comparative genomic hybridization of single micrometastatic tumor cells. *Nucleic Acids Res* 36: e39.
146. Mohlendick B, Bartenhagen C, Behrens B, Honisch E, Raba K, et al. (2013) A Robust Method to Analyze Copy Number Alterations of Less than 100 kb in Single Cells Using Oligonucleotide Array CGH. *PLoS One* 8: e67031.
147. Binder V, Bartenhagen C, Okpanyi V, Gombert M, Moehlendick B, et al. (2014) A New Workflow for Whole-Genome Sequencing of Single Human Cells. *Hum Mutat*.
148. Fragouli E, Wells D, Thornhill A, Serhal P, Faed MJ, et al. (2006) Comparative genomic hybridization analysis of human oocytes and polar bodies. *Hum Reprod* 21: 2319-2328.
149. Hellani A, Coskun S, Benkhalifa M, Tbakhi A, Sakati N, et al. (2004) Multiple displacement amplification on single cell and possible PGD applications. *Mol Hum Reprod* 10: 847-852.
150. Hellani A, Abu-Amero K, Azouri J, El-Akoum S (2008) Successful pregnancies after application of array-comparative genomic hybridization in PGS-aneuploidy screening. *Reprod Biomed Online* 17: 841-847.
151. Lage JM, Leamon JH, Pejovic T, Hamann S, Lacey M, et al. (2003) Whole genome analysis of genetic alterations in small DNA samples using hyperbranched strand displacement amplification and array-CGH. *Genome Res* 13: 294-307.
152. Le Caignec C, Spits C, Sermon K, De Rycke M, Thienpont B, et al. (2006) Single-cell chromosomal imbalances detection by array CGH. *Nucleic Acids Res* 34: e68.
153. Vanneste E, Voet T, Le Caignec C, Ampe M, Konings P, et al. (2009) Chromosome instability is common in human cleavage-stage embryos. *Nat Med* 15: 577-583.
154. Wang Y, Waters J, Leung ML, Unruh A, Roh W, et al. (2014) Clonal evolution in breast cancer revealed by single nucleus genome sequencing. *Nature* 512: 155-160.
155. Alfarawati S, Fragouli E, Colls P, Wells D (2011) First births after preimplantation genetic diagnosis of structural chromosome abnormalities using comparative genomic hybridization and microarray analysis. *Hum Reprod* 26: 1560-1574.
156. Bi W, Breman A, Shaw CA, Stankiewicz P, Gambin T, et al. (2012) Detection of ≥ 1 Mb microdeletions and microduplications in a single cell using custom oligonucleotide arrays. *Prenat Diagn* 32: 10-20.
157. Lu S, Zong C, Fan W, Yang M, Li J, et al. (2012) Probing meiotic recombination and aneuploidy of single sperm cells by whole-genome sequencing. *Science* 338: 1627-1630.
158. Hou Y, Fan W, Yan L, Li R, Lian Y, et al. (2013) Genome analyses of single human oocytes. *Cell* 155: 1492-1506.
159. Ni X, Zhuo M, Su Z, Duan J, Gao Y, et al. (2013) Reproducible copy number variation patterns among single circulating tumor cells of lung cancer patients. *Proc Natl Acad Sci U S A* 110: 21083-21088.
160. Magbanua MJ, Sosa EV, Roy R, Eisenbud LE, Scott JH, et al. (2013) Genomic profiling of isolated circulating tumor cells from metastatic breast cancer patients. *Cancer Res* 73: 30-40.
161. Voullaire L, Slater H, Williamson R, Wilton L (2000) Chromosome analysis of blastomeres from human embryos by using comparative genomic hybridization. *Hum Genet* 106: 210-217.

References

162. Voullaire L, Wilton L, McBain J, Callaghan T, Williamson R (2002) Chromosome abnormalities identified by comparative genomic hybridization in embryos from women with repeated implantation failure. *Mol Hum Reprod* 8: 1035-1041.
163. Wilton L (2005) Preimplantation genetic diagnosis and chromosome analysis of blastomeres using comparative genomic hybridization. *Hum Reprod Update* 11: 33-41.
164. Daphnis DD, Fragouli E, Economou K, Jerkovic S, Craft IL, et al. (2008) Analysis of the evolution of chromosome abnormalities in human embryos from Day 3 to 5 using CGH and FISH. *Mol Hum Reprod* 14: 117-125.
165. Wang J, Fan HC, Behr B, Quake SR (2012) Genome-wide single-cell analysis of recombination activity and de novo mutation rates in human sperm. *Cell* 150: 402-412.
166. Hou Y, Song L, Zhu P, Zhang B, Tao Y, et al. (2012) Single-cell exome sequencing and monoclonal evolution of a JAK2-negative myeloproliferative neoplasm. *Cell* 148: 873-885.
167. Hosch SB, Stoecklein NH, Pichlmeier U, Rehders A, Scheunemann P, et al. (2001) Esophageal cancer: the mode of lymphatic tumor cell spread and its prognostic significance. *J Clin Oncol* 19: 1970-1975.
168. Polzer B (2006) Identifizierung und Charakterisierung metastatischer Vorläuferzellen aus dem Knochenmark beim Prostatakarzinom [Dissertation]: LMU Munich.
169. du Manoir S, Speicher MR, Joos S, Schrock E, Popp S, et al. (1993) Detection of complete and partial chromosome gains and losses by comparative genomic in situ hybridization. *Hum Genet* 90: 590-610.
170. Will D (2011) Genomische Analyse disseminierter Tumorzellen (DTCs) bei Ösophaguskarzinompatienten Identifizierung einer prognostisch relevanten DTC-Subpopulation und Etablierung der aCGH zur hochaufgelösten genomischen Einzelzellanalyse von Chromosom 17 [Dissertation]: Heinrich-Heine-Universität Düsseldorf.
171. Cheung VG, Nowak N, Jang W, Kirsch IR, Zhao S, et al. (2001) Integration of cytogenetic landmarks into the draft sequence of the human genome. *Nature* 409: 953-958.
172. Mosteller F, Tukey JW (1977) Data analysis and regression: a second course in statistics.: Addison-Wesley.
173. Lange T, Nentwich MF, Luth M, Yekebas E, Schumacher U (2011) Trastuzumab has anti-metastatic and anti-angiogenic activity in a spontaneous metastasis xenograft model of esophageal adenocarcinoma. *Cancer Lett* 308: 54-61.
174. Pollack JR, Perou CM, Alizadeh AA, Eisen MB, Pergamenschikov A, et al. (1999) Genome-wide analysis of DNA copy-number changes using cDNA microarrays. *Nat Genet* 23: 41-46.
175. Konings P, Vanneste E, Jackmaert S, Ampe M, Verbeke G, et al. (2012) Microarray analysis of copy number variation in single cells. *Nat Protoc* 7: 281-310.
176. Fiorentino F, Spizzichino L, Bono S, Biricik A, Kokkali G, et al. (2011) PGD for reciprocal and Robertsonian translocations using array comparative genomic hybridization. *Hum Reprod* 26: 1925-1935.
177. Barretina J, Caponigro G, Stransky N, Venkatesan K, Margolin AA, et al. (2012) The Cancer Cell Line Encyclopedia enables predictive modelling of anticancer drug sensitivity. *Nature* 483: 603-607.
178. Borgen E, Pantel K, Schlimok G, Muller P, Otte M, et al. (2006) A European interlaboratory testing of three well-known procedures for immunocytochemical detection of epithelial cells in bone marrow. Results from analysis of normal bone marrow. *Cytometry B Clin Cytom* 70: 400-409.
179. Ylstra B, van den Ijssel P, Carvalho B, Brakenhoff RH, Meijer GA (2006) BAC to the future! or oligonucleotides: a perspective for micro array comparative genomic hybridization (array CGH). *Nucleic Acids Res* 34: 445-450.
180. Pease AC, Solas D, Sullivan EJ, Cronin MT, Holmes CP, et al. (1994) Light-generated oligonucleotide arrays for rapid DNA sequence analysis. *Proc Natl Acad Sci U S A* 91: 5022-5026.

References

181. Hughes TR, Mao M, Jones AR, Burchard J, Marton MJ, et al. (2001) Expression profiling using microarrays fabricated by an ink-jet oligonucleotide synthesizer. *Nat Biotechnol* 19: 342-347.
182. Singh-Gasson S, Green RD, Yue Y, Nelson C, Blattner F, et al. (1999) Maskless fabrication of light-directed oligonucleotide microarrays using a digital micromirror array. *Nat Biotechnol* 17: 974-978.
183. Iwamoto K, Bundo M, Ueda J, Nakano Y, Ukai W, et al. (2007) Detection of chromosomal structural alterations in single cells by SNP arrays: a systematic survey of amplification bias and optimized workflow. *PLoS One* 2: e1306.
184. Johnson DS, Gemelos G, Baner J, Ryan A, Cinnioglu C, et al. (2010) Preclinical validation of a microarray method for full molecular karyotyping of blastomeres in a 24-h protocol. *Hum Reprod* 25: 1066-1075.
185. Ling J, Zhuang G, Tazon-Vega B, Zhang C, Cao B, et al. (2009) Evaluation of genome coverage and fidelity of multiple displacement amplification from single cells by SNP array. *Mol Hum Reprod* 15: 739-747.
186. Treff NR, Su J, Tao X, Levy B, Scott RT, Jr. (2010) Accurate single cell 24 chromosome aneuploidy screening using whole genome amplification and single nucleotide polymorphism microarrays. *Fertil Steril* 94: 2017-2021.
187. Northrop LE, Treff NR, Levy B, Scott RT, Jr. (2010) SNP microarray-based 24 chromosome aneuploidy screening demonstrates that cleavage-stage FISH poorly predicts aneuploidy in embryos that develop to morphologically normal blastocysts. *Mol Hum Reprod* 16: 590-600.
188. Vanneste E, Melotte C, Voet T, Robberecht C, Debrock S, et al. (2011) PGD for a complex chromosomal rearrangement by array comparative genomic hybridization. *Hum Reprod* 26: 941-949.
189. Pinto D, Darvishi K, Shi X, Rajan D, Rigler D, et al. (2011) Comprehensive assessment of array-based platforms and calling algorithms for detection of copy number variants. *Nat Biotechnol* 29: 512-520.
190. Curtis C, Lynch AG, Dunning MJ, Spiteri I, Marioni JC, et al. (2009) The pitfalls of platform comparison: DNA copy number array technologies assessed. *BMC Genomics* 10: 588.
191. Tulpan D (2010) Recent patents and challenges on DNA microarray probe design technologies. *Recent Pat DNA Gene Seq* 4: 210-217.
192. Sharp AJ, Itsara A, Cheng Z, Alkan C, Schwartz S, et al. (2007) Optimal design of oligonucleotide microarrays for measurement of DNA copy-number. *Hum Mol Genet* 16: 2770-2779.
193. De Witte A, Rizzo C, Cifuentes F (2007) Analysis of DNA Copy Number Changes Using 60 mer Oligo-based Microarrays. *Genetic Engineering and Biotechnology News* 27.
194. Cai X, Evrony GD, Lehmann HS, Elhosary PC, Mehta BK, et al. (2014) Single-Cell, Genome-wide Sequencing Identifies Clonal Somatic Copy-Number Variation in the Human Brain. *Cell Rep*.
195. Mead S, Poulter M, Beck J, Uphill J, Jones C, et al. (2008) Successful amplification of degraded DNA for use with high-throughput SNP genotyping platforms. *Hum Mutat* 29: 1452-1458.
196. Agalliu I, Schweitzer PA, Leanza SM, Burk RD, Rohan TE (2009) Illumina DNA test panel-based genotyping of whole genome amplified-DNA extracted from hair samples: performance and agreement with genotyping results from genomic DNA from buccal cells. *Clin Chem Lab Med* 47: 516-522.
197. Rigby PW, Dieckmann M, Rhodes C, Berg P (1977) Labeling deoxyribonucleic acid to high specific activity in vitro by nick translation with DNA polymerase I. *J Mol Biol* 113: 237-251.
198. Pinkel D, Seagraves R, Sudar D, Clark S, Poole I, et al. (1998) High resolution analysis of DNA copy number variation using comparative genomic hybridization to microarrays. *Nat Genet* 20: 207-211.
199. Feinberg AP, Vogelstein B (1983) A technique for radiolabeling DNA restriction endonuclease fragments to high specific activity. *Anal Biochem* 132: 6-13.
200. Lieu PT, Jozsi P, Gilles P, Peterson T (2005) Development of a DNA-labeling system for array-based comparative genomic hybridization. *J Biomol Tech* 16: 104-111.

References

201. Wiegant JC, van Gijlswijk RP, Heetebrij RJ, Bezrookove V, Raap AK, et al. (1999) ULS: a versatile method of labeling nucleic acids for FISH based on a monofunctional reaction of cisplatin derivatives with guanine moieties. *Cytogenet Cell Genet* 87: 47-52.
202. Knijnenburg J, van der Burg M, Tanke HJ, Szuhai K (2007) Optimized amplification and fluorescent labeling of small cell samples for genomic array-CGH. *Cytometry A* 71: 585-591.
203. Yu H, Chao J, Patek D, Mujumdar R, Mujumdar S, et al. (1994) Cyanine dye dUTP analogs for enzymatic labeling of DNA probes. *Nucleic Acids Res* 22: 3226-3232.
204. Pinard R, de Winter A, Sarkis GJ, Gerstein MB, Tartaro KR, et al. (2006) Assessment of whole genome amplification-induced bias through high-throughput, massively parallel whole genome sequencing. *BMC Genomics* 7: 216.
205. Lucito R, West J, Reiner A, Alexander J, Esposito D, et al. (2000) Detecting gene copy number fluctuations in tumor cells by microarray analysis of genomic representations. *Genome Res* 10: 1726-1736.
206. Pugh TJ, Delaney AD, Farnoud N, Flibotte S, Griffith M, et al. (2008) Impact of whole genome amplification on analysis of copy number variants. *Nucleic Acids Res* 36: e80.
207. Cheng J, Vanneste E, Konings P, Voet T, Vermeesch JR, et al. (2011) Single-cell copy number variation detection. *Genome Biol* 12: R80.
208. Schmitt MW, Kennedy SR, Salk JJ, Fox EJ, Hiatt JB, et al. (2012) Detection of ultra-rare mutations by next-generation sequencing. *Proc Natl Acad Sci U S A* 109: 14508-14513.
209. Lipson D, Aumann Y, Ben-Dor A, Linial N, Yakhini Z (2006) Efficient calculation of interval scores for DNA copy number data analysis. *J Comput Biol* 13: 215-228.
210. Olshen AB, Venkatraman ES, Lucito R, Wigler M (2004) Circular binary segmentation for the analysis of array-based DNA copy number data. *Biostatistics* 5: 557-572.
211. Turner NC, Reis-Filho JS (2012) Genetic heterogeneity and cancer drug resistance. *Lancet Oncol* 13: e178-185.
212. Fidler IJ (2012) Biological heterogeneity of cancer: implication to therapy. *Hum Vaccin Immunother* 8: 1141-1142.
213. Burrell RA, McGranahan N, Bartek J, Swanton C (2013) The causes and consequences of genetic heterogeneity in cancer evolution. *Nature* 501: 338-345.
214. Gerlinger M, Rowan AJ, Horswell S, Larkin J, Endesfelder D, et al. (2012) Intratumor heterogeneity and branched evolution revealed by multiregion sequencing. *N Engl J Med* 366: 883-892.
215. Yap TA, Gerlinger M, Futreal PA, Pusztai L, Swanton C (2012) Intratumor heterogeneity: seeing the wood for the trees. *Sci Transl Med* 4: 127ps110.
216. Keats JJ, Chesi M, Egan JB, Garbitt VM, Palmer SE, et al. (2012) Clonal competition with alternating dominance in multiple myeloma. *Blood* 120: 1067-1076.
217. Szerlip NJ, Pedraza A, Chakravarty D, Azim M, McGuire J, et al. (2012) Intratumoral heterogeneity of receptor tyrosine kinases EGFR and PDGFRA amplification in glioblastoma defines subpopulations with distinct growth factor response. *Proc Natl Acad Sci U S A* 109: 3041-3046.
218. Landau DA, Carter SL, Stojanov P, McKenna A, Stevenson K, et al. (2013) Evolution and impact of subclonal mutations in chronic lymphocytic leukemia. *Cell* 152: 714-726.
219. Inukai M, Toyooka S, Ito S, Asano H, Ichihara S, et al. (2006) Presence of epidermal growth factor receptor gene T790M mutation as a minor clone in non-small cell lung cancer. *Cancer Res* 66: 7854-7858.
220. Mroz EA, Tward AD, Pickering CR, Myers JN, Ferris RL, et al. (2013) High intratumor genetic heterogeneity is related to worse outcome in patients with head and neck squamous cell carcinoma. *Cancer* 119: 3034-3042.
221. Maheswaran S, Sequist LV, Nagrath S, Ullkus L, Brannigan B, et al. (2008) Detection of mutations in EGFR in circulating lung-cancer cells. *N Engl J Med* 359: 366-377.
222. Swanton C (2012) Intratumor heterogeneity: evolution through space and time. *Cancer Res* 72: 4875-4882.

References

- 223. Ding L, Ley TJ, Larson DE, Miller CA, Koboldt DC, et al. (2012) Clonal evolution in relapsed acute myeloid leukaemia revealed by whole-genome sequencing. *Nature* 481: 506-510.
- 224. Parkin B, Ouillette P, Li Y, Keller J, Lam C, et al. (2013) Clonal evolution and devolution after chemotherapy in adult acute myelogenous leukemia. *Blood* 121: 369-377.
- 225. Wikman H, Vessella R, Pantel K (2008) Cancer micrometastasis and tumour dormancy. *APMIS* 116: 754-770.
- 226. Ranganathan AC, Zhang L, Adam AP, Aguirre-Ghiso JA (2006) Functional coupling of p38-induced up-regulation of BiP and activation of RNA-dependent protein kinase-like endoplasmic reticulum kinase to drug resistance of dormant carcinoma cells. *Cancer Res* 66: 1702-1711.
- 227. Almendro V, Kim HJ, Cheng YK, Gonen M, Itzkovitz S, et al. (2014) Genetic and phenotypic diversity in breast tumor metastases. *Cancer Res* 74: 1338-1348.
- 228. Almendro V, Cheng YK, Randles A, Itzkovitz S, Marusyk A, et al. (2014) Inference of tumor evolution during chemotherapy by computational modeling and in situ analysis of genetic and phenotypic cellular diversity. *Cell Rep* 6: 514-527.
- 229. Xu X, Hou Y, Yin X, Bao L, Tang A, et al. (2012) Single-cell exome sequencing reveals single-nucleotide mutation characteristics of a kidney tumor. *Cell* 148: 886-895.

7. Acknowledgments.

First of all I would like to thank my supervisor, Prof. Dr Christoph Klein, for giving me the chance to complete my PhD thesis in his laboratory. I am truly grateful for his invaluable support as well as providing funds, infrastructure and other resources without which completion of this thesis would not be possible.

I would also like to sincerely thank the members of the examination committee, Prof. Dr. Thomas Dresselhaus (my Doktorvater), Prof. Dr Gunter Meister, Prof. Dr. Stephan Schneuwly and Prof. Dr. Richard Warth, for investing their time and efforts in all the proceedings related to this thesis.

I would also like to express my gratitude to Dr Bernhard M. Polzer for his time, support and supervision. In particular I would like to express my gratitude for critical revision of the preliminary drafts of this dissertation.

Many thanks to the staff members of The Chair of Experimental Medicine & Therapy Research (the LEXians) and the Projectgroup for Personalized Tumor Therapy at Fraunhofer ITEM Regensburg (the ITEMS), as well as all those who made my time in Regensburg to a life changing experience and invaluable lesson of life.

In particularly I would like to name and thank the following people:

- Dr Milan Obradović, my dear friend – thank you sincerely for your friendship and support. We went through a lot of ups and downs but we've overcome all the obstacles in the end. I wish you all the best.
- Dr Martin Hoffmann for supporting me on the bioinformatics side of the project.
- Dr Stefan Kirsch for countless discussions and critical questions. I learned a lot from this.
- Miodrag, Nina, Manfred, Isa, Sebastian, Giancarlo, Katharina, Gundula, Irene, Lahiri, Daniel, Anya and all the others who accompanied and supported me during my times at the AG Klein.
- Kathrin, Christian, Steffi, Catherin, Karola, Stefanie, Siegfried, Sybille and other ITEMS for their support and creating a nice atmosphere around the lab.

I would like to thank Aileen Rose Lo, MD. Thank you for your unfailing faith in me. You have enlightened my life and helped me at many different levels. Without you it would be so much harder.

Last but not least I would like to thank my parents for their continuous support and unfading faith in my abilities. Po długi zmaganiach, wzlotach i upadkach dotarliśmy do celu. Mamo, Tato – dziękuję Wam bardzo za wszystko.

8. Curriculum vitae.

Zbigniew Tadeusz Czyż

Date of birth: 30.06.1983
Place of birth: Czarnków, Poland

EDUCATIONAL BACKGROUND:

1990 – 1998 Primary Education:
Władysław Broniewski Primary School, Wronki, Poland

1990 – 2002 Secondary Education:
Piotr Skarga High School, Szamotuły, Poland
Graduated with honours.

HIGHER EDUCATION:

2002 – 2007 Master's Degree Program in Biotechnology,
at The August Cieszkowski Agricultural University of Poznan, Poland
Graduated with honours.

2005 – 2007 Master's Degree training,
Executed at The Department of Reproductive Biology and Stem Cells
in The Institute of Human Genetics of the Polish Academy of Sciences,
Poznan, Poland.
Topic: Quantitative analysis of selected molecular markers in *in vitro* culture
of human myoblast populations established through the pre-plate technique.
Supervised by Prof. Dr. Maciej Kurpisz

2007 – 2014 PhD training.
Executed at The Chair of Experimental Medicine & Therapy Research
in the Insitute of Pathology of the Univeristy Hospital Regensbug:
Topic: Development of a reliable single-cell aCGH suitable for clinical
samples.
Supervised by:
Prof. Dr. Christoph A. Klein – primary suprvisor

FURTHER CARRIER:

Since April 2014 Research assistant
Projectgroup for Personalized Tumor Therapy at Fraunhofer ITEM,
Regensburg

PUBLICATIONS:

1.

Molecular profiling of single Sca-1⁺/CD34⁺, - cells--the putative murine lung stem cells.

Hittinger M, Czyz ZT, Huesemann Y, Maneck M, Botteron C, Kaeufl S, Klein CA, Polzer B.
PLoS One. 2013 Dec 31;8(12):e83917. doi: 10.1371/journal.pone.0083917. eCollection 2013.
PMID: 24391845

2.

Reliable single cell array CGH for clinical samples.

Czyz ZT, Hoffmann M, Schlimok G, Polzer B, Klein CA.
PLoS One. 2014 Jan 21;9(1):e85907. doi: 10.1371/journal.pone.0085907. eCollection 2014.
PMID: 24465780

3.

Quantitative measurement of melanoma spread in sentinel lymph nodes and survival.

Ulmer A, Dietz K, Hodak I, Polzer B, Scheitler S, Yildiz M, Czyz Z, Lehnert P, Fehm T, Hafner C,
Schanz S, Röcken M, Garbe C, Breuninger H, Fierlbeck G, Klein CA.
PLoS Med. 2014 Feb 18;11(2):e1001604. doi: 10.1371/journal.pmed.1001604. eCollection 2014 Feb.
PMID: 24558354

4.

Combined genome and transcriptome analysis of single disseminated cancer cells from bone marrow of prostate cancer patients reveals unexpected transcriptomes.

Guzvic M, Braun B, Ganzer R, Burger M, Nerlich M, Winkler S, Werner-Klein M, Czyz ZT, Polzer B, Klein CA.
Cancer Res. 2014 Oct 15. pii: canres.0934.2014. [Epub ahead of print]
PMID: 25320011

5.

Molecular profiling of single circulating tumor cells with diagnostic intention.

Polzer B, Medoro G, Pasch S, Fontana F, Zorzino L, Pestka A, Andergassen U, Meier-Stiegen F, Czyz ZT, Alberter B, Treitschke S, Schamberger T, Sergio M, Bregola G, Doffini A, Gianni S, Calanca A, Signorini G, Bolognesi C, Hartmann A, Fasching PA, Sandri MT, Rack B, Fehm T, Giorgini G, Manaresi N, Klein CA.
EMBO Mol Med. 2014 Oct 30;6(11):1371-86. doi: 10.15252/emmm.201404033.
PMID: 25358515